Collection of replies to reviewer comments.

---

## *REPLY TO:*

# *Interactive comment on* "The SSP greenhouse gas concentrations and their extensions to 2500" *by* Malte Meinshausen et al.

**Anonymous Referee #1**

Received and published: 2 December 2019

This paper describes the new Shared Socioeconomic Pathways (SSP) greenhouse gas scenarios for 2015 to 2500 based on the MAGICC7.0 climate-carbon cycle model. The future projections are combined with historical observationally-based concentration data to provide continuous time series from pre-industrial (1700) to 2500. Projections include monthly and latitudinal variations for 43 greenhouse gases: CO2, CH4, N2O, the major chlorine and bromine-containing ozone depleting substances, and many fluorinated compounds. The paper documents the methodology and assumptions made for five high-priority scenarios and four additional scenarios that will be used to drive climate model simulations for the upcoming CMIP6 activity. The paper also provides some analysis of the expected impacts of the scenarios on global and regional surface temperature and sea level rise, and includes some comparisons with

the previous RCP greenhouse gas scenarios.

This is an important paper which is generally well-written. However, some aspects of the text should be clarified and/or improved prior to publication. These are listed below, along with some other minor corrections.

*REPLY: We thank Referee #1 for the time to go through this extensive manuscript.*

The figures, overall, are too complicated and filled with unnecessary details at this point. Most of the figures have too many panels and many panels are too small to be discernible. I would recommend the authors to put some serious thoughts into what are the most important figures that are essential in terms of conveying the key messages of this paper for the modeling and the general scientific communities. Keep those figures/panels, and move the rest to supplementary material.

*REPLY: Thank you. We moved Figures 6 (the 2005 to 2030 excerpt of historical observations and future concentrations) and 13 (the effect of the latitudinally resolved concentrations in CESM2) to the Supplementary Material and deleted Figure 12 (the temperature and SLR projections under SSPs and RCPs).*

Abstract:

line 38, change to ". . . has quantified"

*REPLY: Done.*

line 41, change to "concentrations"

*REPLY: Thx. Done.*

line 51, ". . .from today 66%...." sentence structure is not right. Do you mean, eg, ". . . from 66% for present day to roughly 68% " ?

*REPLY: Thx. Suggestion implemented.*

line 55, ". . . expected global mean temperatures extend to lower 2100 temperatures" Please reword this. It's not clear what is being said here.

*REPLY: Thank you. We shortened and hopefully clarified the sentence by saying that: "In comparison to the RCPs, the five main SSPs (SSP1-1.9, SSP1-2.6, SSP2-4.5, SSP3-7.0 and SSP5-8.5) are more evenly spaced and extend to lower 2100 radiative forcing and temperatures."*

Line 58, spell out MAM.

*REPLY: Done.*

line 63, I was confused by the term "collective" here. I suggest "societal" instead.

*REPLY: Thx for the suggestion. Implemented.*

line 64, change "manage" to "limit"

*REPLY: Thx for the suggestion. Implemented.*

lines 60-64. This is a very long sentence. I suggest separating into two sentences. Eg, start new sentence on line 63 to read: ". . ... upwards shape. It is a"

*REPLY: Thx for the suggestion. Implemented.*

Main text:

p. 3, CMIP6 was defined three times on this page. Suggest introduction of CMIP-6 at lines 72-73. Please consistently use either CMIP6 or CMIP-6 throughout the text.

*REPLY: Implemented.*

p. 3, line 77, define GHG here as greenhouse gases (GHG). You may consider using GHG, instead of greenhouse gases throughout the text hereafter.

*REPLY: We opted to introduce the abbreviation GHG in the next paragraph. At this location (line 77) it could have led to misunderstandings – given it refers to non-CO2 GHGs..*

p. 3, line 79, insert “minor” after “other”.

*REPLY: Done.*

p. 6, line 170, consider use “concentrations”, instead of “mixing ratios”

*REPLY: Done.*

p.7, line 193, change “CO” to “OC”

*REPLY: Oups. Thanks for spotting that.*

p. 12, line 323, delete “to”

*REPLY: Thank you. Done.*

p. 13, Section 2.4.3, lines 363-365, the change in stratospheric lifetime per BDC change, and the BDC change per warming beyond 1980 levels. These are important points, but how were these numbers obtained? This should be explained and/or references cited.

*REPLY: Thank you and apologies that we insufficiently explained this step in our calibration. The text now reads:*

*“The Brewer-Dobson circulation is assumed to increase 15% per degree of warming beyond 1980, derived from Butchart and Scaife’s finding of an approximately 3% increase per decade (2001) and assuming a 0.2C warming per decade (Meinshausen et al., 2011). Calibrating our gas-cycle models to the results by Holmes et al. (2013), it seemed however that our Brewer-Dobson circulation speed-up shortened the longer-term lifetimes in higher-warming scenarios substantially more than predicted by the results of Holmes et al. (2013). Assuming no change in the height-age distribution of the air parcels that travel through the stratosphere, the speed-*

*up of this meridional circulation could 1:1 lower stratospheric lifetimes. However, assuming shorter residence times could offset some of the effect. We proceeded with a pragmatic approach and calibrated an effectiveness/scaling factor of 0.3 to match methane concentration projections by Holmes et al. (2013). That means that every 1% increase in the Brewer-Dobson circulation, the partial stratospheric lifetimes are reduced by 0.3%. However, we acknowledge that this effectiveness factor possibly summarizes multiple underlying differences between un-scaled MAGICC results and the Holmes et al. 2013 projections that are unrelated to the Brewer-Dobson circulation."*

p. 14, lines 365-366, in addition to scaling of lifetime with the OH abundance, shouldn't you consider scaling of the OH reaction rates due to temperature changes as well, as these rates are temperature-dependent (same as the CH4-OH rate)?

*REPLY: Yes, that is a good point. Somewhat implicitly, MAGICC does indeed account for this temperature dependence of the OH-related sinks for other gases. That is because, the OH-related lifetime for those gases is scaled by the relative change over time of the OH-related and temperature-dependent CH4 partial lifetime. Hence, we clarify that sentence to say: "We assume that partial lifetimes related to the (changing) tropospheric OH sink scale with the OH- and temperature-dependent methane lifetime"*

p. 14, line 371, delete "now"

*REPLY: "Done".*

p. 15, lines 414-418, this sentence is long, awkward, and doesn't flow logically. Con- sider rewrite.

*REPLY: Thank you. And apologies for this sentence that was indeed awkward. We now rewrote it to read "There are large natural $CH_4$ emission sources, predominantly in the northern hemisphere. In addition, anthropogenic emissions are higher in the northern hemisphere. This largely explains the observed atmospheric concentration gradient: At the end of the historical period (2010 to 2014), $CH_4$ concentrations are 80 ppb above the global average in the Northern mid-latitudes while Southern hemispheric concentrations gently slope towards a minimum of 60 ppb below the global average at the pole (Figure 11b in Meinshausen et al., 2017)."*

p. 15, lines 414-418 and hereafter throughout the text, be consistent when you capitalize "Northern hemisphere" and "Southern hemisphere" or not.

*REPLY: Thank you. Done.*

p. 16, line 429, change to "increase strongly"

*REPLY: Thank you. Done.*

p. 20, line 550, change “this” to “these”

*REPLY: Corrected.*

p. 22, lines 600 and 603, remove “as”

*REPLY: Thank you. Corrected.*

p. 24, line 638, “Even stronger. . ..” is awkward. I suggest “More notable. . .”

*REPLY: Suggestion adopted.*

p. 24, line 645, change to: “. . . in China. The similarly short-lived methylene chloride (CH2Cl2) also had ”

*REPLY: Suggestion adopted.*

p. 25, line 670, change to: “. . .for CO2, are miniscule... ”

*REPLY: Thank you. Corrected.*

p. 25, line 672, remove “to”

*REPLY: Thank you. Corrected.*

p. 25, line 673, remove “These”

*REPLY: Thank you. Corrected.*

p. 25, lines 675-676, change to: “... concentrations of methane decrease pronouncedly over the 21st century. CO2, for which lower ”

*REPLY: Thank you. We largely followed this suggestion, but changed the second sentence, so that it reads: “Reflecting the shorter lifetime, concentrations of methane decrease noticeably over the 21st century. The stronger mitigation scenarios include net negative emissions for CO2, so that CO2 concentrations recede over the long term to around 350ppm in case of the SSP1-1.9 scenario.”*

p. 27, line 739, what do you mean by “cooler”? Colder temperatures?

*REPLY: Due to the strong interest of the user community in temperature comparisons, we decided to actually pull this section and turn it into a separate manuscript with the background methodology description it deserves.*

p. 27, line 741, either “relatively comparable” or “closely comparable”, “relatively closely comparable” doesn’t make sense.

*REPLY: ibid. Due to the strong interest of the user community in temperature comparisons, we decided to actually pull this section and turn it into a separate manuscript with the background methodology description it deserves.*

p. 27, line 745, should be “easily communicated”?

*REPLY: ibid. Due to the strong interest of the user community in temperature comparisons, we decided to actually pull this section and turn it into a separate manuscript with the background methodology description it deserves.*

p. 28, lines 759-769, references to Figure 12b are missing.

*REPLY: ibid. Due to the strong interest of the user community in temperature comparisons, we decided to actually pull this section and turn it into a separate manuscript with the background methodology description it deserves.*

p. 29, line 786, MAM is a spring season, not winter.

*REPLY: Now corrected so that it says: “In the DJF and MAM northern hemispheric winter and spring season, ….”*

p. 29, lines 793-4, wording is redundant, change to: “. . .. poleward of 65 degrees North”, or something to that effect.

*REPLY: Thank you. Suggestion taken up.*

p. 29, line 796, change to “4500-year long”

*REPLY: Thank you. Corrected.*

p. 29, lines 801 and 803, what do you mean by “the MAM region” and “the DJF region”?

*REPLY: Apologies. Corrected to now read “MAM period” and “DJF period”.*

p. 28-29 and Figure 13, what about the responses/impacts in the other two seasons, JJA and SON? Whether significant impacts were expected or not, at least there needs to be a note on this?

*REPLY: See below the figure for JJA and SON. As to be expected, the difference in the signal is not as pronounced, if any. That is because the lower summer/autumn northern hemispheric CO2 concentrations due to the seasonality are offset by the North-to-South latitudinal gradient of forcing due to all GHGs. See the JJA and SON figure below.*

*Reflecting these results, we added a sentence: "As one would expect, our analysis does not suggest significant latitudinal temperature perturbations at the 5% level for the JJA and SON periods (not shown), when seasonally lower CO2 concentrations are partially offset by the latitudinal gradient of concentrations in the Northern hemisphere.".*

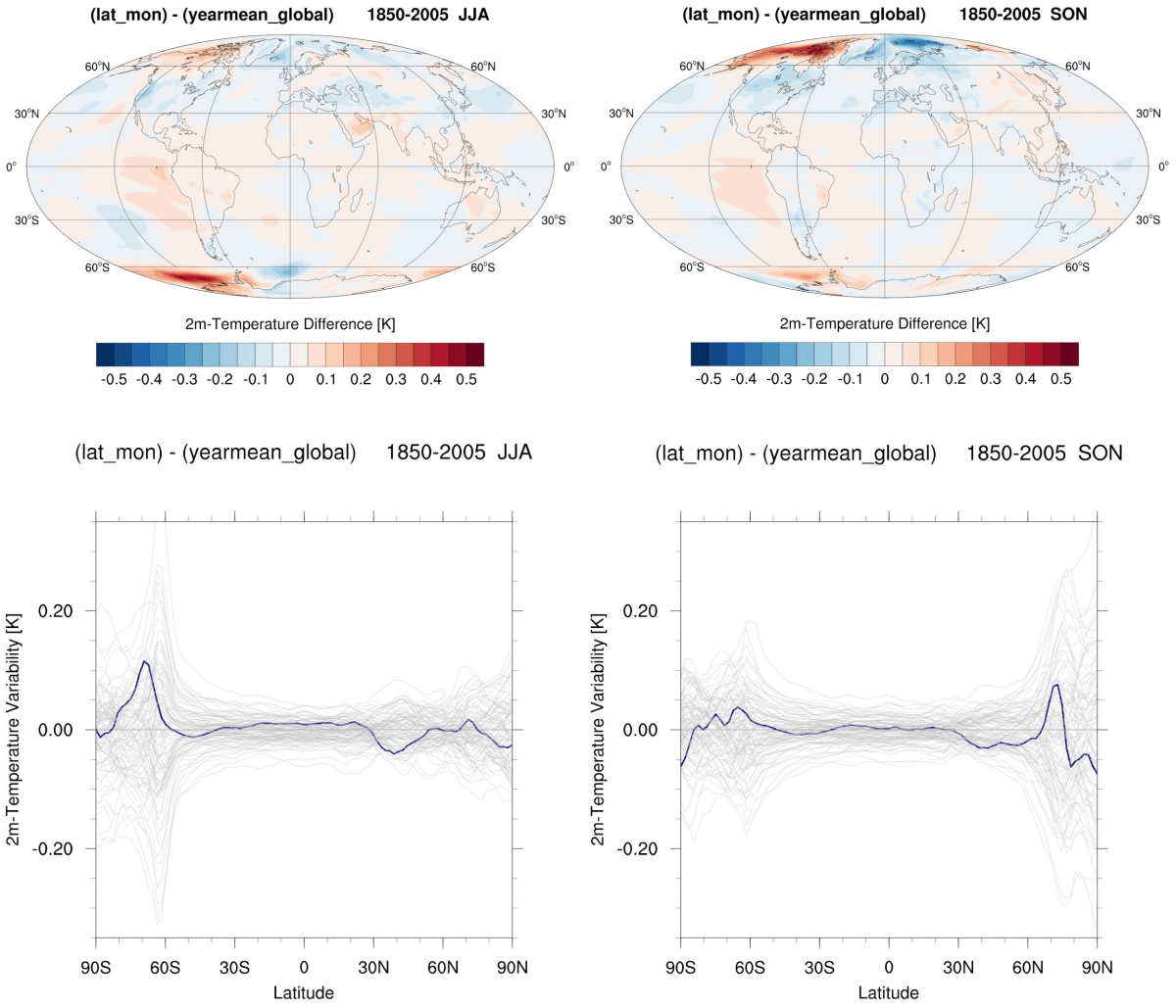


Figure 2: I am not sure the color and line-style grouping for this figure are the best choices or reader-friendly. First I would suggest to use thicker lines for the RCPs so that we can distinguish the SSP lines easily from the RCP lines. Second, why break thick solid lines from thin solid lines just because these are the four scenarios for which

long-term CMIP6 model experiments are planned? Isn't it more meaningful to use the thick vs. thin lines to break the high-priority ("Tier 1" + SSP1-1.9) and "Tier 2", to support the discussion in the text?

*REPLY: Done. Thank you for the suggestion. We now adapted the color code of the SSP scenarios to the official IPCC AR6 color guide. We highlighted (by virtue of the boxed labels) all the high-priority SSPs. We also increased the stroke width for the RCP scenarios and distinguished them from the SSP scenarios by line style rather than color (RCPs are now all dark grey).*

A few minor comments: 1) what is the first vertical blue line, 2010? 2015? Please state.

*REPLY: Done.*

2) Also the small SSP labels, and the x-axis and y-axis labels all need to be bigger and darker. They are hard to read as is.

*REPLY: Done.*

3) Overall, the thin lines are too thin, which make them almost not readable on printout versions.

*REPLY: Corrected. The thinnest line width is now increased from 0.5 to 1.5pt. .*

4) "Total N2O emissions" in panel g should be "Total anthropogenic N2O emissions", to be accurate?

*REPLY: We think it will lead to less confusion, if we adapt the figure caption by stating that these are all anthropogenic emissions. If we inserted that flag only for a single gas, people will wonder whether the Total CH4 emissions are for example both natural and anthropogenic. We hence adapted the caption.*

Here is the adjusted Figure 2:

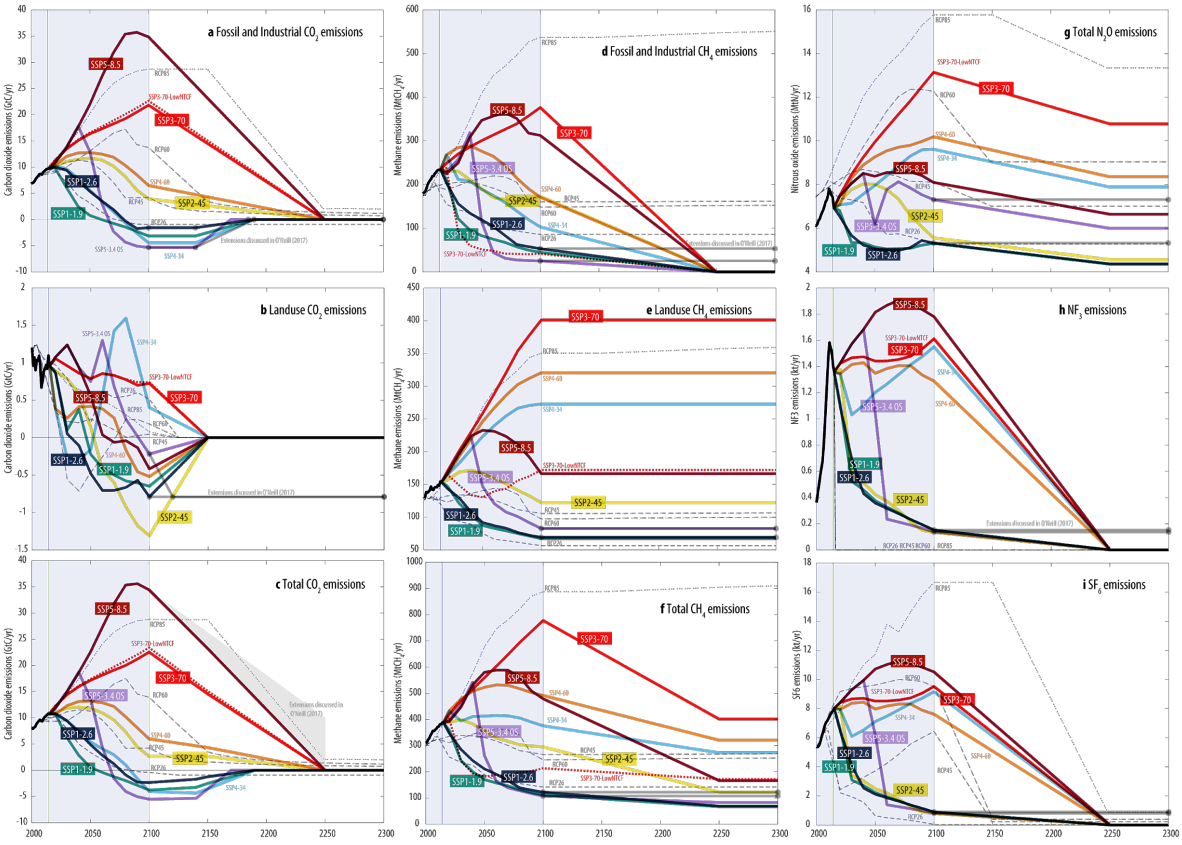


Figure 2

Figure 3, panels eg, are the y-axis showing latitudes? If so, please mark clearly.

*REPLY: The fifty permafrost zonal bands are simplified presentations of the latitudinal (and topographic) distribution of the permafrost in the northern hemisphere. These bin numbers hence do not refer to latitudes. The full description from Schneider von Deimling permafrost module (2012 www.biogeosciences.net/9/649/2012) is provided in their schematic Figure 1 or A1, with the Appendix A describing the assumption about thawing threshold and carbon content distributions across these zonal bands.*

*See e.g. Figure 1 in Schneider von Deimling*

*And the technical Appendix specifies the carbon content assumption.*

*We hence insert a reference in the caption that now reads:*

*"The permafrost zonal bands are a simplified approach to represent the range of thawing thresholds and permafrost carbon contents and are described in Schneider von Deimling et al. (2012)." We also added the additional description "(Southernmost =1) into the y-label caption.*

I assume panels eg are for CO2-related emissions and panels fh are for CH4-related emissions? If so, please indicate clearly in the legends, or at least, explain in the figure caption.

*REPLY: Close, but not quite. The anaerobic decomposition shown in panels f and h will initially produce CH4, but some of the methane is oxidized on its path to the atmosphere and emerges as CO2. Thus, those panels are simply what their titles are, the Anerobic or Aerobic decomposition of the mineral or peatland soil carbon. We added an extra sentence in the caption:*

*"The mineral and peatland soil decomposition under aerobic conditions (panels e and g, respectively), and also the oxidised part of the methane that originates from the anaerobic decomposition (panels f and h) contribute to the net CO2 emissions from permafrost thawing."*

*The slightly adapted figure is now:*

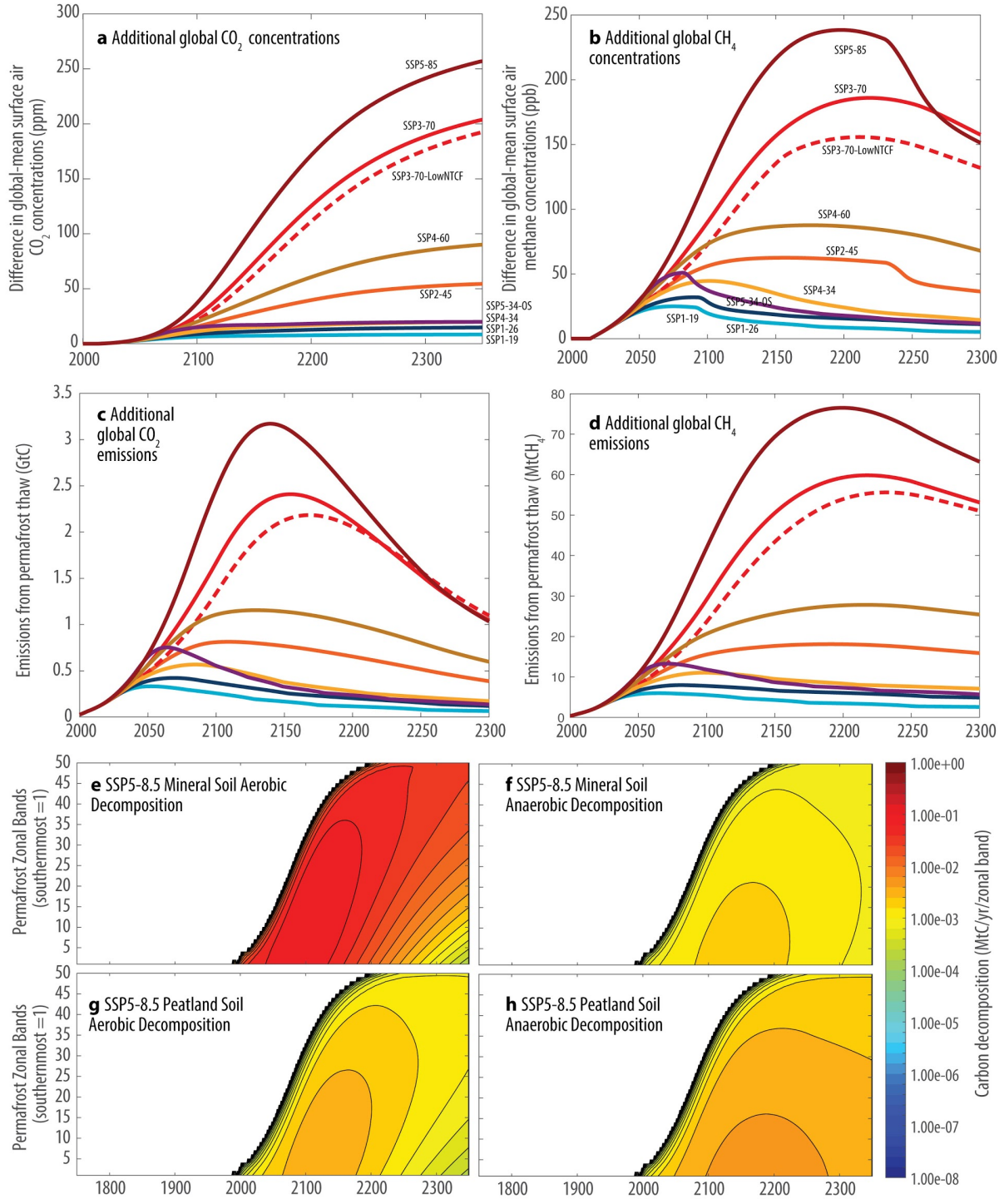


Figure 3

Figure 4, top left panel, what is the black lettering in the upper right? Remove or clarify. I am not sure I understand Figure 4d at all, particularly the top ranges for N2O, CH4.

*REPLY: Thank you. We now expanded the title of Figure 4d and added some additional text. The black lettering is an odd display issue that arises when the journal's submission website converts the submitted PDF. It unfortunately does not arise on our side, so we are unsure how to fix that. Here is the adapted graph.*

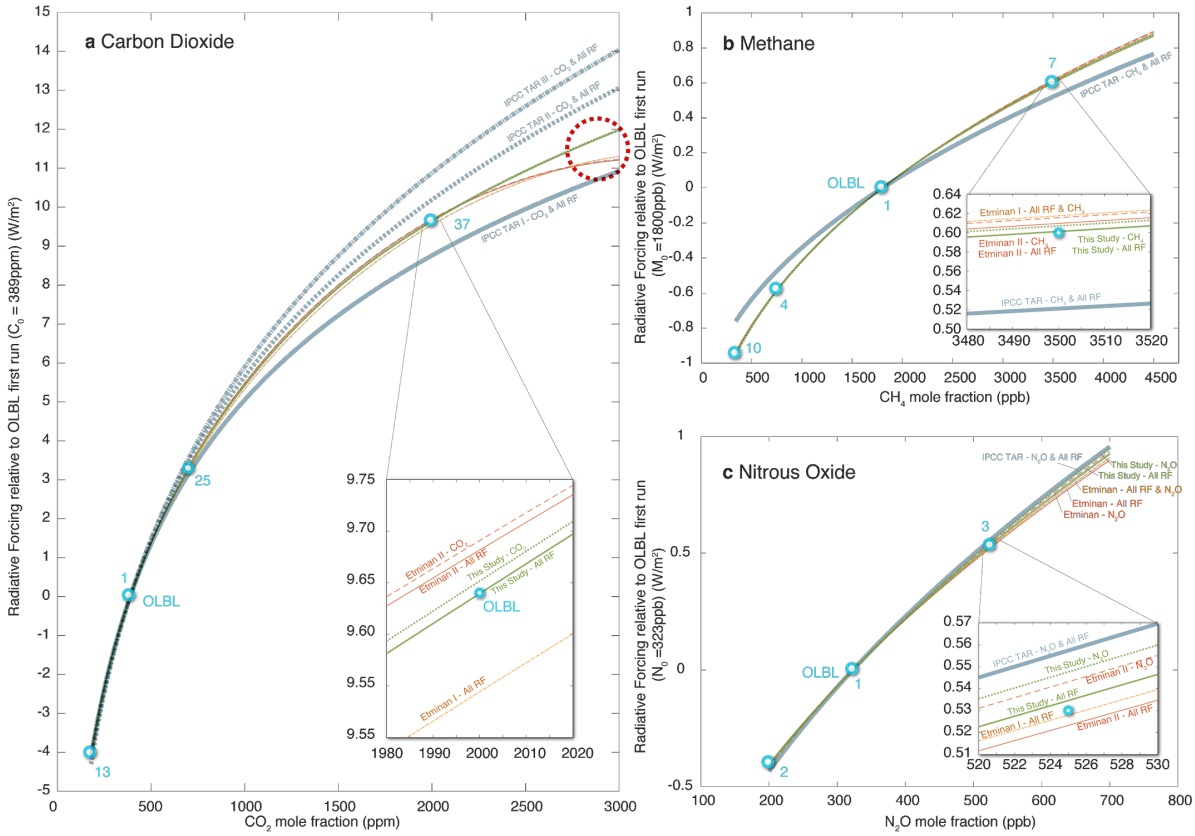


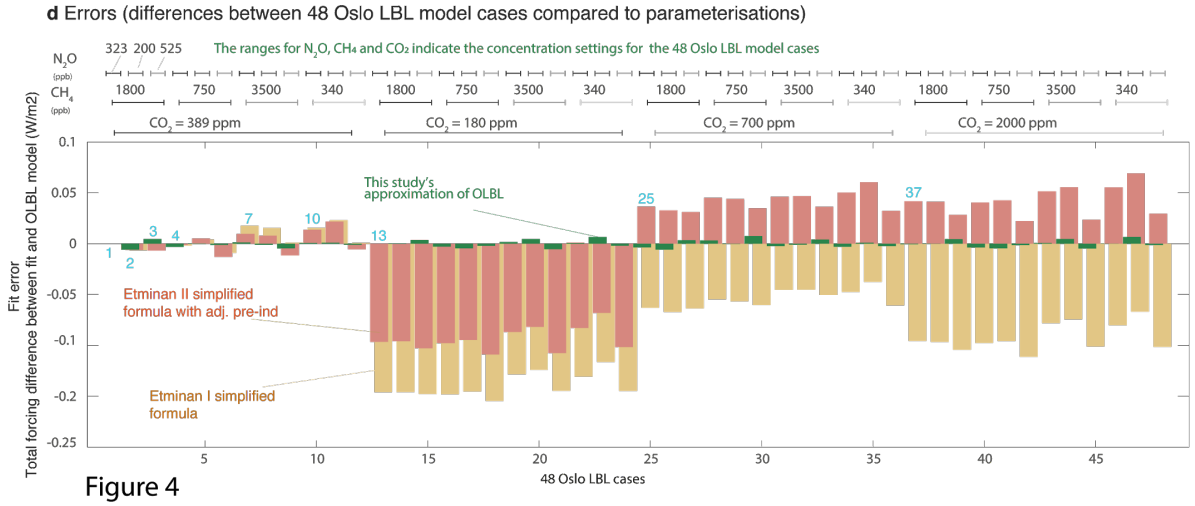


Figure 4

~

Figure 5, I don't see the need of including this figure (or at least many of the subpan- els) in the main text of this paper. There are 10 subpanels in this figure, which include lots of repetitive information illustrating the long term global trend, NH-SH differences, seasonality and their changes w.r.t. time, etc, for just CO2 under the SSP1-1.9 sce- nario. Are these all essential information for the purpose of SSP scenarios? If so, there should be some discussion on why these information are important in the text. At this point, there are almost no references to this figure (except line 507 that briefly reference to figure 5b) throughout the text. Second, many of the labels and the legend are much too small. For example, panel f shows 25 different lines, which I can't tell apart from each other at all. This is the consequence of jamming too many complicated panels into a single figure. There got to be a way that the information can be conveyed through 3-4 subpanels, if the authors have a compelling reason to show figure 5. In the next revision, please indicate at the top of the figure (not just in the caption) that it is CO2 surface mole fraction under the SSP1-1.9 scenario. Also, Make all fonts bigger

and lines thicker and darker.

*REPLY: Thank you. We share the observation that a lot of information is cramped into this "factsheet" figure. For the research community, we offer these kinds of factsheets for every gas and every scenario (see greenhousegases.science.unimelb.edu.au) and would hence like to keep the general format. Thanks to the reviewer's comment that we failed to appropriately explain the various panels in the text, we now added more explanatory text and made presentation changes to this factsheet (bigger fonts, clearer labelling, clarification of "zoom" panels f, g and h). The revised figure with the updated font size and labelling is here:*

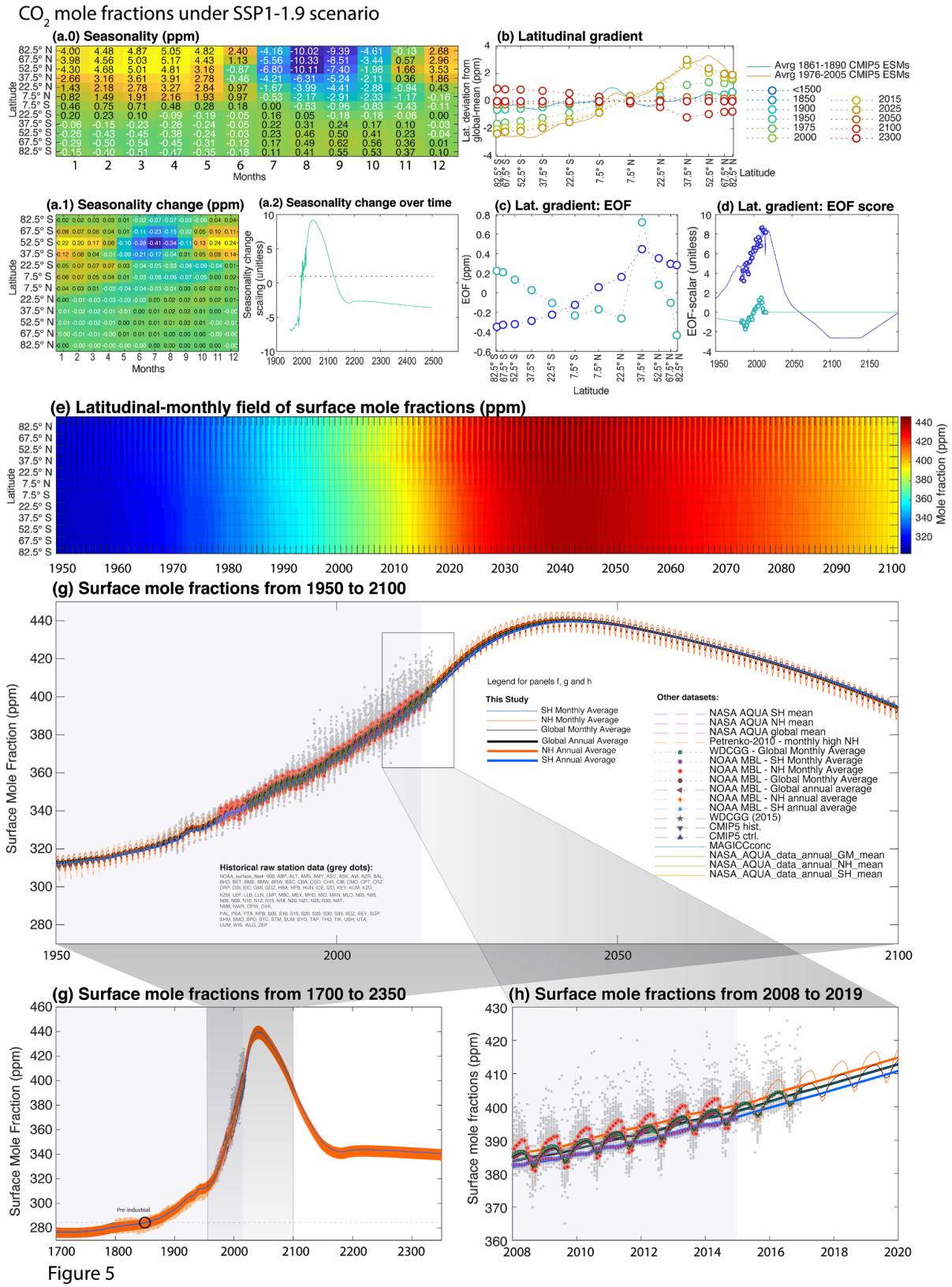


Figure 5

*We amended section 3.1 on the Carbon Dioxide, referring to all subpanels of Figure 5, so that the reader has a textual guidance.*

*The text previously read:*

*"The projected CO2 concentrations range from 393 to 1135 ppm in 2100, with the low scenario SSP1-1.9 decreasing to 350 ppm by 2150. Given the assumption of zero CO2 emissions in the lower scenarios beyond that, the lower end of the projected CO2 concentrations is not projected to decrease much further. On the upper end, under the SSP5-8.5 scenario global-average concentrations are projected to increase up to 2200 ppm by 2250 (Table 4 and Table 5). The latitudinal gradient implies a difference of annual-average northern midlatitudes to South pole concentrations of about 7 ppm. For the future, the applied projection methods result in a zero latitudinal gradient by ~2060 in the lowest SSP1-1.9 scenario (Figure 5b) because CO2 emissions revert from positive to net negative. Under the highest SSP5-8.5 scenario, the northern midlatitude to South Pole difference expands to more than 23 ppm by 2100 (not shown in plot, but viewable in online data repository at greenhousegases.science.unimelb.edu.au)."*

*And is now expanded to read:*

*"The projected CO2 concentrations range from 393 to 1135 ppm in 2100, with the low scenario SSP1-1.9 decreasing to 350 ppm by 2150 (Figure 5g). Given the assumption of zero CO2 emissions in the lower scenarios beyond that, the lower end of the projected CO2 concentrations is not projected to decrease much further. On the upper end, under the SSP5-8.5 scenario global-average concentrations are projected to increase up to 2200 ppm by 2250 (Table 4 and Table 5, and see also online "GHG factsheets" at greenhousegases.science.unimelb.edu.au). The latitudinal gradient implies a difference of annual-average northern midlatitudes to South pole concentrations of about 6 ppm in current times (Figure 5b). As future seasonality is correlated with projected NPP, the CO2 seasonality change pattern (Figure 5a.1) is scaled with the a normalized projected NPP (Figure 5a.2). Future latitudinal gradients are derived by projecting the first two principal components or EOFs, where the first (dark blue line in Figure 5c) is regressed against global emissions – with the implied future scaling factor show in Figure 5d (dark blue line). The second EOF (turquoise line in Figure 5c) is assumed constant in the future (turquoise line in Figure 5d). The applied projection methods result in a continuous projection of CO2 concentration from the observationally derived historical values, including their latitudinal gradients and seasonality (Figure 5h). By approximately 2060, a zero latitudinal gradient is projected in the lowest SSP1-1.9 scenario (Figure 5b) because $CO_2$ emissions revert from positive to net negative. Under the highest SSP5-8.5 scenario, the northern midlatitude to South Pole difference expands to more than 23 ppm by 2100 (not shown in plot, but viewable in online data repository at greenhousegases.science.unimelb.edu.au)."*

Figure 6, this is a key figure, but I would suggest to just keep the mean global, NH, SH lines with the envelopes showing the range of the various scenarios. The rest of the information are too trivial for the sake of this figure and literally unreadable, when included.

*REPLY: Thank you. We took out all the binned averages, i.e. included 12 of the shown timeseries. We consider the main importance of this figure in the three aspects (1) the zoomed-in focus on the transition between historical and future values, (2) the emerging spread between the various scenarios in the future (see SSP 2030 range on the right) and*

*(3) zoomed-in comparison with a few key alternative datasets. Hence, we hope that this version strikes a balance and brings out the key points. We also increased the font sizes. See here the revised figure.*

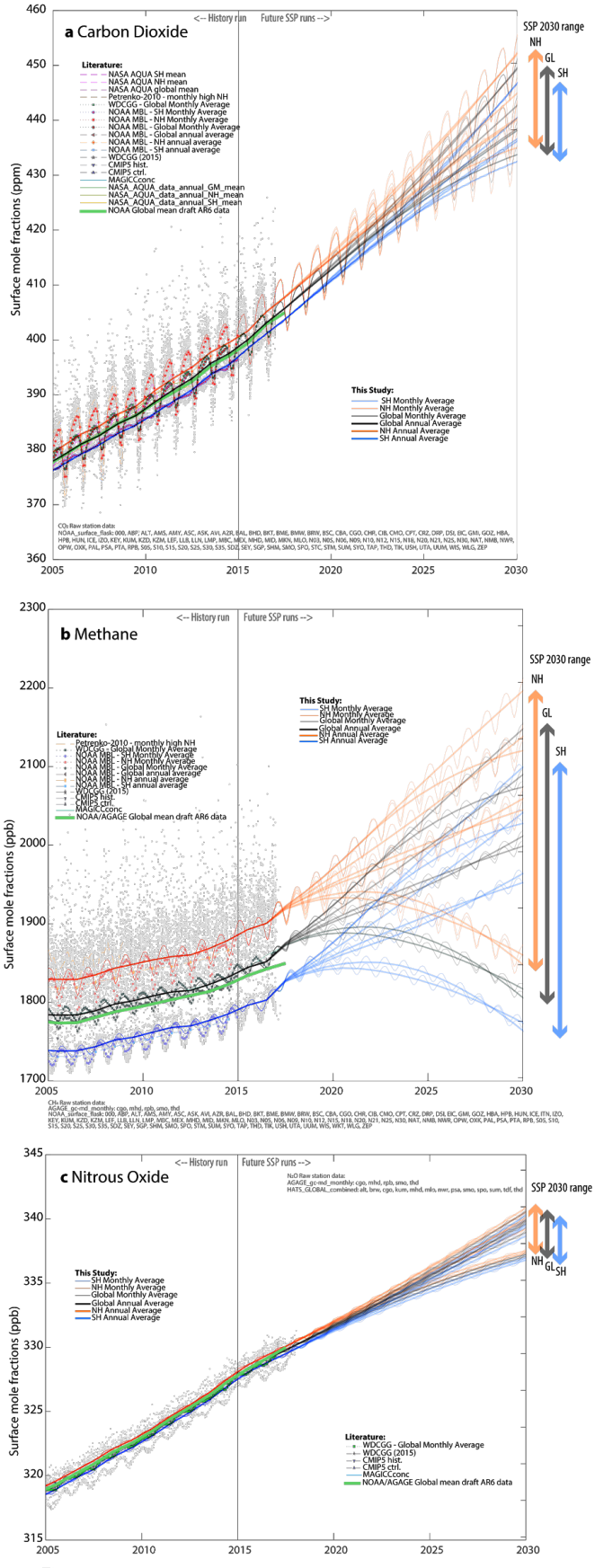
a Carbon Dioxide
<-- History run
Future SSP runs -->
Surface mole fractions (ppm)
SSP 2030 range
NH
GL
SH
Literature:
NASA AQUA SH mean
NASA AQUA NH mean
NASA AQUA global mean
Petrenko-2010 - monthly high NH
WDCGG - Global Monthly Average
NOAA MBL - SH Monthly Average
NOAA MBL - NH Monthly Average
NOAA MBL - Global Monthly Average
NOAA MBL - Global annual average
NOAA MBL - NH annual average
NOAA MBL - SH annual average
WDCGG (2015)
CMIP5 hist.
CMIP5 ctrl.
MAGICCconc
NASA_AQUA_data_annual_GM_mean
NASA_AQUA_data_annual_NH_mean
NASA_AQUA_data_annual_SH_mean
NOAA Global mean draft AR6 data
This Study:
SH Monthly Average
NH Monthly Average
Global Monthly Average
Global Annual Average
NH Annual Average
SH Annual Average
CO2 Raw station data:
NOAA_surface_flasks: 000, ABP, ALT, AMS, AMY, ASC, ASK, AVI, AZR, BAL, BHD, BKT, BME, BMW, BRW, BSC, CBA, CGO, CHR, CIB, CMO, CPT, CRZ, DRP, DSI, EIC, GMI, GOZ, HBA, HPB, HUN, ICE, IZO, KEY, KUM, KZD, KZM, LEF, LLB, LLN, LMP, MBC, MEX, MHD, MID, MKN, MLO, NAT, NMB, NWR, OPW, OXK, PAL, PSA, PTA, RPB, SMO, SOG, SPO, STM, SUM, SYO, TAP, THD, TIK, USH, UTA, UUM, WIS, WLG, ZEP
2005
2010
2015
2020
2025
2030


b Methane
<-- History run
Future SSP runs -->
Surface mole fractions (ppb)
SSP 2030 range
NH
GL
SH
This Study:
SH Monthly Average
NH Monthly Average
Global Monthly Average
Global Annual Average
NH Annual Average
SH Annual Average
Literature:
Petrenko- 2010 - monthly high NH
WDCGG - Global Monthly Average
NOAA MBL - NH Monthly Average
NOAA MBL - SH Monthly Average
NOAA MBL - Global Monthly Average
NOAA MBL - Global annual average
NOAA MBL - NH annual average
NOAA MBL - SH annual average
WDCGG (2015)
CMIP5 hist.
CMIP5 ctrl.
MAGICCconc
NOAA/AGAGE Global mean draft AR6 data
CH4 Raw station data:
2005
2010
2015
2020
2025
2030


c Nitrous Oxide
<-- History run
Future SSP runs -->
N2O Raw station data:
Surface mole fractions (ppb)
SSP 2030 range
NH
GL
SH
This Study:
SH Monthly Average
NH Monthly Average
Global Monthly Average
Global Annual Average
NH Annual Average
SH Annual Average
Literature:
WDCGG - Global Monthly Average
WDCGG (2015)
CMIP5 hist.
CMIP5 ctrl.
MAGICCconc
NOAA/AGAGE Global mean draft AR6 data
2005
2010
2015
2020
2025
2030

Figure 6

Figure 7, As in Fig. 6, many of the labels and lettering are too small, including the species labels. Also, why is there a white square area in the bottom right panel?

*REPLY: Our apologies. We are not sure. Again, this is a graphical element that only pops up after the conversion of the manuscript on the submission website. We hope that the new version corrected the problem.*

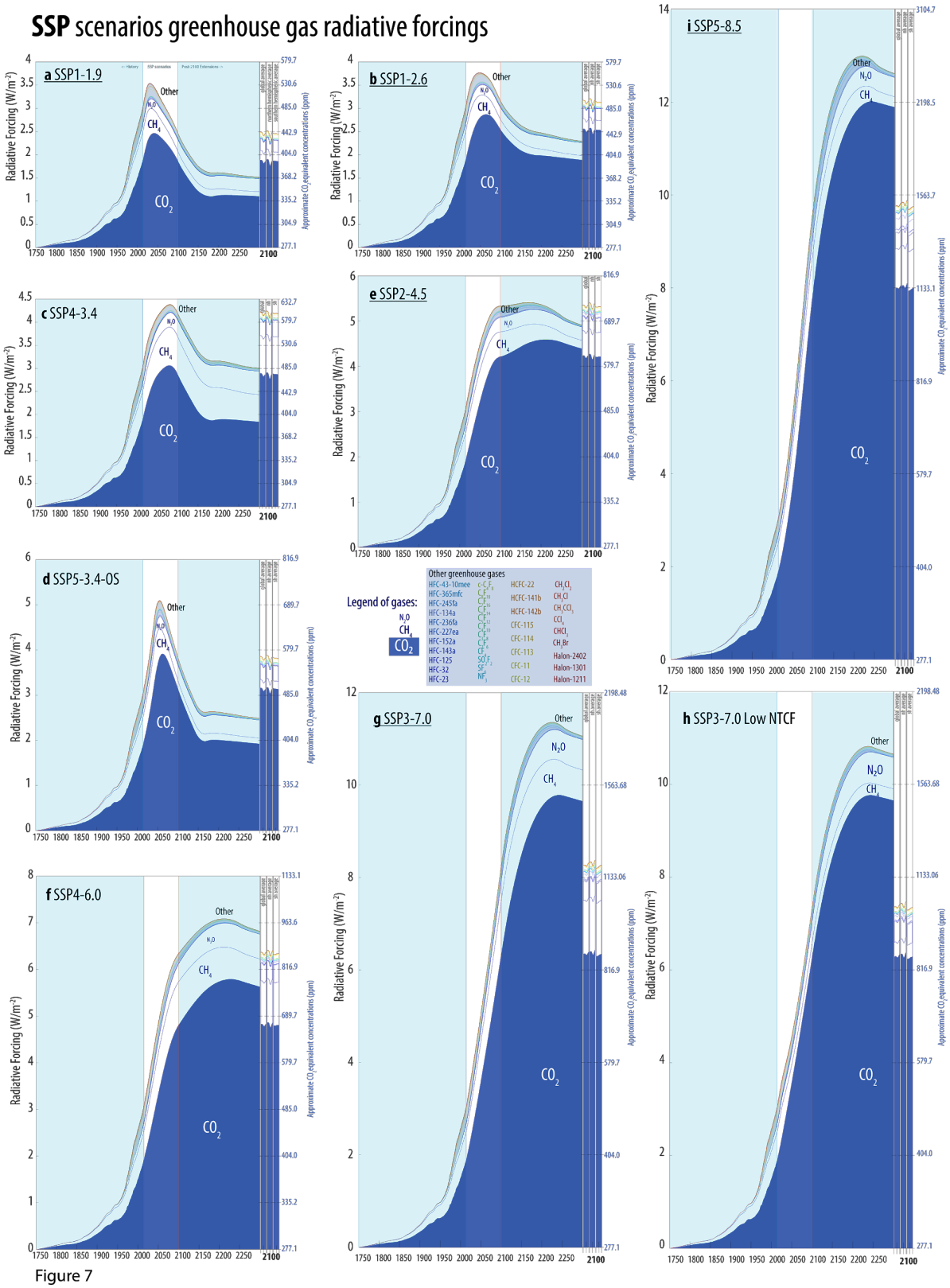


Figure 7

Most important of all, do we really need all these details on time variations of individual gas contribution to radiative forcing? In my view, a condensed bar graph showing the total radiative forcing, with stacked bar graph attribution of individual RF for all nine scenarios will

be adequate and useful. You may also consider lumping all CFCs, other ODSs, HFCs, PFCs, respectively, instead of showing individual gases that no one can tell apart.

*REPLY: We fully appreciate the reviewer's focus on simplicity. We hence made some changes to the graph that hopefully guide the quick reader's eye to the main points, i.e. that the dark blue area is the CO2 forcing, that CH4 and N2O are on top and a bunch of OTHER greenhouse gases then also contributing a small forcing. However, while introducing shading that lumps all 40 other gases together in a very simple grey stripe, we opted for keeping the underlying lines of the individual lines. It might be a slightly different philosophy of how figures shall represent data in the time of less and less paper-printouts. For the younger generation of researchers, zooming into a graph and looking at the details is an important feature that we want to support. The data richness is hence kept for the few inquisitive readers, while the vast majority readers can enjoy the main features of the plot in a zoomed-out version. I hope the reviewer will permit us to cater for both reader groups in this graph. The revised graph, with the simplified grey shaded areas for the OTHER GHGs is shown above.*

Figure 9, this is certainly a very important figure. To make the message clearer and connects better with the discussion in the text, I would suggest to use different symbols or sizes for SSP1-1.9, the four Tier 1 SSPs, and the four Tier 2 SSPs, respectively. If helpful, the authors may consider add a brief discussion on the choice of CH4/CO2 scenarios between Tier 1 and Tier 2 SSPs, or connect back to the discussion in the Introduction section on p. 4.

*REPLY: Thank you. As per the reviewer's suggestion we now created different labels for the high priority "Tier 1 + SSP1-1.9" and other illustrative marker SSPs. See the revised figure here:*

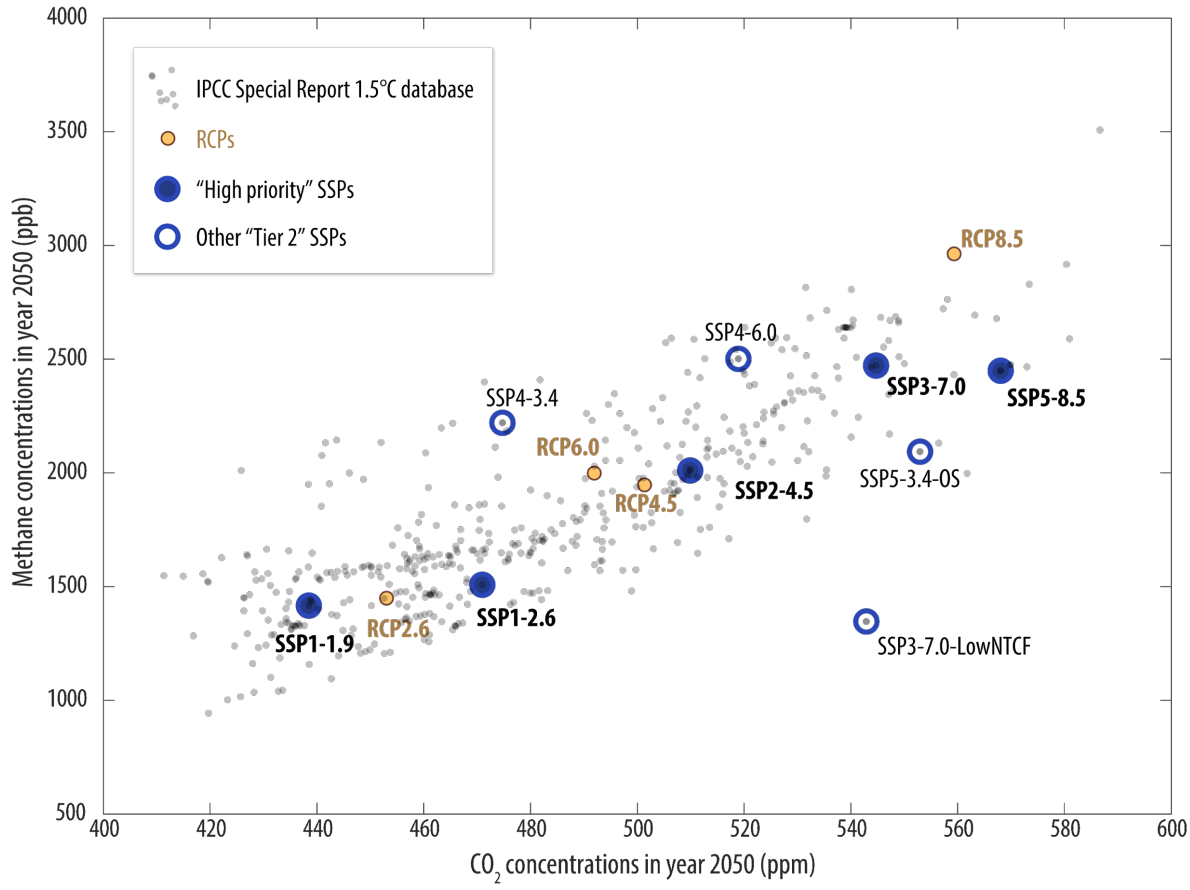


Figure 9

Figure 10: 1) Again, please make x-axis and y-axis labels bigger/darker. 2) The legends on panel a is not consistent with panel b or the rest of the figure. SH, NH, global averages are plotted as thick solid lines. 3) Are the firn measurements necessary here for the scope of this paper? I can see you need them for CO2 and CH4, but CFCs, especially that you have information from the surface networks. 4) What are the gray dots? NOAA monthly measurements from the stations? Do we need to show them here? I assume the SH, NH, global averages from this study are derived using these measurements, but you can just mention in the text how they are calculated using surface observations, without actually showing them in the figure. They make the figure extremely busy, without adding additional information. 5) The diamond symbol + dashed line for Velders et al., (2014) didn't show up in legend in panel. 6) The WMO (2014) and Velders et al (2014b) are both out of date now, which are quite visible by looking at these lines in Figure 10. Why aren't you using the WMO (2018) ODSs, which will have much better agreement with the NOAA measurements, and the results from this work.

*REPLY: We revised the figure now to provide larger labels and deleted the extra literature timeseries that were not strongly visible. The main point arises from the comparison to the Velders et al. (2014) data, which assumes a strong phaseout / no-emission scenario, where concentrations are lifetime-driven. The comparison with the actual NOAA measurements is hence informative as it shows the discrepancy, which is now documented in a number of papers for CFC-11 and other species. Apologies also for the inconsistent legend. We had*

*split the legend (which was valid for all panels) between panels a and b. For clarity, we moved the legend now below the panels. The revised figure is here:*

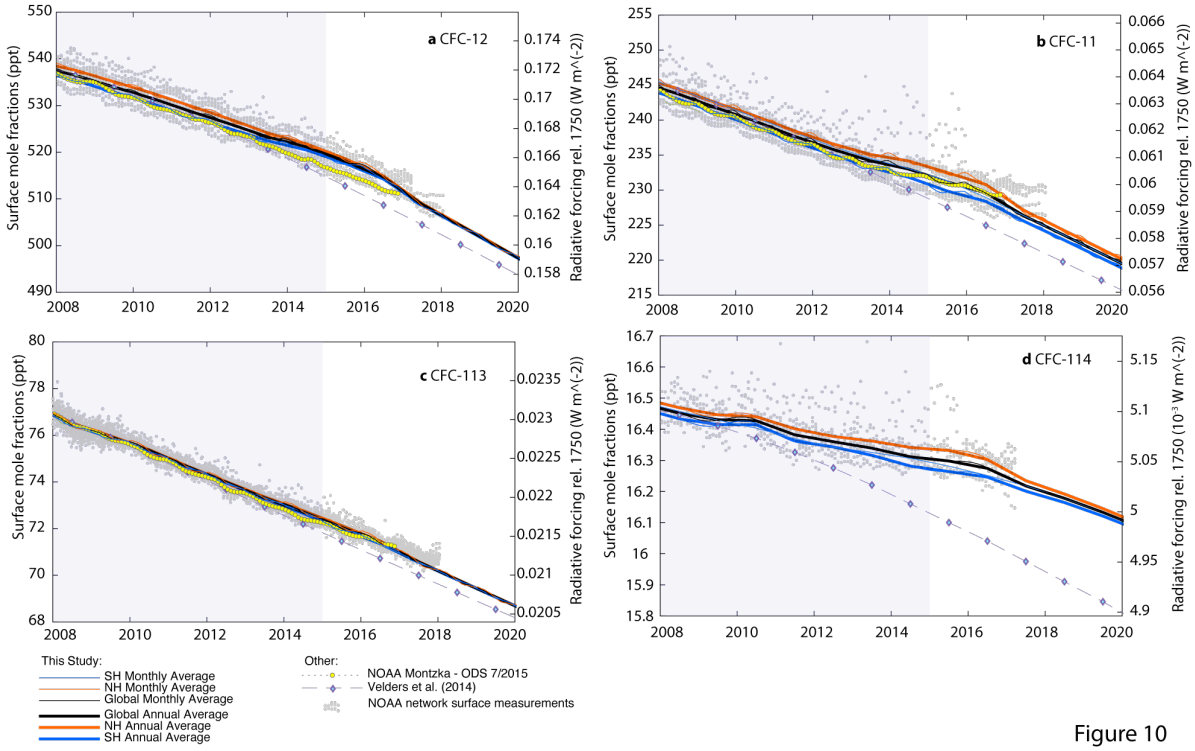


Figure 10

Figure 11, again, it would be useful to use different line styles for high priority SSPs vs. Tier 2 SSPs, which will tie better with the discussion in the text. Use bigger font size and thicker lines so that they are easy to read.

*REPLY: Following the suggestion from the reviewer, we now doubled the line-width for the high priority SSPs and increased the font size for labels and legends. The revised figure is here:*

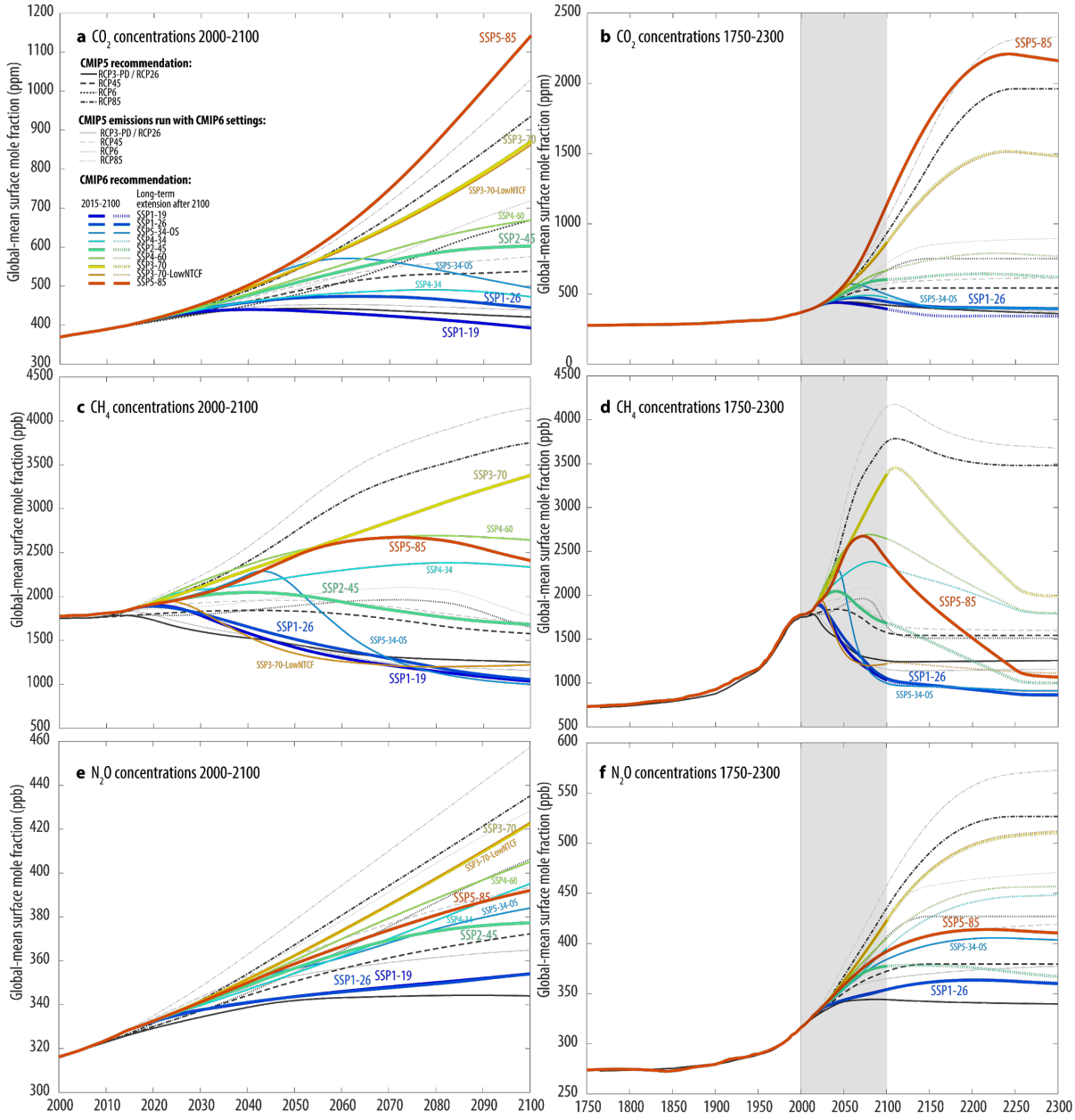


Figure 11

Figure 12, panel a, may be change y-axis title to " . . . temperature change with respect to 1750" to be consistent with panel b? panel b, y-axis, units should be meters (or cm?) not K.

*REPLY: This Figure is now deleted.*

Figure 13 caption, line 1130, change to "January". Also, the final sentence in the caption is confusing:

“In the high upper North during the MAM season, approximately 97 of the 100 control run segment differences are lower.”

Reword this sentence for clarity, and to better summarize the text from lines 801-803 on p. 29.

*REPLY: Thank you. We reworded now as suggested. The new text now reads:*

*“In the high upper North during the MAM season, the comparison with control run segment differences suggest that these ESM model results show a significant warming at the 5% level, given that only 3 to 5 of the 100 control run differences are higher.”*

---

# *REPLY TO*

# *Interactive comment on* “The SSP greenhouse gas concentrations and their extensions to 2500” *by* Malte Meinshausen et al.

**Anonymous Referee #2**

Received and published: 5 December 2019

This paper describes the distribution of greenhouse gases (and some of their impacts) as needed for the CMIP6 experiments, especially ScenarioMIP and AerChemMIP. I find the paper very thorough in its documentation, and is clearly a very useful addition to the CMIP6 papers. I have minor comments listed below, and the authors can decided whether to integrate them in the next version:

*REPLY: Thank you for your overall positive review.*

Line 50-52: I am not convinced that the SSP are more evenly spaced than 2.6-4.5-6.0-8.5. The addition of 1.9 is useful for the lower end, but 6.0 or 7.0 is basically equivalent in terms of distance.

*REPLY: Thank you. The issue is that RCP4.5 and RCP6.0 were very similar up to the middle the of century (also evident from our Figure 9 of mid-century CO2 and CH4 concentrations. As shown in Figure 9, the high-priority SSPs are generally more evenly spaced.*

Line 63-64: “it is a collective choice. . .” seems like a policy statement that I don’t feel belong to the paper.

*REPLY: Thank you. As wider relevance for the general public is often pursued as a last sentence in an abstract or the end of the conclusions, we feel it is appropriate to put the framing of a “choice” to these future scenarios. The scenarios give decision makers a set of tools to weigh various possible future options against each other. As the primary scenarios in the scientific literature, it is hence important that these SSPs are generally understood as reflecting the collective choice of society, not only as an abstract future uncertainty. In order to put the language a bit more neutral though, we deleted the term “hothouse”, and adapted the language from “collective choice” to “societal choice” so that the last sentence of the abstract reads now:*

*“The SSP concentration time series derived in this study provide a harmonized set of input assumptions for long-term climate science analysis; they also provide an indication of the wide set of futures that societal developments and policy implementations can lead to - ranging from multiple degrees of future warming on the one side or approximately 1.5C warming on the other.”*

Line 72: ESMs are driven by many more emissions than CO2

*REPLY: Thank you. We changed this section in order to provide a clearer separation between ESMs and AOGCMs. For GHGs, ESMs are normally not driven with CH4, N2O or any other non-CO2 GHG emissions – at least not in the main CMIP6 experiments to our knowledge.*

*The expanded section now reads (also due to other review comments): “The atmosphere-ocean general circulation models (AOGCMs) are physical climate models that may include biogeochemical model components, such as vegetation or some atmospheric chemistry, but they are not able to project CO2 concentrations from emissions due to an incomplete, imbalanced or non-existent carbon cycle. The climate models that have this ability to project CO2 concentrations from emissions, are often referred to as Earth System Models (ESMs) (Lawrence et al., 2016;Jones et al., 2016). These ESMs are also often run in ‘CO2-concentration driven mode’ for computational ease and to allow for an easier separation between carbon cycle feedbacks and climate responses. As of today in phase 6 of the Coupled Model Intercomparison Project (CMIP6) (Eyring et al., 2016), both AOGCMs and ESMs use concentrations from all non-CO2 greenhouse gases to perform multi-gas experiment (such as the future scenario projections) due to either missing non-CO2 gas cycles or prohibitive computational costs of including such cycles.*

Line 86: the correct reference to the description of the experiments is the GMD papers, not the es-doc site.

*REPLY: Thank you. We provide the GMD paper references and rephrased the reference to es-doc.org site now to read:*

*"… (see search.es-doc.org for a tabular overview of the experiments)."*

*This hopefully avoids the misunderstanding that the es-doc.org site is the primary reference.*

Line 111: while aerosol abundances are important in present-day and early 21st century, this becomes much less of an issue further in the 21st century

*REPLY: We agree. Nevertheless, remnant aerosol emissions, including remainder NH3 and biomass-burning aerosols, will still cause some radiative forcing differences around 2100, if the current scenarios are somewhat representative of the range. Thus, for completeness, we mention here not only GHG concentrations (the topic of this paper) but also aerosols and expand to other forcers for completeness. The sentence now reads: "*
*"Those labels are merely indicative, given that actual radiative forcing uncertainties (and differences across ESMs that implement the same concentrations, aerosol abundances, ozone fields and landuse patterns) are substantial."*

Line 133: it might be beyond the scope of this paper but it would be useful to know how much of the difference in concentrations comes from the updated model. Could the old model be run with the current emissions/harmonization?

*REPLY: Thank you. As the list of the considered GHGs expanded, we rather ran the inverse: We ran the current model also with the RCPs. The results are shown in Figure 11. It is apparent that the new model calibration leads to increased CO2, CH4 and N2O concentrations at least for the upper scenarios. We now added the following text to the end of section 4.4:*

*"When projecting future concentrations under the old RCP emission scenarios, the new calibration choice for the gas cycles of MAGICC (section 2.4) produce increased CO2, CH4 and N2O concentrations compared to the original RCP concentration timeseries, at least for the upper scenarios (Figure 11)."*

Line 188: it might be worth explaining in more details the meaning of "harmonization" and "categorization"

*REPLY: We point the reader now more explicitly to Gidden et al. 2019, where these steps are explained.*

Line 225/line 238/line 553-554: the fact that the paper is from 2015 (WMO 2014) highlights one issue that keeps coming back, that is that the emissions/concentrations of ODSs are out

of phase with the WMO recommendation. This is rather unfortunate, but also points to the fact that the system needed to create seems rather complicated/obscure and therefore limits the possibility to easily generate concentrations from other scenarios.

*REPLY: We agree. At the time when we had to pull together these scenarios and provide them to the CMIP6 community, the WMO 2018 scenarios were not available yet. Admittedly, our documentation paper (this study) is delayed.*

Line 256: “AerChemMIP”

*REPLY: Corrected.*

Line 261 (also lines 268-269): what is the justification for bringing negative emissions to 0? Don’t we have the technology assumption to keep them negative? This seems arbitrary without a justification.

*REPLY: Thank you. In response to this valid point, we now inserted a justification in the text that reads: “We did not assume permanent net-negative CO2 emissions to maintain proximity to the original scenario design and in the light of biophysical and economic limits of negative emissions, as well as potential side-effects (Fuss et al., 2018;Smith et al., 2016)”.*

Line 305: there has been a lot more work on OH concentrations since 2001 and 2011.

*REPLY: We now clarified how these two references are meant to be understood in this sentence, i.e. simply as a description of the underlying modelling skeleton, which has been calibrated (as in section 2.4.1) to the Holmes and Prather et al. studies. The new sentence now reads: “*

*“On top of this, increased CH4 emissions are modelled to affect (alongside several other reactive gas emissions like CO, NMVOC and NOx) tropospheric OH concentrations (as described for our modelling framework in Meinshausen et al., 2011a; based on Ehhalt et al., 2001)”*

Line 327: problem with reference

*REPLY: Apologies. Fixed.*

Line 376: “while we do not entertain. . .” seems very much a lost opportunity. Even if it is only partial, adding knowledge on uncertainty, especially on feedback, would be quite important to discuss and include.

*REPLY: We agree that a fully probabilistic setup is warranted in the future. However, given the main focus of this study, i.e. to provide standardized inputs (without uncertainty) for a large multi-model intercomparison exercise, it was beyond the scope of this study to entertain a probabilistic setup – for the permafrost module and for the other modules.*

Section 2.7: this section seems to be out of place since the discussion focuses on the concentrations

*REPLY: We agree that this section is not directly on concentrations. However, given that the Etminan results substantially shifted the radiative forcing of CH4, we ought to make sure that the underlying modelling framework represents this update. Without it, the projected temperature-dependent concentration projections could not have been undertaken on the basis of the latest findings. Also, we needed to develop new parameterisations for the Etminan Oslo line by line results, as the originally published parameterisations were not valid for the full range of projected concentrations (as our long-term concentrations for SSP5-8.5 exceeded 2000ppm).*

Line 584: It seems rather unfortunate that the research community only has access to a handful of those 475 scenarios. I strongly encourage the authors to identify a path towards a better integration between the two communities.

*REPLY: The IPCC Special Report 1.5C database is publicly available (with registration, see https://data.ene.iiasa.ac.at/iamc-1.5c-explorer/) and can be used for research. Also, under the leadership of Zebedee Nicholls, we are developing a close integration of MAGICC into the IIASA database so that scenarios can be amended by GHG concentration projections and also probabilistic temperature projections. Thus, the reviewer's suggestion is much appreciated, and we are working on it (with our limited resources).*

Section 4.4: it would be amazingly useful (and most likely powerful) if we had on the same graph all those scenarios, including IS92 and SRES!

*REPLY: In terms of emissions, some of us prepared such a graph for the forthcoming IPCC AR6 report. Please register as an Expert reviewer. See section 1.6 in Chapter 1. We however take the reviewer's comment as encouragement to provide more dedicated comparisons also in the concentration and temperature space in future studies.*

Line 691-692: Why is SSP5-8.5 much higher than RCP8.5?

*REPLY: The Integrated Assessment modelling teams intended to approximately match again 2100 forcing levels of 8.5 W/m2. With the specific modelling team behind the chosen illustrative marker SSP5-8.5 scenario (i.e. the REMIND group at the Potsdam Institute for Climate Impact Research) projecting comparatively lower CH4 concentrations and greater abundance and use of fossil fuels, the CO2 concentrations increased more. See also Figure*

*9 on this aspect. More detail to be found in the REMIND SSP5 papers, such as Kriegler et al, 2018 (https://doi.org/10.1016/j.gloenvcha.2016.05.015).*

Section 4.5: I am not sure I fully see the value of this section. It seems that it will be much more useful to do an evaluation of MAGICC against the CMIP6 models.

*REPLY: Section deleted. Such an evaluation is being prepared by us (many things, little time…) and there are some preliminary comparisons available in Nicholls et al., GMDD 2020 (https://www.geosci-model-dev-discuss.net/gmd-2019-375/).*

Line 799-801: based on this, it seems that the whole discussion on latitudinal and seasonal variations could be significantly reduced.

*REPLY: We would argue that while the effect is not beyond the min-max "variability range", there is nevertheless a strong reason to get the latitudinal and seasonal variations correct. After all, there are lot of process amended and introduced in ESMs that would not pass the test of causing a global or zonally averaged temperature signal beyond natural variability min-max ranges. ESMs are not performing well when it comes to estimating high polar warming. The inclusion of latitudinally and seasonally resolved GHG concentrations can therefore possibly help to address this bias.*

Line 955: "AGAGE"

*REPLY: Apologies. Corrected.*

---

## *Reply to*

# *Interactive comment on* "The SSP greenhouse gas concentrations and their extensions to 2500" *by* Malte Meinshausen et al.

**Ron Stouffer**

ronstouffer@gmail.com

Received and published: 14 October 2019

REVIEW:

A Review of “The SSP greenhouse gas concentrations and their extension to 2500” by Meinshausen et al.

General Comments

This paper is documenting the GHG concentration used in CMIP6 and therefore in AR6. It is important to publish such papers. I found the paper to be well written and informative, although the text does need cleaned up in spots as I point out below. I am not an atmospheric chemist so much of the discussion is outside my area of expertise. Given my lack of expertise, I do not think this review is very helpful to the authors.

REPLY: Many thanks for your time to look through the manuscript. Your expertise as a member of the CMIP6 panel is much appreciated.

REVIEW:

Detailed Comments

1. Lines 70 -77 – In CMIP (and the IPCC), AOGCMs are physical climate models. They may have some chemistry/vegetation/etc. incorporated into them BUT they do not close the carbon cycle and therefore need some concentration inputs. ESMs close the carbon cycle and therefore can be run with concentrations or emissions. The paper discussion confuses these things. All AOGCMs need concentrations of CO2 and potentially other GHG. Furthermore, there are concentration driven scenarios in the CMIP6 design (as noted in paper) which require concentrations. The discussion needs cleaned up.

REPLY:

Thank you. We apologise for any confusion that arose from our previous formulation. We reworded now, so that it reads:

*“The atmosphere-ocean general circulation models (AOGCMs) are physical climate models that may include biogeochemical model components, such as vegetation or some atmospheric chemistry, but they are not able to project CO2 concentrations from emissions due to an incomplete, imbalanced or non-existent carbon cycle. The climate models that have this ability to project CO2 concentrations from emissions, are often referred to as Earth System Models (ESMs) (Jones, Arora et al. 2016, Lawrence, Hurtt et al. 2016). These ESMs are also often run in ‘CO2-concentration driven mode’ for computational ease and to allow for an easier separation between carbon cycle feedbacks and climate responses. As of today in phase 6 of the Coupled Model Intercomparison Project (CMIP6) (Eyring, Bony et al. 2016), both AOGCMs and ESMs use concentrations from all non-CO2 greenhouse gases (GHGs) to perform multi-gas experiment (such as the future scenario projections) due to either missing non-CO2 gas cycles or a prohibitive computational burden.”*

2. Line 326 – Figure reference messed up.

REPLY: Thanks. Fixed.

3. Line 446, Figure 4 – In my version, the figure is hard to see. There is black text over top of other text and the figure itself, obscuring the information in the figure.

REPLY: This is a mysterious technical issue as the black text does show up normally as blue marker text in our PDF and EPS readers, but then turns odd in the automatic conversion on the journal's website. We hope that the final version won't face the same technical issue.

4. Line 731 – Text says "Check". It is important to check the data and the figure. It is something that most readers (non-atmospheric chemists like me) would understand.

REPLY: Apologies for these leftovers. Now revised as we deleted the temperature projections from this manuscript.

5. Line 735 – Text says "To Do - show this in figure. . .".

REPLY: Apologies for these leftovers. Now revised as we deleted the temperature projections from this manuscript.

6. Line 749 – five high priority – I thought there are 4 tier 1 scenarios. Type-o? If not, explain.

*REPLY: IPCC WG1 will display five SSP scenarios as their so-called 'high priority' scenarios, which are the four TIER 1 SSP scenarios that were prioritized in the CMIP6 ScenarioMIP protocol in addition to SSP1-1.9, which caters for the renewed interest in a scenario that is potentially 1.5C compliant. We adapted the text accordingly. We attempted to describe this background already earlier in the paper in lines 112ff., where it says: "These nine scenarios comprise five high-priority scenarios for the Sixth Assessment report by the IPCC report, which is the group of four "Tier 1" scenarios highlighted in ScenarioMIP (O'Neill, Tebaldi et al. 2016) in addition to the SSP1-1.9 scenario that reflects most closely a 1.5°C target under the Paris Agreement*. "

7. Line 924 – concentrations already rose to – Awkward in sentence. Change to – concentrations are 411 ppm.

*REPLY: Thanks. Adapted. It now reads "In 2019, atmospheric $CO_2$ concentrations are 411ppm."*

---

## *REPLY TO*

# *Interactive comment on* "The SSP greenhouse gas concentrations and their extensions to 2500" *by* Malte Meinshausen et al.

**Astrid Kerkweg**

a.k erkweg@fz-juelich.de

Received and published: 15 November 2019

Dear authors,

in my role as Executive editor of GMD, I would like to bring to your attention our Editorial version 1.2:

https://www.geosci-model-dev.net/12/2215/2019/

This highlights some requirements of papers published in GMD, which is also available on the GMD website in the 'Manuscript Types' section:

http://www.geoscientific-model-development.net/submission/manuscript_types.html

*REPLY: Thank you for your comments and our apologies for the lateness in getting these replies back into the open review. We appreciate the reference to the GMD manuscript types and realise that our paper is currently not appropriately categorized. It should be categorized as MODEL EXPERIMENT DESCRIPTION PAPER (and not as "development and technical paper" as it is at the moment).*

In particular, please note that for your paper, the following requirements have not been met in the Discussions paper:

- The main paper must give the model name and version number (or other unique identifier) in the title.

*REPLY: In this multi-community exercise of creating GHG concentrations for the SSP scenarios as community resources for the CMIP6 and other intercomparison exercises, it feels odd to single out one or a few models over others. Even though MAGICC7.0 was used for the step from emissions to concentrations, the SSP emission pathways were created by*

*different Integrated Assessment Models, namely IMAGE (SSP1-1.9 and SSP1-2.6), MESSAGE-GLOBIOM (SSP2-45) REMIND-MAGPIE (SSP5-3.4-over and SSP5-8.5) etc. Thus, given the community nature of these SSP concentration datasets, we would prefer keeping the title as is and free of a long list of model names.*

- "Code must be published on a persistent public archive with a unique identifier for the exact model version described in the paper or uploaded to the supplement, unless this is impossible for reasons beyond the control of authors. All papers must include a section, at the end of the paper, entitled "Code availability". Here, either instructions for obtaining the code, or the reasons why the code is not available should be clearly stated. It is preferred for the code to be uploaded as a supplement or to be made available at a data repository with an associated DOI (digital object identifier) for the exact model version described in the paper. Alternatively, for established models, there may be an existing means of access- ing the code through a particular system. In this case, there must exist a means of permanently accessing the precise model version described in the paper. In some cases, authors may prefer to put models on their own website, or to act as a point of contact for obtaining the code. Given the impermanence of websites and email addresses, this is not encouraged, and authors should consider improv- ing the availability with a more permanent arrangement. Making code available through personal websites or via email contact to the authors is not sufficient. After the paper is accepted the model archive should be updated to include a link to the GMD paper."

- Papers describing data sets designed for the support and evaluation of model simulations are within scope. These data sets may be syntheses of data which have been published elsewhere. The data sets must also be made available, and any code used to create the syntheses should also be made available.

The cited text is mainly focused on Code, however, the editorial states that the same criteria adhere to newly developed data sets. Therefore, a version number for the data set should be provided in the title of the manuscript, to enable a distinction of data sets, if in a later stages updates of the same data set are required. Regarding the data availability, permanent access to the data set as published in this article mus be ensured. Therefore, please consider to aquire a DOI for the full data set (e.g. via zenodo).

REPLY: Thank you. In line with the specifications for the MODEL EXPERIMENT DESCRIPTION PAPER, we provide a data availability section. We spend a fair amount of time to provide a user interface that is as easy as possible for all the data to be downloaded, specifically or in bulk, at greenhousegases.science.unimelb.edu.au. All our data is associated to DOI numbers and we provide those now in the revised data availability section. We hope that this is appropriate and sufficient for a MODEL EXPERIMENT DESCRIPTION PAPER where the purpose is to provide the community with a unified dataset that is used by a broad range of GCM and ESM models.

The revised data availability section now reads:
*“A supplementary data table is available with global and annual mean mole fractions. The complete dataset with latitudinally and monthly resolved data in netcdf format is available via the Earth System Grid Federation (ESGF) servers* at https://esgf-

node.llnl.gov/search/input4mips/ with *a total of 1656 files for source version 1.2.1. The license for all data is Creative Commons Attribution-ShareAlike 4.0 International License (CC BY-SA 4.0). The digital identifiers of the produced datasets, as provided by the ESGF servers are specific to the 9 SSP scenarios: (SSP5-3.4-over: 10.22033/ESGF/input4MIPs.9867; SSP5-8.5: 10.22033/ESGF/input4MIPs.9868; SSP2-4.5: 10.22033/ESGF/input4MIPs.9866; SSP4-3.4: 10.22033/ESGF/input4MIPs.9862; SSP3-7.0: 10.22033/ESGF/input4MIPs.9861; SSP3-7.0-lowNTCF: 10.22033/ESGF/input4MIPs.9824; SSP1-1.9: doi.org/10.22033/ESGF/input4MIPs.9864; SSP1-2.6: 10.22033/ESGF/input4MIPs.9865; SSP4-6.0: 10.22033/ESGF/input4MIPs.9863) Additional data formats, i.e. CSV, XLS, MATLAB .mat files of the same data are also available via http://greenhousegases.science.unimelb.edu.au. "*

Please consider to move your paper to the manuscript type "Model experiment description papers", as it might be better placed there (see third point in the above list, which comes from this manuscript type)

*REPLY: Yes, we agree that "model experiment description paper" is a better category.*

Yours,

Astrid Kerkweg

# The SSP greenhouse gas concentrations and their extensions to 2500

Malte Meinshausen[1,2,3], Zebedee Nicholls[1,2], Jared Lewis[1], Matthew J. Gidden[4,5], Elisabeth Vogel[1,2], Mandy Freund[1,6], Urs Beyerle[7], Claudia Gessner[7], Alexander Nauels[1,5], Nico Bauer[3], Josep G. Canadell[8], John S. Daniel[9], Andrew John[1,10], Paul Krummel[11], Gunnar Luderer[3], Nicolai Meinshausen[12], Stephen A. Montzka[13], Peter Rayner[2,1], Stefan Reimann[14], Steven J. Smith[15], Marten van den Berg[16], Guus J.M. Velders[17,18], Martin Vollmer[14], Hsaing Jui (Ray) Wang[19]

[1] Climate & Energy College, The University of Melbourne, Parkville, Victoria, Australia
[2] School of Earth Sciences, The University of Melbourne, Parkville, Victoria, Australia
[3] Potsdam Institute for Climate Impact Research (PIK), Potsdam, Germany
[4] IIASA Institute for Applied Systems Analysis, Laxenburg, Austria
[5] Climate Analytics, Berlin, Germany
[6] Marine and Atmospheric Research, CSIRO, Hobart, Tasmania, Australia
[7] Institute for Atmospheric and Climate Science, Swiss Federal Institute of Technology, Zurich (ETH Zurich), Switzerland
[8] Global Carbon Project, CSIRO Oceans and Atmosphere, Canberra, ACT, Australia
[9] NOAA, Earth System Research Laboratory, Chemical Sciences Division, Boulder, Colorado, USA
[10] Department of Infrastructure Engineering, The University of Melbourne, Parkville, Victoria, Australia
[11] CSIRO Oceans and Atmosphere, Aspendale, Victoria, Australia
[12] Seminar for Statistics, Swiss Federal Institute of Technology (ETH Zurich), Zurich, Switzerland.
[13] NOAA, Earth System Research Laboratory, Global Monitoring Division, Boulder, Colorado, USA
[14] Empa, Laboratory for Air Pollution/Environmental Technology, Swiss Federal Laboratories for Materials Science and Technology, Dübendorf, Switzerland
[15] Joint Global Change Research Institute, Pacific Northwest National Laboratory, College Park, MD, USA
Potsdam, Germany
[16] PBL Netherlands Environmental Assessment Agency, the Netherlands
[17] National Institute for Public Health and the Environment (RIVM), Bilthoven, Netherlands
[18] Institute for Marine and Atmospheric Research Utrecht (IMAU), Utrecht University, Utrecht, The Netherlands
[19] School of Earth and Atmospheric Sciences, Georgia Institute of Technology, Atlanta, GA 30332-0340, USA

*Correspondence to:* M. Meinshausen (malte.meinshausen@unimelb.edu.au)

**Abstract.** Anthropogenic increases of atmospheric greenhouse gas concentrations are the main driver of current and future climate change. The Integrated Assessment community has quantified anthropogenic emissions for the Shared Socioeconomic Pathways (SSP) scenarios, each of which represents a different future socio-economic projection and political environment. Here, we provide the greenhouse gas concentrations for these SSP scenarios – using the reduced complexity climate-carbon cycle model MAGICC7.0. We extend historical, observationally-based concentration data with SSP concentration projections from 2015 to 2500 for 43 greenhouse gases with monthly and latitudinal resolution. $CO_2$ concentrations by 2100 range from 393 to 1135 ppm for the lowest (SSP1-1.9) and highest (SSP5-8.5) emission scenarios respectively. We also provide the concentration extensions beyond 2100 based on assumptions in the trajectories of fossil fuels and land use change emissions, net negative emissions, and the fraction of non-$CO_2$ emissions. By 2150, $CO_2$ concentrations in the lowest emission scenario are approximately 350 ppm and approximately plateau at that level until 2500, whereas the highest fossil-fuel driven scenario projects $CO_2$ concentrations of 1737 ppm and reaches concentrations beyond 2000ppm by 2250. We estimate that the share of $CO_2$ in the total radiative forcing contribution of all considered 43 long-lived greenhouse gases increases from ~~today~~ 66% for present day to roughly 68% to 85% by the time of maximum forcing in the 21st century. For this estimation, we updated simple radiative forcing parameterisations that reflect the Oslo Line by Line model results. In comparison to the RCPs, the five main SSPs (SSP1-1.9, SSP1-2.6, SSP2-4.5, SSP3-7.0 and SSP5-8.5) are more evenly spaced ~~in terms of their expected global mean temperatures~~ and ~~,~~ extend to lower 2100 radiative forcing and temperatures ~~and sea level rise than the RCP set~~. Performing 2 pairs of 6-member historical ensembles with CESM1.2.2, we estimate the effect on surface air temperatures of applying latitudinally and seasonally resolved GHG concentrations. We find that the ensemble differences in the March-April-May (MAM) season provide a regional warming in higher northern latitudes of up to 0.4K over the historical period, latitudinally averaged of about 0.1K, which we estimate to be comparable to the upper bound (~5% level) of natural variability. In comparison to the comparatively straight line of the last 2000 years, the greenhouse gas concentrations since the onset of the industrial period and this studies' projections over the next 100 to 500 years unequivocally depict a 'hockey-stick' upwards shape. The SSP concentration time series derived in this study provide a harmonized set of input assumptions for long-term climate science analysis; they also provide an indication of the wide set of futures that societal developments and policy implementations can lead to - ranging from multiple degrees of future

warming on the one side or approximately 1.5ºC warming on the other. ~~— it is a collective choice whether the hothouse pathway is pursued or whether we manage climate damages to the SSP1-1.9 equivalent of around 1.5°C warming~~.

## 1 Introduction

The climate modelling community periodically undertakes large model intercomparison exercises with the latest and most sophisticated set of climate models, to gain a better understanding of the response of the climate system to a range of potential emission or concentration scenarios (Taylor et al., 2012;Meehl et al., 2007). The atmosphere-ocean general circulation models (AOGCMs) are physical climate models that may include biogeochemical model components, such as vegetation or some atmospheric chemistry, but they are not able to project $CO_2$ concentrations from emissions due to an incomplete, imbalanced or non-existent carbon cycle. The climate models that have this ability to project $CO_2$ concentrations from emissions, are often referred to as Earth System Models (ESMs) (Lawrence et al., 2016;Jones et al., 2016). These ESMs are also often run in '$CO_2$-concentration driven mode' for computational ease and to allow for an easier separation between carbon cycle feedbacks and climate responses. As of today in phase 6 of the Coupled Model Intercomparison Project (CMIP6) (Eyring et al., 2016), both AOGCMs and ESMs use concentrations from all non-$CO_2$ greenhouse gases to perform multi-gas experiment (such as the future scenario projections) due to either missing non-$CO_2$ gas cycles or a prohibitive computational burden.

~~The general circulation models (GCMs) that feature elements such as dynamic vegetation, coupled carbon cycles~~ (Lawrence et al., 2016;Jones et al., 2016) ~~and more sophisticated atmospheric chemistry are referred to as Earth System Models (ESMs). Most of these ESMs participating in the Sixth Model Intercomparison Phase (CMIP 6) (Eyring et al., 2016) could be driven by $CO_2$ emissions. However, many of the ESMs are driven by exogenous greenhouse gas concentrations instead of emissions for many of the scenarios (a) to allow for an easier separation between carbon cycle feedbacks and climate responses, (b) to allow for the inclusion of GCMs in the intercomparison exercrisees, and (c) to take into account non-$CO_2$ long-lived GHG gases, for which the ESM do not include gas cycles yet.~~

This study provides and describes the standardised set of greenhouse gas (GHG) concentration futures for $CO_2$, $CH_4$, $N_2O$ and 40 other minor greenhouse gases. For the historical period, this GHG concentration data for CMIP6 was provided by the companion paper Meinshausen et al. (2017). This study provides the GHG concentration data until 2100 on the basis of the emission scenarios derived from socio-economically explicit Integrated Assessment Models' (IAMs) under the SSP framework (Gidden et al., 2019). We also provide an extension of the concentration data until 2500 on the basis of simplified assumptions.

These concentrations datasets are part of the protocols for several ~~Coupled Model Intercomparison Project phase 6 (CMIP6)~~CMIP6 experiments, most notably ScenarioMIP (O'Neill et al., 2016) and AerChemMIP (Collins et al., 2017), that require concentration-driven runs (see search.es-doc.org for a full description). While greenhouse gases are arguably the most important influence of humankind on future climate in terms of radiative forcing, there is a wide range of other forcers, including anthropogenic aerosols (Hoesly et al., 2018), land-use patterns, aerosol optical properties (Stevens et al., 2017), as well as natural forcers like solar (Matthes et al., 2017) and volcanic effects (Toohey et al., 2016). These forcers are described in the companion papers and compiled in the input4mip interface to be used for the historical and future ESM experiments (Durack and Taylor, 2019), available on https://esgf-node.llnl.gov/projects/input4mips/.

Our future greenhouse gas concentration datasets from 2015 onwards are provided for a total of nine SSP scenarios. These nine scenarios comprise five high-priority scenarios for the Sixth Assessment report by the IPCC report, which is the group of four "Tier 1" scenarios highlighted in ScenarioMIP (O'Neill et al., 2016) in addition to the SSP1-1.9 scenario that reflects most closely a 1.5°C target under the Paris Agreement. Specifically, these "high priority" scenarios for IPCC AR6 are (1) the SSP1-2.6 "2°C-scenario" of the "sustainability" SSP1 socio-economic family, whose nameplate 2100 radiative forcing level is 2.6 W/m$^2$. This SSP1-2.6 scenario approximately corresponds to the previous' scenario generation Representative Concentration Pathway (RCP) 2.6. Secondly, the (2) SSP2-4.5 of the "middle of the road" socio-economic family SSP2 with a nominal 4.5W/m$^2$ radiative forcing level by 2100 - approximately corresponding to the RCP-4.5 scenario. Thirdly, (3), the SSP3-7.0 scenario is a medium-high reference scenario within the "regional rivalry" socio-economic family, while (4), the SSP5-8.5 marks the upper edge of the SSP scenario spectrum with a high reference scenario in a high fossil-fuel development world

throughout the 21st century. The additional high priority scenario that IPCC AR6 considers is SSP1-1.9 to better reflect the research regarding the Paris Agreement's 1.5°C target. It should be noted that the radiative forcing labels, such as "2.6" in the SSP1-2.6 scenario, are indicative "nameplates" only, approximating total radiative forcing levels by the end of the 21st century. Those labels are merely indicative, given that actual radiative forcing uncertainties (and differences across ESMs that implement the same concentrations, ~~and~~ aerosol abundances, ozone fields and landuse patterns) are substantial.

In addition to these five high-priority scenarios, we provide concentrations for four additional SSP scenarios, namely the three remaining "Tier 2" ScenarioMIP experiments, featuring a low reference scenario SSP4-6.0 within the socio-economic context of the an "inequality" dominated world, as well as its moderate mitigation scenario SSP4-3.4. Similarly, there is the geophysically interesting emissions "overshoot" scenario, SSP5-3.4-OS, as it initially follows the high emission SSP5-8.5 scenario until 2030 before exhibiting the steepest annual reduction rates of all SSP scenarios and the most net negative emissions by 2100. Lastly, we also consider the SSP3-7.0-LowNTCF variant of the SSP3-7.0 scenario with reduced near-term climate forcer (NTCF) emissions. Given that the SSP3-7.0 scenario is the one with the highest methane and air pollution precursor emissions, the SSP3-7.0-LowNTCF variant investigates an alternative pathway for the AerChemMIP intercomparison project (Collins et al., 2017) that exhibits very low methane, aerosol and tropospheric ozone precursor emissions - approximately in line with the lowest other SSP scenarios for those species like SSP1-1.9 and SSP1-2.6. Note that the NTCF nomenclature is equivalent to the term Short-Lived Climate Forcer, SLCF, which is now more commonly used by the research community and IPCC context.

The presented historical global-mean and hemispheric-mean surface mole fractions in this study transition smoothly from the end of the historical dataset (Meinshausen et al., 2017), 2014, into the start of the projections, 2015. Also, the latitudinal gradient and seasonality, and their temporal evolution, are consistent with the historical dataset - which in all cases are tied directly to past measurements. We used a reduced complexity carbon-cycle model, MAGICC (Meinshausen et al., 2011c;Meinshausen et al., 2011a), to produce global-mean future greenhouse gas concentration time series for each of the considered SSPs. The same model, albeit an earlier version, was also previously used to provide the RCP greenhouse gas concentrations projections (Meinshausen et al., 2011b). The MAGICC version used for this study (version 7.0) is calibrated to closely represent C4MIP carbon cycle responses, includes a permafrost

module (Schneider von Deimling et al., 2012) and updated radiative forcing and non-$CO_2$ gas cycle parameterisations (in particular for $CH_4$ and $N_2O$) that represent recent literature findings (Prather et al., 2012; Holmes et al., 2013). The calibrated carbon cycle of MAGICC has previously been shown to reflect well the CMIP5 ESM response range (Friedlingstein et al., 2014). Given the nearly two-year time difference between the completion of historical and future greenhouse gas concentrations, we also updated the historical observational datasets to reflect observations until early 2018 for $CO_2$, $CH_4$ and $N_2O$, as well as most other gases considered here.

This study first describes the methods with separate parts for the updated observational data until 2018 (Section 2.1), the emission input data from the IAM scenarios and the input preparation steps undertaken (2.2), the extensions of the emissions and concentrations beyond 2100 (2.3) the MAGICC model setup (2.4), and the projections of latitudinal gradients (2.5) and seasonality (2.6). We also provide a new simplified formula to reflect the Oslo Line By Line model (OLBL) radiative forcing results (Etminan et al., 2016) in order to provide the radiative forcing aggregation of the output (2.7) and discuss additional methodological steps (2.8). We then show the results and compare these to other recent observational datasets (Section 3 "Results"). A discussion section follows (Section 4 "Discussion"), which includes a closer look at the two most dominant GHG forcers $CO_2$ and $CH_4$ and their correlation (4.1), a discussion on the most recent GHG concentration developments (4.2) and the comparison with RCPs concentrations (4.4) as well as temperatures and sea level rise projections (1.1~~4.5~~). We describe the limitations of the dataset (5), which includes issues like the integration of observational and modelled future data, missing uncertainty estimates, potential biases in future seasonality and latitudinal gradients, and a lack of reference scenarios for Montreal-controlled substances. Section 6 concludes.

## 2 Methods

As for the historical concentrations, we provide 43 greenhouse gases future concentration projections, namely $CO_2$, $CH_4$, $N_2O$, 17 ozone depleting substances, namely CFC-11, CFC-12, CFC-113, CFC-114, CFC-115, HCFC-22, HCFC-141b, HCFC-142b, $CH_3CCl_3$, $CCl_4$, $CH_3Cl$, $CH_2Cl_2$, $CHCl_3$, $CH_3Br$, Halon-1211, Halon-1301, Halon-2402, and 23 other fluorinated compounds, namely 11 HFCs (HFC-134a, HFC-23, HFC-32, HFC-125, HFC-143a, HFC-152a, HFC-227ea, HFC-236fa, HFC-245fa, HFC-365mfc,

HFC-43-10mee), $NF_3$, $SF_6$, $SO_2F_2$, and 9 PFCs ($CF_4$, $C_2F_6$, $C_3F_8$, $C_4F_{10}$, $C_5F_{12}$, $C_6F_{14}$, $C_7F_{16}$, $C_8F_{18}$, and c-$C_4F_8$). Our projections refer to atmospheric dry air mole fractions as does the historical data presented in Meinshausen et al. (2017), even though the projections are sometimes loosely referred to as 'concentrations'. For $CO_2$, the usual unit is parts per million (ppm), for $CH_4$ and $N_2O$, the usual unit is parts per billion (ppb) and other gases are usually denoted in parts per trillion (ppt).

### 2.1 Updated observational data

The historical concentrations (until the end of 2014) were derived from various observational datasets of greenhouse gas concentrations, or literature studies in the case of some of greenhouse gases with lower ~~mixing ratios~~concentrations. The observational data was binned by latitudinal and longitudinal boxes, averaged for monthly values and complemented by interpolations. The historical timeseries for every greenhouse gas were separated into three elements as part of the spatio-temporal binning: i) latitudinal gradient, ii) seasonality pattern and iii) global mean. This separation then permitted the use of longer observational timeseries, such as the high latitudinal $CH_4$ firn data – implicitly correcting for the high latitude differences to the global mean that one would expect. Interpolations, regressed latitudinal gradients and seasonality patterns were employed to derive the historical dataset, but no gas cycle models.

With additional observational data being available for 2015, 2016 and 2017, the previously used observational datasources from the AGAGE and NOAA networks (Dlugokencky, 2015a, b;Prinn et al., 2018), including multiple NOAA/ESRL/GMD flask measurements, were updated and used to determine the initial years of the future concentration timeseries. The result of this is that – depending on the gases - the same concentrations are used across all nine SSPs in the initial years (Table 1~~Table 1~~). As outlined below, we employed MAGICC7.0 and its calibrated gas cycles to produce concentration time series from SSP emissions beyond the observationally based period.

### 2.2 Emission data and their harmonisation

For the emission driven MAGICC7 runs that produce the future global-mean greenhouse gas timeseries, we use the SSP emission data for $CO_2$, $CH_4$ and $N_2O$, HFCs, PFCs and $SF_6$ which is available from the SSP database at IIASA (https://tntcat.iiasa.ac.at/SspDb). This emission data has already been subject to several categorisation and harmonisation steps to obtain regionally consistent (in case of $CO_2$ and $CH_4$)

and sectorally resolved data (for more details, see Gidden et al., 2019). We complemented those harmonisation steps to consider the following species in the five RCP regions (OECD90, REF (Economies in Transition), LAM (Latin America), MAF (Middle East and Northern Africa) and ASIA): $CO_2$, $CH_4$ and $N_2O$ in addition to black carbon (BC), carbon monoxide (CO), ammonium ($NH_3$), non-$CH_4$ volatile organic compounds (NMVOC), nitrates (NOx), organic carbon (~~CO~~OC) and sulphate aerosol (SOx). For those 10 species, we also distinguished between fossil & industrial sources and land-use related sources.

Regional landuse $CO_2$ emissions are not provided in the SSP database (Gidden et al., 2019), so we downscaled to the RCP regions based on historical regional emission shares in the year 2015. Given landuse $CO_2$ emissions can be negative in some SSP scenarios, a simple scaling approach in the regional harmonisation would yield unrealistic results (i.e. regions with low or negative current net landuse emissions, like the OECD, would end up with positive emissions and the other world regions would be strongly negative in the future. Instead, we applied a normalisation that assumes a negative 1.5 GtC base level against which historical regional emission shares are continued into the future, scaled with global emissions.

Mathematically, the constant regional scaling factor is hence applied to the offset emission level, so that the future regional emissions $E_r(y)$ in year y are:

$$E_r(y) = E_g(2015) \times s_{2015} + \Big(E_g(y) - E_g(2015)\Big) \times r$$

where

$$r = \frac{E_r(2015) + 1.5}{\sum_{r=1}^{n}(E_r(2015) + 1.5)}$$

With r being the regional share of emissions relative to that 1.5GtC offset level, s being the regional share of emissions in 2015 relative to zero, i.e. $s_{2015} = E_r(2015)/E_g(2015)$, $E_r(y)$ being the regional emissions in year y and $E_g(y)$ being the global emissions, i.e. the sum of the n regional emissions. Specifically, the factors $s_{2015}$ and r for were the following for the regions Asia, Latin America, Middle East and Africa, OECD-90 and Economies in Transition: 0.483, 0.282, 0.189, 0.043, 0.003, for $s_{2015}$ and 0.232 0.209, 0.199, 0.182, 0.178 for r, respectively. This choice has little effect because the regional split up of $CO_2$ emissions only marginally and indirectly affects the latitudinal concentrations in our chosen

method. A very small difference arises for different regional landuse $CO_2$ emission assumptions because MAGICC7 scales albedo effects with landuse $CO_2$ emissions and these albedo effects impact temperatures and in turn the carbon cycle again.

Landuse related $CH_4$ and fossil & industrial $CO_2$ and $CH_4$ emissions were already harmonised with historical emissions and also regionally available (Gidden et al., 2019;Gidden et al., 2018). $N_2O$ emissions were only available as global total from the SSP database based on PRIMAP (Gütschow et al., 2016), which is why we assume constant regional and sectoral emission shares. This assumption does not have a bearing on final global concentrations.

For the emissions of fluorinated gases, that are listed in the Kyoto Protocol and considered here (PFCs, HFCs and $SF_6$), namely $C_2F_6$, $CF_4$, HFC-125, HFC-134a, HFC-143a, HFC-227ea, HFC-23, HFC-245fa, HFC-43-10mee, and $SF_6$, MAGICC7 takes the global and aggregated SSP emissions of the gas baskets as inputs, as provided by the IAM modellers using constant emission shares based on a future gas-specific scenario by Guus Velders (Velders et al., 2015) and described in Gidden et al. (2019). The basket of PFCs, HFCs and $SF_6$ is reported in the SSP database at IIASA (https://tntcat.iiasa.ac.at/SspDb/). Some few data points were corrected in consultation with the respective IAM modelling teams, namely the SSP1-1.9 emission level in 2100 for $CF_4$ and $C_2F_6$, for which we assumed the rate of decline prolonged from the 2080 to 2090 to the 2090 to 2100 period. HFC-32 emissions were complemented from a Kigali-Agreement consistent scenario, which has also been derived from the scenarios by Velders et al. (2015). Those scenarios were published until 2050 and we use in addition an extension up to 2100 by proportional downscaling of the GWP-weighted HFC basket – using SSP GDP and population data with an assumption of constant GDP and population after 2100.

The ozone depleting substances controlled under the Montreal Protocol, namely CFC-11, CFC-12, CFC-113, CFC-114, CFC-115, HCFC-22, HCFC-141b, HCFC-142b, $CH_3Br$, $CH_3Cl$, $CH_3CCl_3$, $CCl_4$, Halon-1202, Halon-1211, Halon-1301, Halon-2402 are here assumed to follow the WMO 2014 scenario (WMO, 2014) from 1951 to 2099, as presented in detail in Velders and Daniel (2014a). For times before 1951 and after 2099, the previous WMO A1 Baseline emission scenario from year 2006 (WMO, 2006) is assumed which is near-zero and close to the respective WMO 2014 values in 1951 and 2099.

Harmonized emissions of aerosol and ozone precursor species are also available for the SSP scenarios (Hoesly et al., 2018), but not discussed in this paper. These non-GHG emissions are used here as part of the complete scenario specification needed to produce future temperature and GHG concentration pathways.

### 2.3 Extension of emissions and concentrations beyond 2100

In 2011, the RCPs were extended beyond 2100 to provide the basis for longer-term scenario studies (Meinshausen et al., 2011b), then called 'Extended Concentration Pathways' (ECPs). Studying this longer-term behaviour of the climate system is of interest for quantities that exhibit a strong long-term commitment or non-linear behaviour (e.g. sea-level rise, ice sheet dynamics). The RCP concentration extensions were – for some gases and scenarios – based on pragmatic extensions of emissions, like an RCP8.5 $CO_2$ emission stabilisation from 2100 to 2150 with a subsequent ramp-down until 2250. For other RCPs, concentrations were held constant and the inverse $CO_2$ emissions exhibited a near-exponential decline.

Here, we present the extensions beyond 2100 of the ScenarioMIP and AerChemMIP SSPs (although we do not use a new acronym like ECPs at the time of the RCPs). The final choices differ, in some respects, from the initial sketch of these extensions that was offered in the ScenarioMIP overview paper (O'Neill et al., 2016). As described below, the collaborative exercise by the IAM modellers and MAGICC team updated the original SSP extension design. In summary, the extension principles are:

1) From 2100 onwards, net negative fossil $CO_2$ emissions are brought back to zero during the 22nd century, while positive fossil $CO_2$ emissions are ramped down to zero by 2250.
2) Land use $CO_2$ emissions are brought back to zero by 2150.
3) Non-$CO_2$ fossil greenhouse gas emissions are ramped down to zero by 2250.
4) Land use-related non-$CO_2$ emissions are held constant at 2100 levels.

In the initial ScenarioMIP design (O'Neill et al., 2016), fossil $CO_2$ emissions for SSP5-3.4-OS and SSP1-2.6 are negative at 2100 levels until 2140 and gradually increase to zero until 2190 and 2185, respectively (**Figure 2**~~**Figure 2**~~, panel a). We did not assume permanent net-negative $CO_2$ emissions to maintain

proximity to the original scenario design and in the light of biophysical and economic limits of negative emissions, as well as potential side-effects (Fuss et al., 2018;Smith et al., 2016). For all scenarios with net negative fossil fuel extensions, we implemented extensions assuming constant emissions until 2140 (as suggested), but reaching zero emissions in 2190. The only exception is the SSP5-3.4-OS scenario, which was ramped back to zero by a slightly earlier date (2170) so that fossil and landuse emissions (in combination with MAGICC7.0's default setting – see section 2.4) met the design criteria of an approximate merge with SSP1-2.6 concentrations in the longer-term, i.e. after 2150.

In the initial ScenarioMIP extension sketch for SSP5-8.5, total $CO_2$ emissions were envisaged to be "less than 10 GtC/yr" by 2250 **Figure 2**~~**Figure 2**~~, panel c). Having considered multiple options, we opted for a straight ramp down of fossil $CO_2$ emissions to zero by 2250 due to its simplicity. Landuse $CO_2$ emissions for SSP1-2.6 in the initial ScenarioMIP design were held constant at 2100 levels indefinitely. SSP5-3.4-OS levels were designed to reach the same net negative landuse $CO_2$ levels by 2120 (**Figure 2**~~**Figure 2**~~, panel b). However, the extensions presented here assume that all landuse $CO_2$ emissions linearly phase-out between 2100 and 2150, as continuing negative landuse $CO_2$ emissions are inconsistent with fixed 2100 landuse and land cover patterns. In the original scenario design suggestion by O'Neill et. al, all non-$CO_2$ greenhouse gas emissions were kept constant at 2100 levels. However, the final extensions presented here assume differentiated extension rules by sector. Specifically, we assumed a linear phase-out of all fossil and industrial non-$CO_2$ emissions by 2250 (incl. aerosols etc) (see e.g. **Figure 2**~~**Figure 2**~~, panel c). Similarly, synthetic industrial gases were assumed to be phased out by 2250 instead of assuming constant emissions (panel g, h). For landuse-related non-$CO_2$ emissions, the assumption has been maintained that 2100 emission levels are held constant. That assumption seemed approximately consistent with constant landuse and land cover patterns as food production activities would continue to produce certain levels of $N_2O$ and $CH_4$ emissions (panel d). In comparison to a uniform approach of holding all emissions constant at 2100 levels, the chosen differentiation to phase out fossil and industrial related emissions over time while holding land-use related emissions constant seemed more consistent with plausible futures.

### 2.4 Projecting global-mean concentrations with the MAGICC climate model

For projecting the SSP greenhouse gas concentrations, we updated several gas cycles and also used MAGICC's permafrost module, which was not switched on when projecting the RCP concentrations. The sections below describe these updates.

#### 2.4.1 Methane cycle

The methane ($CH_4$) cycle in MAGICC projects $CH_4$ concentrations based on anthropogenic $CH_4$ emissions as an input. Internally, MAGICC derives natural $CH_4$ emissions by closing the $CH_4$ budget over a user-defined historical period (here assumed 1994 to 2004, previously 1966 to 1976). The atmospheric $CH_4$ lifetime as modelled in MAGICC changes over time both because of projected changes in tropospheric OH concentrations and an increased stratospheric Brewer-Dobson circulation under increased climate change (Meinshausen et al., 2011a). On top of this, increased $CH_4$ emissions are modelled to affect (alongside several other reactive gas emissions like CO, NMVOC and NOx) tropospheric OH concentrations (as described for our modelling framework in Meinshausen et al., 2011a; based on Ehhalt et al., 2001). Thus, there is a feedback loop where increased $CH_4$ emissions lead to decreased OH-related $CH_4$ sinks and in turn longer $CH_4$ lifetimes and longer lifetimes of other GHGs, such as HCFCs and HFCs. The increased Brewer-Dobson circulation, on the other hand, leads to stronger $CH_4$ removals, lowering the overall lifetime. As a net effect, $CH_4$ lifetimes tend to be shorter in the lower emission scenarios and longer in the higher emission scenarios, such as RCP8.5.

In this study, we calibrate nine of MAGICC's $CH_4$ cycle parameters (see its description and parameter denotations in Appendix A2.1 of Meinshausen et al. (2011c)) to the modelled $CH_4$ projections by Holmes et al. (2013). They included, like MAGICC, the temperature sensitivity of $CH_4$'s OH-related lifetime, thereby updating results of Prather et al. (2012). These newly calibrated parameters are (a) the initial $CH_4$ lifetime $\tau'_{CH4,tropos}$ (9.95 yrs, updated from 9.6 yrs), (b) the temperature-sensitivity of $CH_4$'s OH-related lifetime $S_{\tau CH4}$ (0.07 $K^{-1}$, updated from 0.058 $K^{-1}$), (c) a scaling factor on the sensitivity of $CH_4$'s lifetime to OH-changes $S^{OH}_{scale}$(0.725, formerly 1), which is newly introduced and applies to all $S^{OH}_{x}$ factors shown in equation A30 in Meinshausen (2011c), (d) the unscaled sensitivity of OH to $CH_4$ concentration changes $S^{OH}_{CH_4}$ (-0.5377, updated from the unscaled -0.32), noting that this update largely offsets the effect of the

newly introduced scaling factor $S_{scale}^{OH}$, (e) the other sensitivities of tropospheric OH to changes in $NO_x$, CO, and VOC, namely $S_{NO_x}^{OH}$, $S_{CO}^{OH}$, $S_{VOC}^{OH}$ (updated to 9.3376e-3, -1.13e-4, and -3.142e-4 from 4.2e-3, -1.05e-4, and -3.15e-4, respectively). Also, we updated the partial soil related lifetime of $CH_4$ (150 years rather than 160 years), following ~~to~~ Prather et al. (2012).

The net effect of the newly calibrated MAGICC is that Holmes et al. (2013) $CH_4$ projections are closely matched across the range of RCPs (Supplementary Figure 1, left column). Both OH-related and total $CH_4$ lifetimes exhibit similar changes over time as in Holmes et al. (Supplementary Figure 1~~Error! Reference source not found.~~, middle columns), with the slight upward offset explained by our historical budgeting approach deducting somewhat lower natural $CH_4$ emissions (which MAGICC assumes constant over time) (Supplementary Figure 1, right column).

### 2.4.2 Nitrous oxide projections

Prather et al. (2012) suggested that the RCP projections for $N_2O$ concentrations performed with MAGICC6 were somewhat too low for the lower RCP2.6 scenario and slightly too high for the higher RCP8.5 scenario (although within their uncertainty ranges). Here, we use their model to back out natural emission assumptions and lifetimes to allow a multi-variable calibration of MAGICC7 to the median of the RCP $N_2O$ concentration range suggested and these other variables by Prather et al. (2012) (Supplementary Figure 2).

To set up this calibration, we complement RCP emission pathways by historical $N_2O$ emissions from PRIMAP-hist (Gütschow et al., 2016). We also used observed $N_2O$ concentrations until 2014 (Meinshausen et al., 2017) to complement the future Prather et al. concentrations. The natural $N_2O$ emission levels are calibrated (as part of the overall calibration that optimised lifetimes, budgeting periods and lifetime sensitivities) with a budgeting approach over the 10 years prior to 1991, resulting in a slightly lower assumed natural $N_2O$ emission level of 8.013 MtN-$N_2O$ compared to Prather et al (9.1 MtN-$N_2O$) and AR5 (11.0 MtN-$N_2O$). Nonetheless, the total natural and anthropogenic emissions are similar for present-day conditions, because Prather et al. assumes lower anthropogenic emissions (6.5 MtN-$N_2O$) compared to the RCP pathways, which assume in average 7.9 MtN-$N_2O$. Apart from the budgeting period, MAGICC7's $N_2O$ gas cycle has three further $N_2O$ parameters, which we calibrate to the Prather et al.

results. Those are (a) the initial $N_2O$ lifetime $\tau^0_{N2O}$ (updated from 123 years to 139 years), the sensitivity coefficient $S_{\tau_{N2O}}$ which scales the $N_2O$ lifetime with the factor $\left(\frac{C^t_{N2O}}{C^0_{N2O}}\right)^{S_{\tau_{N2O}}}$, where $C^t_{N2O}$ is the current atmospheric burden at time t, and $C^0_{N2O}$ the pre-industrial burden ($S_{\tau_{N2O}}$ updated from -0.05 to -0.04). Lastly, we calibrated the sensitivity of the stratospheric lifetime, with which $N_2O$'s partial stratospheric lifetime is adjusted in response to a change in the Brewer-Dobson circulation (0.04 percent change of partial lifetime per percent change of meridional flux).

### 2.4.3 Additional gas cycles

We extended the number of fluorinated gases to cover the full range of 43 greenhouse gases in MAGICC (i.e. including HFCs) from 12 to 23 and the number of ozone depleting substances from 16 to 18. Specifically, the newly modelled fluorinated species are perfluorocarbons $C_3F_8$, $C_4F_{10}$, $C_5F_{12}$, $C_7F_{16}$, $C_8F_{18}$, $CC_4F_8$, hydrofluorocarbons HFC-152a, HFC-236fa, HFC-365mfc, as well as $NF_3$, and $SO_2F_2$. The newly modelled ozone depleting substances are methylene chloride $CH_2Cl_2$, with a very short lifetime of 0.4 years, and methyl chloride $CH_3Cl$, with a lifetime of around one year (for lifetimes, see Table 8.A.1 of IPCC AR5 WG1 Chapter 8 (Myhre et al., 2014)). We scale the partial stratospheric lifetime (HFC-152a, 39 years; HFC-236fa, 1800 years; HFC-365mfc, 125 years; $NF_3$, 740 years; and $SO_2F_2$ with 630 years – taken from Table 1-3 in WMO (2014)) with a change of the Brewer Dobson circulation strength. The Brewer-Dobson circulation is assumed to increase 15% per degree of warming beyond 1980, derived from Butchart and Scaife's finding of an approximately 3% increase per decade (Butchart and Scaife, 2001) and assuming a 0.2ºC warming per decade (Meinshausen et al., 2011a). Calibrating our gas-cycle models to the results by Holmes et al. (2013), it seemed however that our Brewer-Dobson circulation speed-up shortened the longer-term lifetimes in higher-warming scenarios substantially more than predicted by the results of Holmes et al. (2013). Assuming no change in the height-age distribution of the air parcels that travel through the stratosphere, the speed-up of this meridional circulation could 1:1 lower stratospheric lifetimes. However, assuming shorter residence times could offset some of the effect. We proceeded with a pragmatic approach and calibrated an effectiveness/scaling factor of 0.3 to match methane concentration projections by Holmes et al. (2013). That means that every 1% increase in the Brewer-Dobson circulation, the partial stratospheric lifetimes are reduced by 0.3%. However, we acknowledge that this effectiveness factor possibly summarizes multiple underlying differences between

un-scaled MAGICC results and the Holmes et al. (2013) projections that are unrelated to the Brewer-Dobson circulation.

~~For every 1% increase in the Brewer-Dobson circulation, the partial stratospheric lifetimes are reduced by 0.3%~~

~~(2012).~~ (2001;Prather et al., 2012)~~The Brewer-Dobson circulation is assumed to increase 15% per degree of warming beyond 1980 levels(Butchart and Scaife, 2001;Meinshausen et al., 2011a).~~ For the partial lifetimes related to the (changing) tropospheric OH sink, we assume a scaling of the lifetimes with relative changes over time of the OH- and temperature dependent methane lifetime. ~~For the partial lifetimes related to the tropospheric OH sink, we assume a scaling with the OH abundance (which is largely driven by $CH_4$, VOCs, CO and NOx – see above)~~.

### 2.4.4 Permafrost feedbacks

Earth system feedbacks from permafrost melting and its associated $CO_2$ and $CH_4$ releases were underrepresented in CMIP5 climate models, leading – inter alia – to an ad-hoc adjustment of remaining carbon budgets by 27 GtC (100 $GtCO_2$) in the IPCC Special Report on 1.5°C warming. Also, they were not part of the concentration projections for the RCP scenarios. Here, we ~~now~~ include a representation of permafrost feedbacks based on the MAGICC permafrost (Schneider von Deimling et al., 2012), leading to additional cumulative $CO_2$ emissions of 25 to 88 GtC by 2100, 42 to 378 GtC by 2200 and 51 to 542 GtC by 2300 for the lowest (SSP1-1.9) and highest (SSP5-8.5) scenario, respectively (***Table 2*** ~~***Table 2***~~). Thus, our permafrost module is in line with the IPCC Special Report on 1.5°C warming assumptions for the lowest scenarios (25 GtC versus 27 GtC). While we do not entertain the probabilistic version in this study, our default settings are comparable to the median values reported in Schneider von Deimling (2012). In the highest scenarios (SSP5-8.5), these permafrost related Earth System Feedbacks cause $CO_2$ concentrations that are up to 200 ppm higher by 2200 (**Figure 3** ~~**Figure 3**~~a). A later study included a more complex offline model with deep carbon deposits, a vertical soil resolution and abrupt thaw processes like thermokarst lake formations. Generally, the results are comparable, although our settings might underestimate 21$^{st}$ century contributions and overestimate long-term cumulative emissions in comparison to Schneider von Deimling (2015).

In addition to elevated $CO_2$ concentrations, the permafrost module also estimates future $CH_4$ emissions related to permafrost thawing, i.e. annual emissions of up to 75 $MtCH_4$/yr in the highest SSP5-8.5 scenario by 2200. Cumulatively, 0.34 GtC to 1.07 GtC of carbon are projected to be released as 451 $MtCH_4$ to 1431 $MtCH_4$ over the course of the 21st century across the 9 considered SSP scenarios (Table 2~~Table 2~~), with even more coming in the 22nd century. The extra emissions lead to 10-240 ppb higher $CH_4$ concentrations in 2200 (Figure 3~~Figure 3~~b). Most of the carbon decomposition is assumed to happen as aerobic decomposition in the mineral soils, stretching from the more southerly zonal permafrost bands to the higher latitudes from now to 2200 (**Figure 3**~~**Figure 3**~~ e to h).

### 2.5 Projecting latitudinal gradients

Compared to the previous input datasets for CMIP intercomparisons, which consisted of global-mean values only, latitudinal gradients (and seasonality) are new elements. For the historical period, these latitudinal gradients and seasonally changing surface air concentrations can be estimated from the large set of in situ and flask sampling sites with monthly sampling resolution. Further back in time, when there was insufficient latitudinal coverage, the latitudinal gradient was decomposed into two empirical orthogonal functions (EOFs, the principal components). The multiplier or score (also known as the principal component time series) for the first EOF was regressed against global anthropogenic emissions. Except for $CO_2$, the score for the second EOF was kept constant. For $CO_2$, we assumed a simplified approach by both assuming a zero intercept for the regression of global emissions versus the first EOF and a phase-out back in time of the second EOF score. These lead to the simplified and uncertain assumption that the pre-industrial $CO_2$ gradient was zero (Figure 9b in Meinshausen et al. (2017)). For a more detailed description of the interpolation and assimilation algorithms for the historical data, see Meinshausen et al. (2017).

For the future, there are obviously no observations from which the changes in the latitudinal gradients can be derived. We hence apply the regression procedure from the historical dataset into the future i.e. we project the score of the first EOF of the latitudinal gradient of each greenhouse gas with its global emissions. That makes the simplifying assumption that, in the future, the sources (and sinks) of these gases remain approximately constant in terms of their latitudinal location (not in terms of their magnitude). For $CO_2$ in the very low emission scenarios, like SSP1-1.9 with net negative $CO_2$ emissions,

that leads to a plausible reversal of the latitudinal gradient if the northern hemisphere is the main location for the natural and anthropogenically induced net $CO_2$ sink.

There are large natural $CH_4$ emission sources, predominantly in the northern hemisphere. Also, anthropogenic emissions are higher in the northern hemisphere. This largely explains the observed atmospheric concentration gradient: At the end of the historical period (2010 to 2014), $CH_4$ concentrations are 80 ppb above the global average in the Northern mid-latitudes while Southern hemispheric concentrations gently slope towards a minimum of 60 ppb below the global average at the pole ~~For $CH_4$, which exhibits also large natural sources, predominantly in the northern hemisphere, anthropogenic emissions resulted in a derived latitudinal gradient up to 80 ppb above the global average in the northern midlatitudes while Southern hemispheric concentrations gently slope towards a minimum of 60 ppb below the global average at the pole at the end of the historical datasets~~ (Figure 11b in Meinshausen et al., 2017). As for $CO_2$, we use anthropogenic $CH_4$ emissions to extrapolate the first EOF score into the future. Given that $CH_4$ emissions do not converge to zero in any scenario, let alone become negative, the strong North-South gradient is maintained in all scenarios.

### 2.6 Projecting seasonality

Seasonality of concentrations is by far most strongly pronounced for $CO_2$, given the large seasonal sink (photosynthesis) and source (heterotrophic respiration) pattern of the northern hemispheric terrestrial biomass. Projecting future seasonality changes depends on a correct understanding of the past seasonality changes and how those seasonality changes are related to changes in ecosystem productivity (Forkel et al., 2016;Graven et al., 2013;Welp et al., 2016), increased cropland productivity (Gray et al., 2014) and other factors. Here, we use the net ecosystem productivity (NPP) as a proxy for future seasonality changes and regress the historically derived seasonality change EOF score with modelled future net ecosystem exchange by MAGICC7. NPP in MAGICC7 is projected to ~~strongly~~ increase strongly in the highest SSP5-8.5 scenario, while following a maximum-then-decline pattern in the lower SSP1-1.9 scenario. At the end of the historical period, the total seasonality is derived to have a minimum concentration deviation of -10.1 ppm in Northern mid-latitude August. Given these projected NPP changes in the high SSP5-8.5 scenario, the projected total seasonality increases to approximately twice that by 2100, a projection that comes with a high degree of uncertainty.

For all other gases for which we identified a significant seasonal cycle in the historical observational data, we assume that the relative seasonality (i.e. the magnitude of monthly anomalies relative to the annual mean) stays constant, i.e. that the absolute seasonality concentration changes scale with global-mean concentrations.

### 2.7 Simplified formula to reflect radiative forcing from $CO_2$, $CH_4$ and $N_2O$

In order to present $CO_2$, $CH_4$ and $N_2O$ in our compilation of 43 greenhouse gases and their relative importance for future effective radiative forcings (ERFs), we use simplified radiative forcing formula (for radiative forcing after stratospheric temperature adjustments) that represent the Oslo line-by-line model results – which now takes into account the short-wave absorption of $CH_4$, among other aspects (Etminan et al., 2016). While Etminan et al. provided simplified formulas for their Oslo line-by-line model results, we here adjust those simplified formulas, resulting in a virtual elimination of the model fit errors by Etminan of up to 3.6% for $CO_2$ (see Table 1 in Etminan et al. (2016) and our Figure 4~~Figure 4~~d and Table 3~~Table 3~~ below). Aside from slight model mis-fits, the original Etminan simplified formula for $CO_2$ has a validity range of only up to 2000 ppm $CO_2$ concentrations. Their simplified formula is an adaptation of the classical approach to approximate radiative forcing by $\alpha * ln\left(\frac{C}{C_0}\right)$, where $\alpha$ is a scaling coefficient, $C$ the $CO_2$ concentration at time t and $C_0$ the concentration at the reference state, normally the pre-industrial reference value. Etminan et al. introduce the overlap of the absorption spectra between $CO_2$ and $N_2O$ and also modulate the logarithmic approximation by quadratic and linear terms. When using their suggested coefficients ($a_1$, $b_1$ and $c_1$ in their Table 1), the factor $\alpha$ in front of the $ln\left(\frac{C}{C_0}\right)$ part reaches a maximum at $C_0 - \frac{b_1}{2a_1}$, i.e. at around 1777 ppm, when assuming $C_0$ as the pre-industrial concentration(277.15 ppm). For $CO_2$ concentrations beyond 1777 ppm, the alpha value decreases, leading to an unrealistic flattening off above 2000 ppm (and eventual decline well above 3000 ppm). The highest projected SSP concentration (SSP5-8.5) reaches beyond the nominated validity range of 2000 ppm. Hence, we adapt the $CO_2$ radiative forcing formula to assume a constant $\alpha$, once $\alpha$ reaches its maximal value (which is around 1808 ppm with our optimised parameter settings – see Table 3~~Table 3~~).

In summary, building on the work of Etminan, our optimised modifications of the simplified radiative forcing expressions for $CO_2$, $CH_4$ and $N_2O$ as presented in Table 3~~Table 3~~ have the two advantages of

(a) representing the 48 Oslo line-by-line model results within rounding errors and also (b) extending its likely validity range in line with previous forcing approximations (and pending examinations by line-by-line models) to higher $CO_2$ concentrations. However, there is one disadvantage of our simplified formula. While our formula starts from fixed $C_0$, $N_0$, and $M_0$ values at pre-industrial levels, the formulas presented in Etminan cater for the option to set $C_0$, $N_0$ and $M_0$ at any value within the validity range. Hence, our formula would have to be applied twice to calculate the difference in terms of radiative forcing between a $C_1$, $N_1$, $M_1$ and a $C_2$, $N_2$, $M_2$ concentration state, if both are different from pre-industrial levels $C_0$, $N_0$ and $M_0$.

We also take into account new findings regarding rapid adjustments (Smith et al., 2018). In the multi-model analysis by Smith et al. (2018), $CO_2$ is suggested to have a slightly (~5%) higher effective radiative forcing than its instantaneous radiative forcing after stratospheric temperature adjustments alone, an adjustment also used here. While the tropospheric rapid adjustments in the case of $CO_2$ is substantial, it is largely offset by the corresponding water vapour adjustment and the cloud-related rapid adjustments (Figure 3 in Smith et al., 2018). Following Smith et al. (2018), we assume that rapid adjustments largely cancel out for $CH_4$.

### 2.8 Data-flow, mean-preserving higher resolutions, and merging with historical files.

In this study's projections, the data is provided in 15° latitudinal bands with monthly resolution. These are constructed from the global-mean time series generated by MAGICC7, with the modulation towards latitudinal annual means by the time-changing latitudinal gradients (section 2.5). These latitudinal annual means are then turned into monthly data values using the latitudinally and monthly resolved seasonality fields.

There are two additional post-processing steps involved. For one, the mean-preserving interpolation routines from Section 2.1.9 of Meinshausen et al. (2017) are used to generate a monthly surface air mole fraction field at a finer 0.5° latitudinal resolution. The other step is merging the projections with the historical concentrations. To ensure a smooth transition from the previously derived historical concentration fields to the ones derived in this study, we use the latitudinally resolved differences in the month of December 2014 between the historical fields derived in Meinshausen et al. (2017) and the raw

data produced here. We then add those December 2014 differences to the 2015 future datasets, phasing them out linearly over 12 months.

## 3 Results

This study's projected greenhouse gas concentrations provide the 'official' greenhouse gas concentrations for the SSP scenarios. They help enable the CMIP6 exercises and span a wide range of possible futures. Below, the results are presented for the various gases. The complete data repository of all projected mole fractions in various data formats, with interactive plots and factsheets is available at http://greenhousegases.science.unimelb.edu.au. The subset of the data recommended for the nine SSPs that are part of the ScenarioMIP and AerChemMIP experiments in netcdf format is also available on https://esgf-node.llnl.gov/search/input4mips/.

### 3.1 Carbon Dioxide

The projected $CO_2$ concentrations range from 393 to 1135 ppm in 2100, with the low scenario SSP1-1.9 decreasing to 350 ppm by 2150 (**Figure 5**g). Given the assumption of zero $CO_2$ emissions in the lower scenarios beyond that, the lower end of the projected $CO_2$ concentrations is not projected to decrease much further. On the upper end, under the SSP5-8.5 scenario global-average concentrations are projected to increase up to 2200 ppm by 2250 (**Table 4**~~**Table 4**~~ and **Table 5**~~**Table 5**~~, and see also online "GHG factsheets" at greenhousegases.science.unimelb.edu.au). The latitudinal gradient implies a difference of annual-average northern midlatitudes to South pole concentrations of about ~~7~~ 6 ppm in current times (**Figure 5**b). As future seasonality is correlated with projected NPP, the CO2 seasonality change pattern (**Figure 5**a.1) is scaled with the a normalized projected NPP (**Figure 5**a.2). Future latitudinal gradients are derived by projecting the first two principal components or EOFs, where the first (dark blue line in **Figure 5**c) is regressed against global emissions – with the implied future scaling factor show in **Figure 5**d (dark blue line). The second EOF (turquoise line in **Figure 5**c) is assumed constant in the future (turquoise line in **Figure 5**d). ~~For the future,~~ T~~t~~he applied projection methods result in a continuous projection of $CO_2$ concentration from the observationally derived historical values, including their latitudinal gradients and seasonality (**Figure 5**h). By approximately 2060, a zero latitudinal gradient ~~by ~2060~~is projected in the lowest SSP1-1.9 scenario (**Figure 5**~~**Figure 5**~~b) because $CO_2$ emissions revert

from positive to net negative. Under the highest SSP5-8.5 scenario, the northern midlatitude to South Pole difference expands to more than 23 ppm by 2100 (not shown in plot, but viewable in online data repository at greenhousegases.science.unimelb.edu.au).

### 3.2 Methane

Global-mean $CH_4$ surface air mole fractions across the SSP scenarios are projected to range from 999.7 ppb to 3372 ppb by 2100, with maximal northern hemispheric averages being ~60 ppb higher than the global average (Table 4~~Table 4~~). The largest difference between average Northern and Southern hemispheric concentrations (up to 120 ppb by 2100, Table 5~~Table 5~~) is in the highest $CH_4$ emissions scenario (SSP3-7.0) and whilst the smallest difference (~70 ppb) is seen in the scenarios with the lowest global $CH_4$ emissions (SSP1-1.9, SSP1-2.6 and SSP5-3.4OS). While SSP5-8.5 is projected to be the scenario with the highest radiative forcing, because of high $CO_2$ emissions, SSP5-8.5 is not the highest $CH_4$ emissions scenario, with both SSP3-7.0 and SSP4-6.0 suggesting higher total $CH_4$ emission by 2100 (and in our extensions beyond 2100) (Figure 2~~Figure 2~~f).

### 3.3 Nitrous Oxide

$N_2O$ concentrations are not projected to decrease at any point before 2200, regardless of the SSP scenario we consider. Even under the lowest emissions scenarios, SSP1-1.9 and SSP1-2.6, current global-average concentrations are projected to increase from 328.5 ppb in 2015 to 361 ppb by 2100 (Table 5~~Table 5~~). Under the highest $N_2O$ scenarios (SSP3-7.0 and SSP3-7.0-lowNTCF), concentrations are projected to increase to 422 ppb by 2100 and over 500 ppb by 2500. Both seasonality and the latitudinal gradient is rather subdued for $N_2O$, as it is both a long-lived greenhouse gas and does not exhibit strong seasonal variability in either sources or sinks.

### 3.4 Ozone Depleting Substances and other chlorinated substances

As all ozone depleting substances' emissions are assumed to follow a single emission scenario as a result of the Montreal Protocol (Velders and Daniel, 2014b), the SSP concentration scenarios exhibit no substantial variation across their projected concentrations. For example, by 2100, CFC-11 and CFC-12 concentrations are assumed to vary from 51.4 to 56.2 ppt, and from 114.3 ppt to 133.5 ppt, respectively

(Table 4~~Table 4~~). These differences across the concentration scenarios are hence not a result of different emission assumptions but solely due to factors that influence the substances' lifetimes. The stratospheric partial lifetime of these substances is affected by a change in the meridional Brewer-Dobson circulation, assumed to strengthen with increasing climate forcing. The tropospheric OH-related partial lifetime is scaled by changing OH concentrations. Those OH concentrations are in turn mainly affected by $CH_4$ abundances and emissions of other reactive gases (CO, NMVOC, NOx). Overall, the concentrations and radiative forcing contributions of all ozone depleting substances are assumed to strongly reduce until 2100 and beyond, following the phase-out schedules under the Montreal Protocol (Figure 10~~Figure 10~~). See section 4.2 for a discussion of the unexpectedly slow declines of CFC-11 (Montzka et al., 2018) and other species, though.

### 3.5 Other fluorinated greenhouse gases

The fluorinated gas' emissions with a virtually zero ozone depleting potential - HFCs, PFCs, $SF_6$ and $NF_3$ - vary across the SSP scenarios. Most SSP scenarios assume strong decreases for several of these substances (e.g. $NF_3$ and $SF_6$,), while SSP5-8.5 assumes strong increases for most of the 21st century (Figure 2~~Figure 2~~h,i). Until recently, these fluorinated gases were not controlled under the Montreal Protocol. With the 2016 Kigali Amendment, however, a select number of HFCs have been included in the Montreal Protocol and GWP-weighted emissions of these particular HFCs will have to be phased-down globally in coming decades. When aggregating all ~~this~~ these non-ozone depleting fluorinated gases into HFC-134a equivalent concentrations, the SSP scenarios project a wide range of 2100 values, ranging from 278 ppt to more than ten-fold that value, i.e. 2985 ppt (last row in Table 4~~Table 4~~). While the HFC projections are derived from the IAM modelling team assumptions regarding the SSPs, several of the resulting HFC projections would exceed the phase-out emission levels agreed to in the Kigali Agreement.

### 3.6 Radiative forcing since 1750

In this section, we aggregate all 43 greenhouse gases' radiative forcing effect using the updated radiative forcing formula for $CO_2$, $CH_4$, and $N_2O$ and standard radiative efficiencies from IPCC AR5 (section 2.7). Across the nine SSP scenarios, it is apparent that $CO_2$ makes the largest contribution to future warming (blue parts in Figure 7~~Figure 7~~), constituting between 68% and 85% of GHG radiative forcing by 2100,

and 68% to 92% of radiative forcing by the time of maximum GHG-induced radiative forcing (*Table 6~~Table 6~~*). In the scenario with the greatest radiative forcing, SSP5-8.5, radiative forcing in 2100 is projected to be approximately 8 W/m$^2$ and 9.7 W/m$^2$ for $CO_2$ or all GHGs, respectively (right-axis bars in Figure 7~~Figure 7~~i). This greenhouse gas induced radiative forcing is projected to increase to nearly 13 W/m$^2$ by 2250 under SSP5-8.5. On the lower side, the SSP1-1.9 scenario exhibits a $CO_2$ radiative forcing of around 1 W/m$^2$ in 2150 and beyond, with total greenhouse gas induced forcing stabilising around 1.5 W/m$^2$ – equivalent to $CO_2$ concentrations of approximately 370 ppm (right axis in panel a of Figure 7~~Figure 7~~).

## 4 Discussion

In this section, we discuss the SSP greenhouse gas concentration projections in relation to the last 2000 years of observations and cumulative carbon emissions, which are an important metric for mitigation efforts. We also provide a comparison to previous RCP pathways.

### 4.1 $CO_2$ and $CH_4$ concentrations

After $CO_2$, the greenhouse gas with the second largest radiative forcing contribution in the 21$^{st}$ century is $CH_4$ (Figure 7~~Figure 7~~). To a large extent, greenhouse gas induced future warming is hence influenced by the concentrations of $CO_2$ and $CH_4$. Two examples in which methane and $CO_2$ forcings and their relative strength are important. i: Firstly, discussions about the benefit of the mitigation of short-lived forcers often accounts for $CH_4$ as a short-lived forcer, which usually contributes most of the climate benefits of any short-lived forcer mitigation strategy (Rogelj et al., 2015;Rogelj et al., 2014). Hence, when the climate benefits of reducing short-lived forcers are compared to those of reducing $CO_2$ emissions, the actual comparison is mostly between $CH_4$ and $CO_2$. Secondly, deriving the remaining carbon budget from Earth System Model runs from single or a few scenario runs is contingent on those scenarios showing a representative level of $CH_4$ versus $CO_2$ concentrations. Here, we consider mid-21$^{st}$ century $CH_4$ and $CO_2$ concentrations across the range of SSP scenarios. We place them in the context of the RCP scenarios as well as 475 scenarios of the IPCC Special Report on 1.5°C emissions database (https://data.ene.iiasa.ac.at/iamc-1.5c-explorer/) (Figure 9~~Figure 9~~). We focus on mid-century concentrations as they are close to the expected point of peak warming in the scenarios that are in line

with the Paris Agreement temperature targets of 1.5°C and well below 2.0°C. The comparison shows that SSP1-1.9 and SSP1-2.6 result in relatively similar $CH_4$ concentrations by 2050, albeit their $CO_2$ concentrations differ by approximately 7% (437 ppm versus 469 ppm, respectively, Table 5~~Table 5~~). The other scenario with low $CH_4$ concentrations in 2050, i.e. SSP3-7.0-lowNTCF, falls outside the scenario space considered here, namely the SR.15 database (https://data.ene.iiasa.ac.at/iamc-1.5c-explorer/, see Figure 9~~Figure 9~~ below). This is by design, as this scenario is the result of adapting a high emission scenario (SSP3-7.0) so that it features very low short-lived climate forcer emissions (Collins et al., 2017). See also Appendix C in Gidden et al. (2019) for a detailed comparison of SSP3-7.0 and SSP3-7.0-lowNTCF emissions. The comparison of mid-century $CO_2$ and $CH_4$ concentrations also reveals that the main reason for higher implied warming of SSP4-3.4 in comparison to SSP1-2.6 are elevated $CH_4$ concentrations. Thus, to a limited extent, the SSP4-3.4 and SSP1.2.6 scenarios represent a similar pair of scenarios to the SSP3-7.0 and SSP3-7.0-lowNTCF scenarios, but for a lower level of cumulative $CO_2$ emissions.

### 4.2 Most recent concentration observations

While updating the historical observations for our future concentrations, several recent trends are noteworthy. We discuss these in this section, covering $CH_4$, ozone depleting substances ~~as~~ CFC-11, CFC-12, CFC-113 as well as HFC-23 and $SF_6$.

Regarding $CH_4$, atmospheric observations show a plateauing of $CH_4$ concentrations from 1999 to 2005 ~~as~~ followed by an increased growth rate from 2007 (Nisbet et al., 2016). Available literature suggests that changes in natural and anthropogenic sources and OH-related sinks are involved (Rigby et al., 2017), for example reduced biomass burning emissions (Worden et al., 2017) or reduced thermogenic fossil-fuel related emissions (Schaefer et al., 2016) to explain the plateau of concentrations until 2006, but large uncertainties remain, particularly related to natural wetland and inland water sources (Saunois et al., 2016). Schaefer et al. (2016) suggest that the renewed onset of increasing $CH_4$ concentrations could be related to increased emissions from the agricultural sector.

Our $CH_4$ concentration time series, both the historical ones and the future projections from 2015 onwards, capture this observed increase in the trend Figure 6~~Figure 6~~b) – although there is uncertainty as to

whether the underlying processes and emission sources are correct. Nevertheless, our employed simple model MAGICC7 also captures this temporary plateau of $CH_4$ concentrations when run in an emission-driven model, possibly not the earlier parts though (left column in Supplementary Figure 1). Note that the transition in 2017 from observationally-driven concentrations to our model-driven concentration timeseries exhibits a slight offset in concentrations (section 5.3), as MAGICC7 inferred a slightly stronger increase in $CH_4$ concentrations over 2016 based on the IAM's emissions, than observed (Figure 6~~Figure 6~~).

For nitrous oxide, there appears to be a small downward adjustment in the growth rate around 2014, with atmospheric growth in years 2016 and 2017 being slightly lower than in 2014 (Figure 6~~Figure 6~~c), although observed 2018 growth rates picked up again and the slight offset seems to be well within the noise of recent growth rate variations. For a close comparison of recent observations and our concentration timeseries, see the $CH_4$- and nitrous oxide-related factsheets at http://greenhousegases.science.unimelb.edu.au.

Recent observations regarding substances whose production is largely phased out under the Montreal Protocol are also notable (Montzka et al., 2018;Rigby et al., 2019). CFC-11 measurements show some elevated northern hemisphere values from 2013 onward and the global average concentrations are 5-10 ppt above published projections from 2012 to 2017, which consider compliance with projected Montreal Protocol controls, even though the global concentration continues to decline (Velders and Daniel, 2014b) (see panel h in online CFC-11 factsheets at http://greenhousegases.unimelb.edu.au). Our projections reflect the elevated atmospheric concentrations until 2016, but then continue on the assumption of compliance with the Protocol and those additional emission sources to be halted. By analyzing measurement data from sites around the world, it was also concluded that the additional CFC-11 emissions – roughly a 25% increase since 2012– originate in part from the eastern Asian region (Rigby et al., 2019;Montzka et al., 2018), and an updated study has identified that about half of the global increase can be attributed to 2 provinces in eastern China (Rigby et al., 2019). Although less pronounced, CFC-12 and CFC-113 concentrations have also not declined as expected since 2013, although for neither of these gases emissions are thought to have actually increased in recent years, as is the case for CFC-11 (Figure 10~~Figure 10~~b). ~~Even stronger~~More notable is the diversion of projected and recently observed concentrations for CFC-114, when comparing against the recent Velders and Daniel projections (2014b).

For a discussion of recent concentrations of CFC-13, and inferred emissions of CFC-13 (which also seem to increase due to Asian sources) and the two isomers of CFC-114 as well as CFC-115, see Vollmer et al. (2018).

Chloroform ($CHCl_3$) exhibited a concentration decline since 2000 but is increasing again in the global atmosphere (see Chloroform Factsheet available in the online data repository at http://greenhousegases.science.unimelb.edu.au). Fang et al. (2019) point to a recent strong growth of chloroform emissions in China. ~~Similarly, t~~The similarly short-lived methylene chloride ($CH_2Cl_2$) also had almost stagnant atmospheric concentrations around the year 2000, but high growth has been observed in subsequent years, almost doubling atmospheric global-average concentrations from around 20 ppt to 40 ppt by 2017 (Hossaini et al., 2015). See also Chapter 1 of the 2018 Ozone Assessment Report (Engel et al., 2018).

Emissions of HFC-23 originate almost completely as a by-product of the production of HCFC-22. Under the Kyoto Protocol, abated emissions of HFC-23 are eligible to be credited in project based offset mechanisms – leading to a bulk of offset credits under the Clean Development Mechanism and also two former Joint Implementation projects in Russia (Schneider, 2011). It has been shown that so-called 'perverse incentives' likely resulted in additional production – in order to broaden the magnitude of claimable abatement credits (Schneider and Kollmuss, 2015). Given that the monetary value of those offsets credits far exceeded the abatement costs, the Kigali Amendment to the Montreal Protocol in October 2016 lead to a new regulatory approach for HFC emissions (Velders et al., 2015). Nevertheless, rather high individual station measurements (classified as "pollution" events) lead to high monthly average concentrations at the Gosan South Korean station. Together with accelerating growth trends for HFC-23 since 2015, this could point to a continued large increase of emissions (see panel h in HFC-23 related factsheets on http://greenhousegases.science.unimelb.edu.au). Similarly, $SF_6$ concentrations continue to increase at unprecedented rates. They will remain high for a long time (without other anthropogenic interventions) due to $SF_6$'s very long lifetime. The commonly assumed lifetime so far (also assumed in this study) has been 3200 years (Myhre et al., 2013), although recent findings about a loss mechanism in the polar vortex suggest a lower new best estimate of 850 years (Ray et al., 2017).

### 4.3 The long-term projections in the context of last 2000 years

As the historical compilation of greenhouse gas concentrations based on firn and ice core records indicated, multiple literature studies indicate relatively flat concentration of $CO_2$, $CH_4$ and $N_2O$ over the past 2000 years. Historical fluctuations over the last 2000 years of a few ppm or ppb, e.g. around 1650 for $CO_2$, are miniscule in comparison to recently observed concentration changes since the onset of industrialisation and projected future changes (**Figure 8**~~**Figure 8**~~). For example, $CO_2$ concentrations could reach ~~to~~ levels beyond 1500 ppm in the SSP3-7.0 and SSP5-8.5 scenarios and even reach beyond 2000pm by 2200 under SSP5-8.5. ~~Those~~ $CO_2$ concentrations in excess of 1500ppm have likely not been present on Earth for more than 40 million years ((Fig. 4 in Royer, 2006) – i.e. before the current Antarctic and Northern hemisphere ice sheets formed. Reflecting the shorter lifetime, concentrations of methane ~~can reduce~~ decrease pronouncedly over the 21st century. ~~For $CO_2$, for which~~ The stronger mitigation ~~lower~~ scenarios foresee the option of net negative emissions for $CO_2$, so that $CO_2$, concentrations ~~also~~ recede over the long term to around 350ppm in case of the SSP1-1.9 scenario. Reflecting the longer lifetime and base level of agricultural emissions, $N_2O$ concentrations are not foreseen to drop below current levels in any of the investigated SSP scenarios over the coming 500 years (**Figure 8**~~**Figure 8**~~).

### 4.4 Comparing SSP and RCP concentrations

For every generation of climate scenarios, whether these are the IS92, SRES, RCP or now the SSP scenarios, it is pertinent to clarify the differences and similarities of the new scenario set to the previous one(s). In particular due to the unavoidable delay in the analysis and use of the climate projections in the impact communities, clarifying the comparability to previous scenarios is paramount. Here, we compare both the greenhouse gas concentrations and an indication of global climate effects (section 1.1~~4.5~~).

Four RCP scenarios are now replaced in the SSP generation of scenarios with five "high priority' scenarios (4 ScenarioMIP "Tier1" cases plus SSP1-1.9) in addition to 4 additional scenarios that investigate additional forcing levels (see panels a,c in **Figure 11**~~**Figure 11**~~). Aside from this difference in the sheer number of scenarios, compared to the RCPs, the actual concentration levels differ substantially for most corresponding SSP scenarios. For example, the SSP5-8.5 scenario features substantially higher $CO_2$ concentrations by 2100 and beyond than the RCP8.5 scenario (panels a,b in

Figure 11~~Figure 11~~). Somewhat compensating though, the $CH_4$ concentrations by 2100 are substantially lower under the SSP5-8.5 scenario compared to the RCP8.5 scenarios (Figure 11~~Figure 11~~c), and that difference is even more pronounced by 2300 due to the different extension principles followed for RCP extensions (Meinshausen et al., 2011b) and those for SSPs (section 2.3). Specifically, the SSP5-8.5 fossil and industrial $CH_4$ emissions are assumed to be phased out by 2250 with land use-related $CH_4$ emissions kept constant at 2100 under the SSP5-8.5 extension. That contrasts with the RCP8.5 extension, in which a long term $CH_4$ concentration stabilisation at very high levels of 3500 ppb was implemented. Similarly, for $N_2O$, the new SSP5-8.5 scenario implies lower concentrations by 2100 and beyond compared to the RCP8.5 (Figure 11~~Figure 11~~e,f). Under the SSP family, the SSP3-7.0 becomes the scenario with the highest emissions and concentrations for both $CH_4$ and $N_2O$.

On the lower side of the scenarios, the most marked differences are that the new SSP1-2.6 has higher $CO_2$ concentrations, compared to the previous RCP2.6 and SSP1-1.9 has the lowest $CO_2$ concentrations (Figure 9~~Figure 9~~ and Figure 11~~Figure 11~~a). $CH_4$ concentrations are very similar across these three scenarios by the middle of the century, whereas by the end of the 21st century, the new SSP1-1.9 and SSP1-2.6 scenarios show reduced levels of only 1000 ppb, substantially below today's $CH_4$ concentration levels. For $N_2O$, the story is the other way around: SSP1-1.9 and SSP1-2.6 follow almost identical concentration trajectories while the previous RCP2.6 scenario is lower.

~~**4.5 Comparing SSP and RCP temperature and sea level rise implications**~~

~~A key interest to the user communities of the new SSP scenarios is their comparability with previous RCP scenarios, not only in terms of concentrations (section 4.4) but also more aggregated in terms of their overall global mean temperature and sea level rise implications. While a comprehensive assessment will require the corresponding analysis of CMIP5 and forthcoming CMIP6 ESM results, we here provide an initial assessment using a consistent modelling setup for both RCP and SSP scenarios. Specifically, we run MAGICC7.0 in a probabilistic setting that captures a skewed-normal climate sensitivity likely range from 2°C to 5°C with a best estimate of 3°C – with corresponding parameters being drawn consistently from the historical constraining study described in Meinshausen et al.(2009). The methodological setup of using an adapted climate sensitivity range is also used in Rogelj et al. (2012), when comparing SRES and RCP scenarios. In addition, we updated the $CO_2$, $CH_4$ and $N_2O$ forcing parameterisations in~~

MAGICC7.0 as described above (section 2.7). Here, we also use the probabilistic MAGICC sea level model introduced by Nauels et al. (2017) and include our permafrost module (section 2.4.4). Note that a fully calibrated version of MAGICC7 (version 7.x) will be available after the analysis of the CMIP6 ESM data. In addition, we normalised the SSP global mean surface air temperature (GMSAT) and global mean sea level rise data to the AR5 reference period 1986-2005 to facilitate a comparison with published key RCP data by IPCC AR5 (Table SPM.2 of the IPCC WGI AR5 SPM).

When comparing the results of these temperature and sea level rise projections with those of IPCC AR5, it is noteworthy that our default MAGICC7.0 setting yields similar results for low scenarios RCP2.6 as IPCC AR5 did. However, at the high end, our illustrative probabilistic setting yields much warmer projections of up to nearly 6.0°C by 2100 for median projections under the RCP8.5 scenarios – compared to median projections around 5.0°C (CHECK) for RCP8.5 relative to pre-industrial levels provided by IPCC AR5 (**Figure 12** a). The main reason is the higher than previously assumed upper climate sensitivity range (5°C), included permafrost feedbacks as well as substantially higher methane forcing (section 2.7). Using the previous probabilistic setup for MAGICC6, our results are closely comparable to those reported by IPCC AR5 (TO DO – SHOW THAT IN FIGURE). A comparison with forthcoming CMIP6 ensemble results will show whether the new default settings are too warm compared to the Earth System Model ensemble. [MM1]

When considering relative differences across SSP and RCP scenarios, we note that SSP5-8.5 is closely comparable to RCP8.5, although somewhat cooler. That might be due to lower methane concentrations in SSP5-8.5 compared to RCP8.5 (**Figure 9**) and also higher sulfur and BC aerosol emissions (Figure 5 in Gidden et al., 2019). The SSP2-4.5 scenario is relatively closely comparable to the RCP4.5 scenario. While the former RCP6.0 scenario has been relatively close to RCP4.5, even undercutting RCP4.5 emissions for much of the early 21st century, the new SSP3-7.0 is more evenly spaced in between SSP2-4.5 and SSP5-8.5. The RCP4.5 and RCP6.0 similarity and overcrossing brought both communication challenges and opportunities. The opportunity is that it can be easier communicated and "shown" that a higher or lower early-century emission level is not 1:1 correlated with a higher or lower emission level for the rest of the century. In fact, the second highest 2020 $CO_2$ emissions after RCP8.5 were associated with the RCP2.6 scenario that implied the lowest temperature change by the end of the century. In the five high priority SSP scenarios, the ranking is much more evenly spaced. That has the communication

~~opportunity for simplicity and clarity about which scenario is higher or lower than another one, which had been a challenge when comparing RCP4.5 and RCP6.0. The opportunity of showing cross-overs and that early concentration levels not necessarily dictate late-century concentration levels is mostly indicated by the SSP5-3.4-OS scenario, which initially follows the highest SSP5-8.5 scenario before embarking on very low and strongly negative emissions. The strong peak & decline shape is interesting from a geophysical point of view. This strong increase and decrease shape even of temperatures (**Figure 12**a) featured by SSP5-3.4-OS has not been part of the RCP scenario family and hence could provide new insights about the asymmetric nature of carbon cycle and heat uptake/release patterns during a strong drawdown phase of $CO_2$ versus the historical steady increase.~~

~~For sea level rise, the comparison of MAGICC7.0 results between SSPs and RCPs and between the latter and the IPCC-AR5-RCP results is closely reflecting our results for temperature projections. While AR6-RCP2.6 range remains close to the AR5 equivalent range for RCP2.6, the AR6-RCP8.5-2081-2100 median is about 0.1 m higher than for the AR5-RCP8.5, with the upper bound of the 90% model range close to 1.1 m instead of around 0.8 m for the AR5 equivalent. In this context, it is important to note that the AR5 consistent sea level model setup presented in Nauels et al. (2017) is applied, without accounting for any additional potentially nonlinear contributions, in particular from the Antarctic ice sheet, that have been discussed since IPCC-AR5 (DeConto and Pollard, 2016;Edwards et al., 2019;Golledge et al., 2019). Hence, the GMSLR differences shown here are the result of the updated MAGICC model as well as the different GHG concentrations underlying the new SSP pathways and the resulting differences in warming of the atmosphere and ocean.~~

### ~~4.6~~4.5 Estimating the effect of latitudinally and seasonally resolved GHG concentrations on surface air temperatures in ESMs

A much-improved assimilation process results from considering seasonally and latitudinally resolved GHG concentration – as individual station monthly mean measurements can easily be "bias" corrected to account for their latitudinal and seasonal variations to inform the global mean. In addition, however, the latitudinally and seasonally resolved GHG concentration data we provide also offers an opportunity to drive Earth System models with more accurate forcings, so that a comparison of the ESM historical runs with observational data can be performed – excluding ESM biases that might result from GHG

concentrations that are applied with a globally uniform GHG concentration levels or spatial fields that are sometimes rather dissimilar from observations (Figures S46 and S47 in Supplementary of Meinshausen et al., 2017). In order to test the approximate magnitude of applying either globally uniform ("yearmean-global") or latitudinally and seasonally resolved GHG concentrations ("lat-mon"), we performed 6 historical ensemble members of the CESM1.2.2 model (Hurrell et al., 2013) under each setup. To increase the signal to noise ratio, we then took the averages over the 155 years of model simulations from 1850 to 2005 across the 6 ensembles, resulting in 930 years of model data under each experiment. Given the seasonality of the data, we average the DJF and MAM monthly means in the "lat-mon" experiment and subtract the the reference scenario's "yearmean-global" respective average. In the DJF and MAM northern hemispheric winter and spring season, one would expect a slight positive warming signal in the higher northern latitudes – given the latitudinal gradient of methane concentrations and the seasonally higher $CO_2$ concentrations. Indeed, we observe a regional warming signal of up to 0.4K over Northern American and Eurasian land masses, which is – in the DJF season – however latitudinally overcompensated by a strong cooling signal in the North Atlantic (**Figure 12**~~**Figure 13**~~ a). In the MAM season, the slight cooling signal in the North Atlantic does not fully offset the warming over the land-masses (**Figure 12**~~**Figure 13**~~b), resulting in a latitudinally averaged warming signal of approximately 0.1K ~~in the high polar north above~~poleward of 65 degrees North (**Figure 12**~~**Figure 13**~~d). Given the high natural variability in the higher latitudes, we consider the significance of this warming signal by comparing our warming signal to corresponding differences of arbitrarily chosen control run segments. From an approximately 4500-year long control run for CESM1.2.2 at pre-industrial conditions, we randomly chose hundred pairs of 930-year long segments to compute the variability of the differences. It turns out that our warming signals are within the min-max range of those 100 sample pairs regarding the latitudinally averaged warming differences, indicating that the expected warming signal due to applying latitudinally and seasonally resolved GHG concentration data is not beyond the variability range. For the MAM ~~region~~period, there are only a few (approximately 3-5) of the paired differences that result in a higher warming signal though, suggesting that the GHG warming signal might be comparable in magnitude to the variability to be expected at a 5% confidence level. In the DJF ~~region~~period, a strong North Atlantic cooling is reducing the latitudinally aggregated warming signal. Whether that North Atlantic cooling is a result of natural variability in our modestly sized 6-member ensembles or whether it

is a dynamical response to generally higher latitude forcing (and possible reduced overturning in the North Atlantic thermohaline circulation branch) cannot be detected from our initial ESM runs.

As one would expect, our analysis does not suggest significant latitudinal temperature perturbations at the 5% level for the JJA and SON periods (not shown), when seasonally lower $CO_2$ concentrations are partially offset by the latitudinal gradient of concentrations in the Northern hemisphere

## 5 Limitations

In this section, we provide a number of key limitations that come with the SSP concentration datasets. Some of these limitations arise from the underlying emission scenario data (section 5.1 and 5.2), some due to imperfect matches between recent observational and model results (section 5.3), some are intrinsic model limitations (section 5.4 and 5.5). Likely the largest limitation is that - by design - this study provides default concentration timeseries for the future but does not represent the uncertainty range of future greenhouse gas concentrations for each scenario (section 5.6).

### 5.1 Limited emission variations across scenarios for gases other than $CO_2$, $CH_4$ and $N_2O$.

The main focus of Integrated Assessment Models rests on projecting sectorally resolved energy, transport, industry, waste, agricultural and landuse emissions for $CO_2$, $CH_4$ and $N_2O$ as well as air pollutant emissions. The other industrial greenhouse gases in the basket of gases of the Kyoto Protocol, namely hydrofluorocarbons (HFCs), perfluorocarbons (PFCs), $SF_6$ and $NF_3$ are often modelled as a group or in subgroups. Subsequent downscaling mechanisms can then yield individual gas timeseries, although they often lack specific process dynamics, i.e. follow the same growth and decline trajectory independent of their actual end-use applications. This is certainly a limitation of many of the forward-looking PFC projections.

In terms of the ozone-depleting substances (ODS), a feature, or limitation, is that the presented SSP scenarios do not capture baseline or reference scenarios or in fact any emission-driven scenario variation

at all. This is because the future ODS emissions are strongly constrained by the Montreal Protocol phase-out schedules. The real-world uncertainty in ODS emissions comes from non-compliance to the Protocol and from uncertainties in emission factors from banks and bank magnitudes. In our study, in which we assume identical emissions in all of our different scenarios, future variations in concentrations are hence purely climate-driven, i.e. illustrate the effect that circulation or atmospheric chemistry changes across the scenarios can have on the ODS lifetimes. It might be worth considering whether, for future assessments, the climate community's scenarios and the ozone community's scenarios could not be commonly designed. For example, some of the scenarios could include ODS emission futures that reflect lower or even non-compliance with the Montreal Protocol to allow studies on the "world avoided" (Morgenstern et al., 2008;Velders et al., 2007). An integration of scenarios used for the Ozone Assessments and the climate assessments may be desirable.

Finally, another limitations is that a few minor long-lived greenhouse gases are not included in this compilation of 43 gases, such as CFC-13 or the isomer CFC-114a (Vollmer et al., 2018).

### 5.2 Individual scenario features and overall scenario spectrum

Despite all the multi-year design efforts by large research international communities, there are some inevitable limitations of the overall group of scenarios. In particular, the final set of scenarios might be more appropriate for the earth system research community than for those interested in exploring policy relevant outcomes. For example, one of the scenarios that features new characteristic is the SSP5-3.4-OS scenario. That scenario assumes the greatest net negative emissions after an initial high emissions growth rate. Its high-peak-then-strong-decline feature tests the biophysical models and will be pivotal to examine the asymmetry of the ramp-up and ramp-down characteristics of the carbon cycle, ocean heat uptake and multiple other Earth System properties. Yet, for policy purposes, that is substantially outside the target space of the Paris Agreement, aiming to keep temperatures to below 2°C warming.

A possible shortcoming for the climate science and impact community is that the new SSP generation of scenarios does not provide a very closely matching overlap with the RCP scenarios, as multiple scenario features are substantially different (see e.g. $CO_2$ and $CH_4$ concentrations in **Figure 9**~~**Figure 9**~~). Thus, from a climate science perspective, maintaining a single multi-gas scenario unaltered from the previous

generation of scenarios could have provided a useful reference point with which to quantify the change in our climate system knowledge for future projections. Given the amount of human and material resources used for the CMIP6 runs, it is however a question of balance between historical comparability and the capability to link to earlier studies and putting resources into the most relevant, up-to-date, scenarios. However, there is also a desire to use the best available forcing data to simulate the historical period. Because the actual historical evolution of concentrations and SLCF emissions has been different in detail from previous scenarios, and historical emission and concentration estimates are updated over time (e.g. Hoesly et al., 2018), the community has thus far decided to use the most up to date data for each subsequent CMIP exercise.

### 5.3 Transition issues from observational to modelled concentrations.

MAGICC has been calibrated to allow a smooth continuation from historical time series to future projections. For some gases, this transition is possibly suboptimal. For example, atmospheric measurements since 2013 produced some rather high chloroform ($CHCl_3$) concentrations in the northern hemisphere, which lead to a stronger latitudinal gradient assumption in the assimilation framework for those recent years. The future projections are not reflecting a continuation of this high implied emission spike and hence revert to a lower latitudinal gradient and slightly smaller global-mean chloroform concentrations (see panel f in the Chloroform factsheet available on http://greenhousegases.science.unimelb.edu.au). A similar transition issue is also present for HFC-23, HFC-245fa, HFC-43-10mee, $CH_2Cl_2$, Halon-1301 and even more pronounced for HFC-32, whose actual global emissions seem to increase much stronger than assumed in the 2020s in our Kigali-aligned emission scenario by Velders et al. (2015).

### 5.4 Main limitations due to sequential scenario generation process

The sequential and concentration-driven nature of the main ESM CMIP6 experiments poses the challenge that future projections of greenhouse gas concentrations are required before the ESM results can be evaluated. In other words, the best estimate of future $CO_2$ concentrations, given a certain emission pathway, will certainly differ at the end of the CMIP6 analysis cycle from the setting with which the MAGICC7 climate model was driven with for this study. This sequential problem could only be avoided

with an altered experimental design, performing most future ESM experiments in an emission-driven, but computationally more demanding, design. An advantage of the concentration driven runs is that climate feedbacks and carbon cycle feedbacks can more easily be separated.

In addition to the inconsistencies introduced by the sequential and concentration-driven nature of future climate scenario experiments, there are clearly limitations of MAGICC and its chosen default parameter settings for this study. A full evaluation of the extent to which the chosen parameters yield a concentration response that is representative of the higher complexity atmospheric chemistry model projections that are part of CMIP6 will be of key interest for future studies.

### 5.5 Variable natural emissions.

Except for the interactive carbon cycle, this study assumes constant natural emissions levels for substances like $CH_4$, $N_2O$, $CH_3Br$, $CH_3Cl$ and others. This is clearly a limitation, as under climate change and human management of the land and ocean, the magnitude of these natural emissions (indirectly influenced by human activities) will change over time. Future research could build knowledge of the time-varying natural emission sources into the projection model used.

### 5.6 No uncertainty estimates

A major limitation of our study is the lack of uncertainty estimates. Given the primary purpose of this study of providing a single reference concentration projection as input dataset for the CMIP6 experiments, uncertainty ranges around the projections are not necessary. However, in multiple other potential applications of this dataset, properly derived uncertainty information could have opened up new use cases. For example, simple inversion studies could attempt to derive seasonally varying sink and source patterns from our observationally based historical monthly and latitudinally resolved concentration patterns. Without the appropriate uncertainty information, any inversion approach will have to make ad-hoc assumptions.

## 6 Conclusion

The projected human-induced increase of atmospheric greenhouse gas abundances over the 21st century swamps all observed variations for the last 2000 years (Figure 8~~Figure 8~~). The new SSP scenarios span an even broader range of $CO_2$ concentration futures, with the higher end (SSP5-8.5) yielding higher concentrations than the previous RCP8.5 scenario and the lower end SSP1-1.9 scenario resulting in $CO_2$ emissions down to 350 ppm in the longer term (2150). Also, in a more technical aspect, the SSP concentrations are breaking new ground. For the first time, the greenhouse gas projections are available for 43 greenhouse gases, with latitudinal and seasonal variations captured. For example, by 2050, Northern hemispheric concentrations in the SSP3-7.0 scenario are 1.2% and 4.3% higher than Southern hemispheric averages for $CO_2$ and $CH_4$, respectively - with corresponding non-negligible implications for radiative forcing (Table 5~~Table 5~~).

Given the substantial efforts that go into the data collection by observational network communities, a worthwhile effort in continuation from the present study would be to build a real-time framework to provide a system that updates GHG historical and future projections, including uncertainties, for a wide range of - perhaps also updated - scenarios from the integrated assessment community. While updates of observations, gas cycle models or emission scenarios in between the major IPCC or WMO Assessments are useful for a range of scientific studies, the new GHG projections data could be frozen every several years to provide a new range of benchmark scenarios for Earth System Models. Efforts to provide more frequent updates for emissions data are also underway (e.g.Hoesly et al., 2018).

More than 20 years ago, the IPCC started to put forward future concentration scenarios, the so-called IS-92 scenarios. Back then in 1992, $CO_2$ concentrations were at 356 ppm (Keeling et al., 1976;Keeling and Whorf, 2004). ~~Today, in 2019~~In 2019, atmospheric $CO_2$ concentrations ~~already rose to~~are ~~411ppm~~411ppm. In equilibrium and assuming a central climate sensitivity of 3°C, these $CO_2$ concentrations of 411ppm alone would imply a temperature change of 1.7°C above pre-industrial levels (using the simple and standard $CO_2$ forcing formula of $RF = 5.35 * \ln(C/C_0)$ with C being the current and $C_0$ being the pre-industrial concentrations). While zero $CO_2$ emissions would yield decreasing concentrations, it becomes clear that only a future emission trajectory that effectively reduces atmospheric $CO_2$ concentration levels below today's levels would provide a reasonable chance to keep warming at or

below 1.5°C in the longer term. And even such 1.5°C of warming could come with multi-meter sea level rise by 2300 (Mengel et al., 2018) and the likely demise of coral reefs (Frieler et al., 2013). Thus, while the shown scenarios span a scientifically valid wide range of plausible futures, from a climate impact point of view - and trying to achieve the Paris Agreement targets - all except for the lowest scenarios investigated in this study will hopefully remain hypothetical futures.

## 7 Data Availability

A supplementary data table is available with global and annual mean mole fractions. The complete dataset with latitudinally and monthly resolved data in netcdf format is available via the Earth System Grid Federation (ESGF) servers at https://esgf-node.llnl.gov/search/input4mips/ with a total of 1656 files for source version 1.2.1. The license for all data is Creative Commons Attribution-ShareAlike 4.0 International License (CC BY-SA 4.0). The digital identifiers of the produced datasets, as provided by the ESGF servers are specific to the 9 SSP scenarios: (SSP5-3.4-over: 10.22033/ESGF/input4MIPs.9867; SSP5-8.5: 10.22033/ESGF/input4MIPs.9868; SSP2-4.5: 10.22033/ESGF/input4MIPs.9866; SSP4-3.4: 10.22033/ESGF/input4MIPs.9862; SSP3-7.0: 10.22033/ESGF/input4MIPs.9861; SSP3-7.0-lowNTCF: 10.22033/ESGF/input4MIPs.9824; SSP1-1.9: doi.org/10.22033/ESGF/input4MIPs.9864; SSP1-2.6: 10.22033/ESGF/input4MIPs.9865; SSP4-6.0: 10.22033/ESGF/input4MIPs.9863) Additional data formats, i.e. CSV, XLS, MATLAB .mat files of the same data are also available via http://greenhousegases.science.unimelb.edu.au.

## 8 Author contributions.

Together with EV, MM designed the study. ZN and MG performed the emission data collation, downscaling and harmonisation steps. MM, EV, and MF build the MATLAB libraries for this project. MF, ZN and MM did the verification of the final data product in comparison to the historical datasets. The new MAGICC parameterisations were developed by MM, ZN, and AJ. MAGICC runs for the concentration projections and postprocessing of the data was performed by MM, ZN, EV, and MF. ZN coordinated the transfer of data to the Input4MIP project. JL, ZN and AN performed the MAGICC temperature and SLR projections. UB setup and performed the CESM1.2.2 runs with CG leading the

analysis. GV contributed the future ODS and halogenated emission projections. MM produced the figures with Figure 8~~Figure 8~~ being produced by JL and MM. All authors contributed to writing and commenting on the manuscript.

## 9 Acknowledgements

We would like to thank the broad community of scientists, lab technicians, research assistants and respective funding agencies that make the observational records of greenhouse gas concentrations possibly, specifically those of the AGAGE~~A~~ and NOAA networks. See Meinshausen et al., 2017 for a detailed acknowledgement. Without those observational records, our ability to project greenhouse gas into the future would not be possible. We also would like to thank the IAM modelling teams, especially the IMAGE, MESSAGE-Globiom, AIM, REMIND-MagPie and GCAM4 teams, who created chosen SSP benchmark emission scenarios underlying this study. The author team thanks for the discussions with the IAM modellers on the design of the SSP extensions, especially Keywan Riahi, Detlef van Vuuren, David Klein and Shinichiro Fujimori. Lastly, the authors acknowledge the web-teams that make the use of the datasets possible. Specifically, we would like to thank Paul Durack for handling the data integration for the ESGF server. Also, we would warmly like to thank Melissa Makin and Usha Nattala and Uli Felzmann from the Faculty of Science IT team at the University of Melbourne, who made it possible that the full datasets, factsheets and interactive plots of this study are available in a user-accessible fashion on greenhousegases.unimelb.edu.au. A deep thank goes to Christopher Holmes, who helped tremendously in providing data and code to calibrate MAGICC to abundance projections presented in Prather et al. (2012) and Holmes et al. (2013). We thank Keith Shine for very helpful discussions on section 2.7. MM thankfully acknowledges the support by the Australian Research Council Future Fellowship grant FT130100809. This work was undertaken in collaboration with partners in the European Union's Horizon 2020 research and innovation programme CRESCENDO (grant no. 641816), of which the University of Melbourne is an unfunded partner.

## 10 Tables

**Table 1** - Derivation and construction of future CMIP6 mixing ratio fields for the greenhouse gas concentration series from 2015 onwards. Note that in addition to the steps shown below, a post-processing step was implemented to scale any differences in the December 2014 values between the raw future data and the previously submitted historical greenhouse gas concentration data. Those data differences in monthly latitudinal values for Dec 2014 were linearly scaled to zero until Dec 2015 in order to provide for a smooth transition between historical and future datasets (section 2.8). See section 2.1 for a description of how the observational data was updated.

| Gas | Time period | Observational data source | Global and annual-mean $C_{global}$ | Seasonality $\hat{S}_{l,m}$ | Seasonality Change $\Delta S_{l,m}$ | Latitudinal gradient $\hat{L}$ |
|---|---|---|---|---|---|---|
| $CO_2$ | 2015 - 2016 | NOAA ESRL Carbon Cycle Cooperative Global Air Sampling Network, 1968-2016.<br><br>Version: 2017-07-28 (updated from historical run version: 2015-08-03), monthly station averages (Dlugokencky, 2015b;NOAA ESRL GMD, 2014b, c, d, a) | Calculated based on observational data source as described in Meinshausen et al. (2017) | Mean over 1984-2013 period. | Leading EOF of residuals from observation – extended into future with projected GPP from MAGICC7.0 calibrated carbon cycle to the UVIC C4MIP model (Friedlingstein et al., 2006). (This is a change from the historical GHG methodology, when we used only observational temperature and $CO_2$ concentrations) . | Two leading EOFs and their scores derived from latitudinal residuals from annual mean values. |
| | 2016 to 2500 | n/a | MAGICC7.0 $CO_2$ global-mean projections driven by harmonized SSP GHG emissions (Gidden et al., 2019) or extended emissions beyond 2100 (section 2.3). | | | The score for the first EOF is regressed against global annual fossil fuel & industry emissions from SSP scenarios. Score for the second EOF assumed constant in future. |
| $CH_4$ | 2015-2016 | AGAGE monthly station means, incl. pollution events ('.mop') (Cunnold et al., 2002) & NOAA | Calculated based on observational data source as described | Mean over 1985-2013 period. Applied as relative | Absolut seasonality changing given that it is applied | Two leading EOFs and their scores derived from latitudinal residuals from annual mean values. The score for the first EOF is regressed against |

| | | | | | | |
|---|---|---|---|---|---|---|
| | | ESRL monthly station data (Dlugokencky, 2015a); Version 2017-07-28; | in Meinshausen et al. (2017). | seasonality, i.e. percent deviation from global-mean. | relative to global-mean. | global annual fossil fuel & industry emissions from SSP scenarios. Score for the second EOF assumed constant in future. |
| | 2016-2500 | n/a | MAGICC7.0 $CH_4$ global-mean projections driven by harmonized SSP emissions extended emissions beyond 2100 (section 2.3). | | | |
| $N_2O$ | 2015 to 2016 | AGAGE monthly station means, incl. pollution events (Prinn et al., 1990) (Version Dec 2017) & Combined Nitrous Oxide data (monthly station averages) from the NOAA/ESRL Global Monitoring Division; Version Thu, Jan 25, 2018 1:50:47 PM | Calculated based on observational data source as described in Meinshausen et al. (2017). | Mean over 1985-2013 period. Applied as relative seasonality, i.e. percent deviation from global-mean. | Absolut seasonality changing given that it is applied relative to global-mean. | Two leadings EOFs and their scores derived from latitudinal residuals from annual mean values; The score for the first EOF is regressed against global total $N_2O$ emissions to extrapolate into the future. Score for the second EOF assumed constant in future. |
| | 2016 to 2500 | n/a | MAGICC7.0 $N_2O$ global-mean projections driven by harmonized SSP emissions (Gidden et al., 2019) extended emissions beyond 2100 (section 2.3). | | | |
| Other greenhouse gases | 2015 to 2017 | Data input sources as described in Meinshausen (2017) with several data inputs updated to newer versions of the | Calculated based on observational data source as described in Meinshausen et al. (2017). | Depending on the gas, either assumed zero or mean over recent | Either zero or absolute seasonality changing given that it is applied relative to | The leading EOF and its score derived from residuals from observations; with the score for the leading EOF regressed against global total $CH_4$ |

| | | | | | | |
|---|---|---|---|---|---|---|
| | | data, namely: AGAGE monthly station means, incl. pollution events (Prinn et al., 2018) (Version Dec 2017); 04-Feb-18 update of NOAA/ESRL/GMD data (Montzka et al., 2015), were appropriate. | | historical period, normally 1990-2013, period. See online factsheets at greenhousegases.science.unimelb.edu.au for a gas-to-gas depiction of the seasonality. | global-mean – depending on the gas. | emissions to extrapolate into the future. |
| | 2016/2017 to 2500 | n/a | MAGICC7.0 driven by harmonized SSP emissions or WMO (2014) scenario A1 emission projections (with extensions beyond 2100). | | | |

1050

***Table 2 -*** *Cumulative $CO_2$ and $CH_4$ emissions from MAGICC's permafrost module under the considered SSPs. The permafrost module has 50 zonal bands, a mineral and peatland soil module and 50 latitudinal zonal bands. See Schneider von Deimling et al. (Schneider von Deimling et al., 2012) for a detailed description. See* **Figure 3**~~**Figure 3**~~ *for timeseries of induced $CO_2$ and $CH_4$ atmospheric concentration changes.*

| | Time horizon | SSP1-1.9 | SSP1-2.6 | SSP2-4.5 | SSP3-7.0-LowNTCF | SSP3-7.0 | SSP4-3.4 | SSP4-6.0 | SSP5-3.4-OS | SSP5-8.5 |
|---|---|---|---|---|---|---|---|---|---|---|
| **Cumulative $CO_2$ emissions** (GtC) | 2100 | 25 | 31 | 46 | 54 | 65 | 38 | 56 | 48 | 88 |
| | 2200 | 42 | 58 | 121 | 252 | 288 | 78 | 167 | 83 | 378 |
| | 2300 | 51 | 74 | 173 | 410 | 444 | 99 | 248 | 101 | 542 |
| **Cumulative $CH_4$ emissions** ($MtCH_4$) | 2100 | 451 | 549 | 789 | 919 | 1,089 | 670 | 953 | 835 | 1,431 |
| | 2200 | 884 | 1,231 | 2,527 | 5,083 | 5,911 | 1,639 | 3,467 | 1,744 | 7,999 |
| | 2300 | 1,177 | 1,774 | 4,246 | 10,505 | 11,673 | 2,404 | 6,170 | 2,389 | 15,096 |

1055

**Table 3 -** Simplified expressions for radiative forcing relative to pre-industrial (1750) levels by changes of surface air mole fractions of $CO_2$, $CH_4$, $N_2O$ – reflecting the Oslo Line-by-line model results. This table can be compared to Table 1 in Etminan et al. (2016), but note that their formulae can be directly applied to any sets of (C, Co), (M, Mo) and (N, No) within the range of fitting, unlike the case here where Co, Mo and No are pre-specified at pre-industrial levels.

| Gas | Simplified Expression | Coefficients | Maximal absolute fit error % ($Wm^{-2}$) |
|---|---|---|---|
| $CO_2$ | $C_{\alpha_{max}} = C_0 - \frac{b_1}{2a_1} \approx 1808\, ppm$<br>$\alpha' = d_1 - \frac{{b_1}^2}{4a_1}, \quad for\ C > C_{\alpha_{max}}$<br>$\alpha' = d_1 + a_1(C - C_0)^2 + b_1(C - C_0), for\ C_0 < C < C_{\alpha_{max}}$<br>$\alpha' = d_1, \quad for\ C < C_0$<br>$\alpha_{N2O} = c_1 * \sqrt{N}$<br>$RF_{CO_2} = (\alpha' + \alpha_{N2O}) * ln\left(\frac{C}{C_0}\right)$ | $a_1$ = -2.4785e-07 $Wm^{-2}ppm^{-2}$<br>$b_1$ =0.00075906 $Wm^{-2}ppm^{-1}$<br>$c_1$ = -0.0021492 $Wm^{-2}ppb^{-0.5}$<br>$d_1$ = 5.2488 $Wm^{-2}$<br>$C_0$ = 277.15 ppm | 0.11% (0.0037 $Wm^{-2}$) |
| $N_2O$ | $RF_{N2O} = \left(a_2\sqrt{C} + b_2\sqrt{N} + c_2\sqrt{M} + d_2\right) * \left(\sqrt{N} - \sqrt{N_0}\right)$ | $a_2$ =-0.00034197 $Wm^{-2}ppm^{-1}$<br>$b_2$ = 0.00025455 $Wm^{-2}ppb^{-1}$<br>$c_2$ =-0.00024357 $Wm^{-2}ppb^{-1}$<br>$d_2$ = 0.12173 $Wm^{-2}ppb^{-0.5}$<br>$N_0$ = 273.87 ppb | 1.5% (0.0059 $Wm^{-2}$) |
| $CH_4$ | $RF_{CH_4} = \left(a_3\sqrt{M} + b_3\sqrt{N} + d_3\right) * \left(\sqrt{M} - \sqrt{M_0}\right)$ | $a_3$ =-8.9603e-05 $Wm^{-2}ppb^{-1}$<br>$b_3$ = -0.00012462 $Wm^{-2}ppb^{-1}$<br>$d_3$ = 0.045194 $Wm^{-2}ppb^{-0.5}$<br>$M_0$ = 731.41 ppb | 0.55% (0.0032 $Wm^{-2}$) |

**Table 4 -** Overview of future scenario range of individual GHG concentrations. The table indicates the minimum and maximum surface air mole fra
across the 9 SSP scenarios considered in this study. For spreadsheets with annual data tables per scenario, see greenhousegases.science.unimelb.e
The third column indicates the region, with global ('GL'), Northern hemispheric ('NL') and Southern hemispheric ('SH') data shown for $CO_2$, CH
$N_2O$. The last three rows provide the equivalence concentrations. The CFC-11-eq concentrations summarize – in terms of radiative forcing equiva
all greenhouse gases aside from $CO_2$, $CH_4$, $N_2O$ and CFC-12. The CFC-12-eq concentrations summarize all the ozone depleting substances (
controlled under the Montreal Protocol, while HFC-134a-eq summarizes the remaining fluorinated gases. Altogether $CO_2$, $CH_4$, $N_2O$, CFC-12-e
HFC-134a-eq together represent the radiative forcing of the entirety of the 43 greenhouse gases considered here (cf. Table 5 in Meinshausen et al., 2

| GAS | UNIT | REG | 2015 | 2025 | 2050 | 2075 | 2100 | 2150 | 2200 | 2250 | 2300 |
|---|---|---|---|---|---|---|---|---|---|---|---|
| **$CO_2$** | ppm | GL | 399.9 | 426.5 - 432.4 | 437.6 - 562.8 | 419.7 - 801.7 | 393.5 - 1135.2 | 349 - 1737.3 | 343.4 - 2108.3 | 343.3 - 2206.4 | 342 - 2161.7 |
| | | NH | 401.7 | 428.2 - 434.9 | 437.8 - 567.2 | 419.5 - 808.5 | 392.9 - 1142.3 | 348.5 - 1742 | 343.4 - 2110.7 | 343.3 - 2206.4 | 342 - 2161.7 |
| | | SH | 398.2 | 424.9 - 429.9 | 437.5 - 558.3 | 419.9 - 794.9 | 394.1 - 1128.2 | 349.5 - 1732.6 | 343.4 - 2106 | 343.3 - 2206.3 | 342 - 2161.7 |
| **$CH_4$** | ppb | GL | 1841.9 | 1865.1 - 2049.1 | 1358.8 - 2503.7 | 1184.3 - 2934.1 | 999.7 - 3372.2 | 961.8 - 3096.2 | 927.6 - 2571.6 | 875.2 - 2107.1 | 864.4 - 1988.1 |
| | | NH | 1889.7 | 1910.3 - 2098.2 | 1400 - 2554.8 | 1224.3 - 2989.5 | 1038.8 - 3430.7 | 1000.6 - 3151.1 | 966.1 - 2622.8 | 913.1 - 2154.7 | 902.4 - 2035.7 |
| | | SH | 1794.1 | 1820 - 1999.9 | 1317.5 - 2452.5 | 1144.3 - 2878.7 | 960.6 - 3313.7 | 922.9 - 3041.3 | 889.1 - 2520.3 | 837.2 - 2059.5 | 826.4 - 1940.5 |
| **$N_2O$** | ppb | GL | 328.2 | 334.9 - 336.4 | 343.5 - 361.9 | 348.5 - 391 | 353.9 - 422.4 | 361.2 - 472.5 | 363.4 - 498.5 | 362.2 - 508.7 | 360 - 512 |
| | | NH | 328.5 | 335.1 - 336.7 | 343.8 - 362.2 | 348.8 - 391.3 | 354.2 - 422.7 | 361.5 - 472.8 | 363.7 - 498.8 | 362.5 - 509 | 360.3 - 512.3 |
| | | SH | 327.9 | 334.6 - 336.1 | 343.2 - 361.6 | 348.2 - 390.7 | 353.6 - 422.1 | 360.9 - 472.2 | 363.2 - 498.3 | 361.9 - 508.4 | 359.7 - 511.8 |
| **$SF_6$** | ppt | GL | 8.6 | 11.3 - 11.9 | 14.3 - 21.7 | 16.1 - 32.7 | 17.2 - 43.5 | 18.5 - 60.7 | 19.1 - 70.5 | 19.1 - 73.1 | 18.8 - 72 |
| **$NF_3$** | ppt | GL | 1.4 | 2.3 - 2.5 | 3.3 - 5.8 | 3.8 - 9.3 | 4 - 12.7 | 4.2 - 17.4 | 4.1 - 19.2 | 3.9 - 18.5 | 3.6 - 16.6 |
| **$SO_2F_2$** | ppt | GL | 2.1 | 2.8 - 3 | 2.4 - 4 | 1.6 - 4.4 | 1.1 - 4.1 | 0.5 - 2.9 | 0.2 - 1.8 | 0.1 - 0.8 | 0 - 0.2 |
| **$CF_4$** | ppt | GL | 81.8 | 88.3 - 89.7 | 96.1 - 106.3 | 99.2 - 123.2 | 101.3 - 136 | 103.8 - 154.6 | 105.3 - 165.7 | 105.7 - 169.4 | 105.6 - 169.2 |
| **$C_2F_6$** | ppt | GL | 4.5 | 5.1 - 5.2 | 5.7 - 6.9 | 5.8 - 8.6 | 5.8 - 10 | 5.8 - 12.2 | 5.8 - 13.4 | 5.7 - 13.8 | 5.7 - 13.7 |
| **$C_3F_8$** | ppt | GL | 0.6 | 0.7 - 0.8 | 0.9 - 1.1 | 0.9 - 1.5 | 0.9 - 1.8 | 0.9 - 2.2 | 0.9 - 2.5 | 0.9 - 2.6 | 0.9 - 2.5 |
| **c-$C_4F_8$** | ppt | GL | 1.4 | 1.7 - 1.8 | 2.1 - 2.6 | 2.2 - 3.5 | 2.3 - 4.1 | 2.4 - 5 | 2.5 - 5.5 | 2.5 - 5.6 | 2.4 - 5.5 |
| **$C_4F_{10}$** | ppt | GL | 0.2 | 0.2 - 0.2 | 0.2 - 0.3 | 0.2 - 0.3 | 0.2 - 0.4 | 0.2 - 0.5 | 0.2 - 0.5 | 0.2 - 0.5 | 0.2 - 0.5 |
| **$C_5F_{12}$** | ppt | GL | 0.1 | 0.1 - 0.1 | 0.1 - 0.2 | 0.1 - 0.2 | 0.1 - 0.2 | 0.1 - 0.2 | 0.1 - 0.2 | 0.1 - 0.2 | 0.1 - 0.2 |
| **$C_6F_{14}$** | ppt | GL | 0.3 | 0.3 - 0.4 | 0.4 - 0.5 | 0.4 - 0.7 | 0.4 - 0.8 | 0.4 - 1 | 0.4 - 1.1 | 0.4 - 1.1 | 0.4 - 1.1 |
| **$C_7F_{16}$** | ppt | GL | 0.1 | 0.2 - 0.2 | 0.2 - 0.3 | 0.2 - 0.3 | 0.2 - 0.4 | 0.2 - 0.5 | 0.2 - 0.6 | 0.2 - 0.6 | 0.2 - 0.6 |
| **$C_8F_{18}$** | ppt | GL | 0.1 | 0.1 - 0.1 | 0.1 - 0.1 | 0.1 - 0.2 | 0.1 - 0.2 | 0.1 - 0.2 | 0.1 - 0.3 | 0.1 - 0.3 | 0.1 - 0.3 |
| **HFC-23** | ppt | GL | 27.9 | 31.5 - 32 | 28.7 - 29.9 | 25.8 - 27 | 22.8 - 24.1 | 17.2 - 19.4 | 12.8 - 16 | 9.5 - 13.1 | 7.1 - 10.7 |

| | | | | | | | | | | | |
|---|---|---|---|---|---|---|---|---|---|---|---|
| **HFC-32** | ppt | GL | 9.8 | 6.5 - 7.5 | 0.1 - 0.7 | 0 - 0.2 | 0 - 0 | 0 - 0 | 0 - 0 | 0 - 0 | 0 - 0 |
| **HFC-43-10MEE** | ppt | GL | 0.3 | 0.3 - 0.3 | 0.1 - 0.4 | 0 - 0.4 | 0 - 0.4 | 0 - 0.2 | 0 - 0.1 | 0 - 0 | 0 - 0 |
| **HFC-125** | ppt | GL | 17.8 | 52.1 - 78.6 | 49.8 - 371.6 | 31.5 - 744.8 | 22.7 - 988.8 | 14.2 - 809.2 | 8.5 - 458.2 | 3.4 - 137 | 0.8 - 13.7 |
| **HFC-134A** | ppt | GL | 84.8 | 109.6 - 143.7 | 36.1 - 239.4 | 11.4 - 358 | 6.6 - 423.3 | 4.4 - 286.9 | 2.5 - 145.5 | 0.6 - 24.6 | 0 - 0.2 |
| **HFC-143A** | ppt | GL | 16.7 | 36.7 - 50.9 | 39 - 234.3 | 29.6 - 509.6 | 23.7 - 745.9 | 16.1 - 748.4 | 10.4 - 500.9 | 5.4 - 213.3 | 2.2 - 53.1 |
| **HFC-152A** | ppt | GL | 7.5 | 4.6 - 8.2 | 0.2 - 6.5 | 0.1 - 7.6 | 0.1 - 6.5 | 0.1 - 3.8 | 0 - 1.8 | 0 - 0.1 | 0 - 0 |
| **HFC-236FA** | ppt | GL | 0.1 | 0.2 - 0.3 | 0.3 - 1.3 | 0.3 - 3.1 | 0.3 - 5.3 | 0.3 - 7.9 | 0.3 - 8.2 | 0.2 - 6.7 | 0.2 - 4.9 |
| **HFC-227EA** | ppt | GL | 1.1 | 1.8 - 2.4 | 1.4 - 6.4 | 0.8 - 9.8 | 0.5 - 10.9 | 0.2 - 8.2 | 0.1 - 4.7 | 0 - 1.5 | 0 - 0.2 |
| **HFC-245FA** | ppt | GL | 2.2 | 3.6 - 5.8 | 1.1 - 18.4 | 0.5 - 34.5 | 0.5 - 39.1 | 0.4 - 24.5 | 0.2 - 12.1 | 0 - 1.3 | 0 - 0 |
| **HFC-365MFC** | ppt | GL | 0.9 | 1.2 - 1.6 | 0.2 - 2.5 | 0.1 - 3.8 | 0.1 - 4.3 | 0 - 2.7 | 0 - 1.3 | 0 - 0.2 | 0 - 0 |
| **$CCL_4$** | ppt | GL | 82.1 | 67.4 - 67.4 | 32.4 - 32.7 | 13.3 - 13.8 | 5 - 5.5 | 0.6 - 0.8 | 0.1 - 0.1 | 0 - 0 | 0 - 0 |
| **$CHCL_3$** | ppt | GL | 10.4 | 8.8 - 9.7 | 5.8 - 9.5 | 5.5 - 9 | 5.5 - 8.3 | 5.4 - 7.4 | 5.4 - 6.4 | 5.4 - 5.5 | 5.4 - 5.4 |
| **$CH_2CL_2$** | ppt | GL | 37.8 | 24.7 - 46.7 | 8 - 59.2 | 7.7 - 86.2 | 7.8 - 90 | 7.6 - 63 | 7.3 - 35.5 | 7.1 - 8 | 7.1 - 7.1 |
| **$CH_3CCL_3$** | ppt | GL | 3.2 | 0.4 - 0.4 | 0 - 0 | 0 - 0 | 0 - 0 | 0 - 0 | 0 - 0 | 0 - 0 | 0 - 0 |
| **$CH_3CL$** | ppt | GL | 549.8 | 546.5 - 577.6 | 466.1 - 582.4 | 425.6 - 566 | 421.6 - 556.5 | 418.5 - 536.2 | 394 - 509.7 | 363.7 - 479.1 | 358.2 - 475.9 |
| **$CH_3BR$** | ppt | GL | 6.7 | 6.5 - 6.9 | 5.3 - 6.9 | 5 - 6.8 | 4.9 - 6.6 | 4.7 - 6.3 | 4.6 - 5.9 | 4.4 - 5.5 | 4.4 - 5.5 |
| **CFC-11** | ppt | GL | 231.5 | 204.4 - 204.4 | 137.8 - 138.9 | 86.3 - 89.4 | 51.4 - 56.2 | 17.3 - 22.4 | 5.5 - 8.7 | 1.7 - 3.4 | 0.5 - 1.3 |
| **CFC-12** | ppt | GL | 518 | 471.6 - 471.7 | 364.3 - 366 | 277.6 - 283.6 | 208.7 - 220.2 | 114.3 - 133.5 | 61.2 - 81.4 | 32.5 - 49.6 | 17.3 - 30.3 |
| **CFC-113** | ppt | GL | 72.1 - 72.1 | 64.7 - 64.7 | 48.7 - 48.9 | 36.1 - 37 | 26.4 - 28 | 13.7 - 16.2 | 6.9 - 9.4 | 3.5 - 5.5 | 1.7 - 3.2 |
| **CFC-114** | ppt | GL | 16.3 - 16.3 | 15.8 - 15.8 | 13.9 - 13.9 | 12 - 12.1 | 10.3 - 10.6 | 7.5 - 8.1 | 5.4 - 6.2 | 3.8 - 4.7 | 2.7 - 3.6 |
| **CFC-115** | ppt | GL | 8.5 - 8.5 | 8.8 - 8.8 | 9.1 - 9.1 | 9 - 9 | 8.6 - 8.7 | 7.7 - 7.9 | 6.9 - 7.2 | 6.2 - 6.6 | 5.5 - 6 |
| **HCFC-22** | ppt | GL | 233.7 - 233.7 | 237.2 - 241.1 | 49.9 - 59.5 | 4.5 - 8.8 | 0.3 - 1.4 | 0 - 0 | 0 - 0 | 0 - 0 | 0 - 0 |
| **HCFC-141B** | ppt | GL | 24.2 - 24.2 | 27.2 - 27.7 | 14.1 - 16.2 | 3.5 - 5.2 | 0.8 - 1.4 | 0.3 - 0.5 | 0.2 - 0.3 | 0 - 0 | 0 - 0 |

| | | | | | | | | | | | |
|---|---|---|---|---|---|---|---|---|---|---|---|
| **HCFC-142B** | ppt | GL | 22.1 - 22.1 | 21.2 - 21.5 | 8.7 - 9.8 | 1.9 - 3 | 0.4 - 0.9 | 0 - 0.1 | 0 - 0 | 0 - 0 | 0 - 0 |
| **HALON-1211** | ppt | GL | 3.7 - 3.7 | 2.6 - 2.6 | 0.7 - 0.8 | 0.2 - 0.2 | 0 - 0 | 0 - 0 | 0 - 0 | 0 - 0 | 0 - 0 |
| **HALON-1301** | ppt | GL | 3.3 - 3.3 | 3.3 - 3.3 | 2.8 - 2.8 | 2.1 - 2.1 | 1.5 - 1.6 | 0.6 - 0.8 | 0.3 - 0.4 | 0.1 - 0.2 | 0 - 0.1 |
| **HALON-2402** | ppt | GL | 0.4 - 0.4 | 0.4 - 0.4 | 0.2 - 0.2 | 0.1 - 0.1 | 0 - 0 | 0 - 0 | 0 - 0 | 0 - 0 | 0 - 0 |
| **CFC-11-EQ** | ppt | GL | 818.9 - 818.9 | 848.9 - 908.6 | 528.3 - 1102.9 | 371 - 1599.7 | 305.6 - 1975 | 235 - 1698.5 | 189.8 - 1126.9 | 155 - 563.5 | 135.3 - 323.9 |
| **CFC-12-EQ** | ppt | GL | 1047.8 - 1047.9 | 967.1 - 969 | 627.8 - 637.9 | 433 - 444.4 | 320.6 - 329.5 | 175.3 - 197.1 | 99.2 - 124.3 | 58.4 - 82.2 | 38.7 - 57.5 |
| **HFC-134A-EQ** | ppt | GL | 271.1 - 271.1 | 388.3 - 485.4 | 327.5 - 1259.5 | 286.2 - 2274 | 277.9 - 2984.9 | 254.7 - 2638 | 223.2 - 1755.3 | 186.7 - 864 | 165.4 - 483.5 |

**Table 5 -** Overview of $CO_2$, $CH_4$ and $N_2O$ concentrations in the eight SSP scenarios considered in this study with global-average ('GL'), No hemispheric ('NH') and Southern hemispheric ('SH') surface air mole fractions. For annual and latitudinally resolved mole fractions and other green gases, see supplementary material or greenhousegases.science.unimelb.edu.au.

| SSP1-1.9 | | | 2015 | 2025 | 2050 | 2075 | 2100 | 2150 | 2200 | 2250 | 2300 | 2400 | 2500 |
|---|---|---|---|---|---|---|---|---|---|---|---|---|---|
| $CO_2$ | ppm | GL | 399.9 | 426.5 | 437.6 | 419.7 | 393.5 | 349.0 | 343.4 | 343.3 | 342.0 | 339.2 | 336.9 |
| | | NH | 401.7 | 428.2 | 437.8 | 419.5 | 392.9 | 348.5 | 343.4 | 343.3 | 342.0 | 339.2 | 336.9 |
| | | SH | 398.2 | 424.9 | 437.5 | 419.9 | 394.1 | 349.5 | 343.4 | 343.3 | 342.0 | 339.2 | 336.9 |
| $CH_4$ | ppb | GL | 1,842.0 | 1,875.2 | 1,427.9 | 1,184.3 | 1,036.4 | 969.8 | 928.9 | 881.3 | 1,112.0 | 870.9 | 871.4 |
| | | NH | 1,889.7 | 1,919.9 | 1,468.8 | 1,224.3 | 1,075.6 | 1,008.6 | 967.2 | 919.2 | 909.6 | 908.8 | 909.3 |
| | | SH | 1,794.2 | 1,830.6 | 1,387.0 | 1,144.3 | 997.2 | 931.1 | 890.5 | 843.4 | 833.8 | 833.0 | 833.5 |
| $N_2O$ | ppb | GL | 328.2 | 335.1 | 343.6 | 349.0 | 354.0 | 361.4 | 363.9 | 362.7 | 360.6 | 358.2 | 357.1 |
| | | NH | 328.5 | 335.4 | 343.8 | 349.3 | 354.3 | 361.7 | 364.2 | 363.0 | 360.9 | 358.5 | 357.4 |
| | | SH | 327.9 | 334.8 | 343.3 | 348.7 | 353.7 | 361.2 | 363.6 | 362.4 | 360.3 | 357.9 | 356.8 |
| **SSP1-2.6** | | | **2015** | **2025** | **2050** | **2075** | **2100** | **2150** | **2200** | **2250** | **2300** | **2400** | **2500** |
| $CO_2$ | ppm | GL | 399.9 | 427.7 | 469.3 | 471.0 | 445.6 | 411.1 | 403.2 | 399.7 | 396.0 | 389.5 | 384.3 |
| | | NH | 401.7 | 429.6 | 470.4 | 471.2 | 445.3 | 410.9 | 403.2 | 399.7 | 396.0 | 389.5 | 384.3 |
| | | SH | 398.2 | 425.7 | 468.2 | 470.8 | 445.9 | 411.4 | 403.2 | 399.7 | 396.0 | 389.4 | 384.3 |
| $CH_4$ | ppb | GL | 1,842.0 | 1,865.1 | 1,519.4 | 1,248.4 | 1,056.4 | 977.4 | 927.6 | 875.2 | 1,112.0 | 863.5 | 864.0 |
| | | NH | 1,889.7 | 1,910.3 | 1,561.5 | 1,288.8 | 1,095.9 | 1,016.4 | 966.1 | 913.1 | 902.4 | 901.5 | 901.9 |
| | | SH | 1,794.2 | 1,820.0 | 1,477.3 | 1,208.0 | 1,016.9 | 938.4 | 889.1 | 837.2 | 826.4 | 825.6 | 826.0 |
| $N_2O$ | ppb | GL | 328.2 | 334.9 | 343.5 | 348.5 | 353.9 | 361.2 | 363.4 | 362.2 | 360.0 | 357.5 | 356.4 |
| | | NH | 328.5 | 335.1 | 343.8 | 348.8 | 354.2 | 361.5 | 363.7 | 362.5 | 360.3 | 357.8 | 356.7 |
| | | SH | 327.9 | 334.6 | 343.2 | 348.2 | 353.6 | 360.9 | 363.2 | 361.9 | 359.7 | 357.2 | 356.1 |
| **SSP2-4.5** | | | **2015** | **2025** | **2050** | **2075** | **2100** | **2150** | **2200** | **2250** | **2300** | **2400** | **2500** |
| $CO_2$ | ppm | GL | 399.9 | 429.0 | 506.9 | 575.5 | 602.8 | 626.3 | 643.1 | 637.0 | 621.3 | 597.8 | 579.2 |
| | | NH | 401.7 | 431.2 | 509.2 | 577.3 | 603.6 | 626.8 | 643.4 | 637.0 | 621.3 | 597.8 | 579.2 |
| | | SH | 398.2 | 426.9 | 504.5 | 573.6 | 602.0 | 625.7 | 642.8 | 637.0 | 621.3 | 597.8 | 579.2 |
| $CH_4$ | ppb | GL | 1,841.9 | 1,960.7 | 2,020.2 | 1,815.7 | 1,683.2 | 1,479.6 | 1,255.4 | 1,038.1 | 1,112.0 | 999.2 | 997.3 |
| | | NH | 1,889.7 | 2,008.0 | 2,066.6 | 1,860.7 | 1,727.7 | 1,522.4 | 1,296.6 | 1,077.6 | 1,040.9 | 1,038.7 | 1,036.8 |

| | | | | | | | | | | | | | |
|---|---|---|---|---|---|---|---|---|---|---|---|---|---|
| | | SH | 1,794.2 | 1,913.3 | 1,973.9 | 1,770.8 | 1,638.6 | 1,436.7 | 1,214.2 | 998.6 | 961.8 | 959.7 | 957.8 |
| **$N_2O$** | ppb | GL | 328.2 | 336.0 | 356.2 | 371.5 | 377.3 | 378.3 | 375.9 | 371.4 | 367.0 | 362.0 | 359.8 |
| | | NH | 328.5 | 336.3 | 356.5 | 371.8 | 377.6 | 378.6 | 376.2 | 371.7 | 367.2 | 362.3 | 360.1 |
| | | SH | 327.9 | 335.7 | 355.9 | 371.2 | 377.0 | 378.0 | 375.6 | 371.1 | 366.7 | 361.7 | 359.5 |
| **SSP3-7.0** | | | **2015** | **2025** | **2050** | **2075** | **2100** | **2150** | **2200** | **2250** | **2300** | **2400** | **2500** |
| **$CO_2$** | ppm | GL | 399.9 | 432.3 | 540.6 | 683.0 | 867.2 | 1,235.3 | 1,456.8 | 1,513.7 | 1,482.8 | 1,423.6 | 1,371.1 |
| | | NH | 401.7 | 434.8 | 543.9 | 686.8 | 871.6 | 1,238.3 | 1,458.3 | 1,513.7 | 1,482.8 | 1,423.6 | 1,371.1 |
| | | SH | 398.2 | 429.9 | 537.3 | 679.2 | 862.8 | 1,232.4 | 1,455.3 | 1,513.6 | 1,482.7 | 1,423.6 | 1,371.1 |
| **$CH_4$** | ppb | GL | 1,841.9 | 2,006.5 | 2,472.0 | 2,934.1 | 3,372.2 | 3,096.2 | 2,571.6 | 2,107.1 | 1,112.0 | 1,959.1 | 1,938.4 |
| | | NH | 1,889.7 | 2,055.4 | 2,524.2 | 2,989.5 | 3,430.7 | 3,151.1 | 2,622.8 | 2,154.7 | 2,035.7 | 2,006.7 | 1,986.0 |
| | | SH | 1,794.2 | 1,957.7 | 2,419.8 | 2,878.7 | 3,313.7 | 3,041.3 | 2,520.3 | 2,059.5 | 1,940.5 | 1,911.5 | 1,890.8 |
| **$N_2O$** | ppb | GL | 328.2 | 336.4 | 361.8 | 390.7 | 421.8 | 471.4 | 497.2 | 507.2 | 510.5 | 514.3 | 516.0 |
| | | NH | 328.5 | 336.7 | 362.1 | 391.0 | 422.1 | 471.7 | 497.4 | 507.5 | 510.8 | 514.6 | 516.3 |
| | | SH | 327.9 | 336.1 | 361.5 | 390.4 | 421.5 | 471.1 | 496.9 | 506.9 | 510.2 | 514.0 | 515.7 |
| **SSP3-7.0-lowNTCF** | | | **2015** | **2025** | **2050** | **2075** | **2100** | **2150** | **2200** | **2250** | **2300** | **2400** | **2500** |
| **$CO_2$** | ppm | GL | 399.9 | 432.4 | 538.8 | 677.5 | 858.7 | 1,221.5 | 1,447.2 | 1,509.7 | 1,482.8 | 1,426.1 | 1,374.1 |
| | | NH | 401.7 | 434.9 | 542.2 | 681.4 | 863.2 | 1,224.6 | 1,448.7 | 1,509.7 | 1,482.8 | 1,426.1 | 1,374.1 |
| | | SH | 398.2 | 429.9 | 535.5 | 673.5 | 854.1 | 1,218.5 | 1,445.7 | 1,509.7 | 1,482.7 | 1,426.1 | 1,374.1 |
| **$CH_4$** | ppb | GL | 1,841.9 | 1,940.3 | 1,358.8 | 1,202.5 | 1,219.9 | 1,203.5 | 1,164.6 | 1,129.1 | 1,112.0 | 1,088.0 | 1,068.8 |
| | | NH | 1,889.7 | 1,985.6 | 1,400.0 | 1,244.0 | 1,262.1 | 1,245.3 | 1,205.9 | 1,170.1 | 1,152.9 | 1,129.0 | 1,109.8 |
| | | SH | 1,794.2 | 1,895.0 | 1,317.5 | 1,161.0 | 1,177.8 | 1,161.8 | 1,123.2 | 1,088.2 | 1,071.0 | 1,047.1 | 1,027.9 |
| **$N_2O$** | ppb | GL | 328.2 | 336.4 | 361.9 | 391.0 | 422.4 | 472.5 | 498.5 | 508.7 | 512.0 | 515.8 | 517.5 |
| | | NH | 328.5 | 336.7 | 362.2 | 391.3 | 422.7 | 472.8 | 498.8 | 509.0 | 512.3 | 516.1 | 517.8 |
| | | SH | 327.9 | 336.1 | 361.6 | 390.7 | 422.1 | 472.2 | 498.3 | 508.4 | 511.8 | 515.5 | 517.2 |
| **SSP4-3.4** | | | **2015** | **2025** | **2050** | **2075** | **2100** | **2150** | **2200** | **2250** | **2300** | **2400** | **2500** |

| | | | | | | | | | | | | | |
|---|---|---|---|---|---|---|---|---|---|---|---|---|---|
| **$CO_2$** | ppm | GL | 399.9 | 427.3 | 472.9 | 490.2 | 473.4 | 408.8 | 396.2 | 395.2 | 392.4 | 387.5 | 383.4 |
| | | NH | 401.7 | 429.3 | 474.0 | 490.3 | 472.5 | 408.0 | 396.2 | 395.2 | 392.4 | 387.5 | 383.4 |
| | | SH | 398.2 | 425.3 | 471.8 | 490.1 | 474.3 | 409.5 | 396.2 | 395.2 | 392.4 | 387.5 | 383.4 |
| **$CH_4$** | ppb | GL | 1,841.9 | 2,030.9 | 2,223.4 | 2,370.0 | 2,336.3 | 2,177.6 | 2,023.8 | 1,842.7 | 1,112.0 | 1,786.8 | 1,786.2 |
| | | NH | 1,889.7 | 2,078.9 | 2,271.3 | 2,417.9 | 2,383.2 | 2,223.4 | 2,068.6 | 1,886.6 | 1,832.2 | 1,830.7 | 1,830.1 |
| | | SH | 1,794.1 | 1,983.0 | 2,175.4 | 2,322.2 | 2,289.5 | 2,131.7 | 1,978.9 | 1,798.8 | 1,744.5 | 1,743.0 | 1,742.3 |
| **$N_2O$** | ppb | GL | 328.2 | 335.7 | 353.9 | 373.7 | 394.7 | 425.2 | 441.1 | 446.8 | 448.2 | 449.9 | 450.7 |
| | | NH | 328.5 | 336.0 | 354.2 | 374.0 | 395.0 | 425.5 | 441.3 | 447.1 | 448.5 | 450.2 | 451.0 |
| | | SH | 327.9 | 335.4 | 353.6 | 373.4 | 394.4 | 424.9 | 440.8 | 446.5 | 447.9 | 449.6 | 450.4 |
| **SSP4-6.0** | | | **2015** | **2025** | **2050** | **2075** | **2100** | **2150** | **2200** | **2250** | **2300** | **2400** | **2500** |
| **$CO_2$** | ppm | GL | 399.9 | 428.3 | 515.6 | 606.9 | 668.4 | 741.0 | 783.9 | 786.2 | 768.7 | 739.1 | 714.0 |
| | | NH | 401.7 | 430.5 | 518.2 | 609.2 | 669.7 | 741.8 | 784.3 | 786.2 | 768.7 | 739.1 | 714.0 |
| | | SH | 398.2 | 426.0 | 513.0 | 604.7 | 667.1 | 740.1 | 783.4 | 786.2 | 768.7 | 739.1 | 714.0 |
| **$CH_4$** | ppb | GL | 1,841.9 | 2,049.1 | 2,503.7 | 2,688.5 | 2,645.5 | 2,382.6 | 2,111.4 | 1,864.6 | 1,112.0 | 1,791.0 | 1,785.6 |
| | | NH | 1,889.7 | 2,098.2 | 2,554.8 | 2,739.6 | 2,695.8 | 2,431.2 | 2,158.3 | 1,909.8 | 1,844.7 | 1,836.3 | 1,830.9 |
| | | SH | 1,794.1 | 1,999.9 | 2,452.5 | 2,637.3 | 2,595.3 | 2,334.1 | 2,064.4 | 1,819.3 | 1,754.1 | 1,745.7 | 1,740.4 |
| **$N_2O$** | ppb | GL | 328.2 | 335.9 | 359.7 | 383.4 | 404.7 | 435.8 | 451.2 | 456.1 | 456.8 | 457.7 | 458.1 |
| | | NH | 328.5 | 336.2 | 360.0 | 383.7 | 405.0 | 436.1 | 451.4 | 456.4 | 457.1 | 457.9 | 458.4 |
| | | SH | 327.9 | 335.6 | 359.4 | 383.2 | 404.4 | 435.5 | 450.9 | 455.8 | 456.5 | 457.4 | 457.8 |
| **SSP5-3.4-OS** | | | **2015** | **2025** | **2050** | **2075** | **2100** | **2150** | **2200** | **2250** | **2300** | **2400** | **2500** |
| **$CO_2$** | ppm | GL | 399.9 | 432.2 | 549.3 | 554.5 | 496.6 | 409.4 | 404.7 | 401.8 | 398.5 | 392.4 | 387.5 |
| | | NH | 401.7 | 434.7 | 551.9 | 553.8 | 495.6 | 408.7 | 404.7 | 401.8 | 398.5 | 392.4 | 387.5 |
| | | SH | 398.2 | 429.7 | 546.7 | 555.1 | 497.7 | 410.1 | 404.7 | 401.8 | 398.5 | 392.4 | 387.5 |
| **$CH_4$** | ppb | GL | 1,841.9 | 1,964.3 | 2,125.1 | 1,205.4 | 999.7 | 961.8 | 941.9 | 916.8 | 1,112.0 | 910.5 | 910.6 |
| | | NH | 1,889.7 | 2,012.6 | 2,168.8 | 1,245.2 | 1,038.8 | 1,000.6 | 980.5 | 955.2 | 950.1 | 948.9 | 948.9 |
| | | SH | 1,794.2 | 1,916.0 | 2,081.4 | 1,165.5 | 960.6 | 922.9 | 903.3 | 878.5 | 873.4 | 872.2 | 872.2 |
| **$N_2O$** | ppb | GL | 328.2 | 336.3 | 356.3 | 371.1 | 383.8 | 398.4 | 404.7 | 405.1 | 403.6 | 401.9 | 401.1 |
| | | NH | 328.5 | 336.6 | 356.6 | 371.4 | 384.1 | 398.7 | 405.0 | 405.4 | 403.9 | 402.1 | 401.4 |
| | | SH | 327.9 | 336.0 | 356.1 | 370.8 | 383.6 | 398.1 | 404.4 | 404.8 | 403.3 | 401.6 | 400.8 |

| SSP5-8.5 | | | 2015 | 2025 | 2050 | 2075 | 2100 | 2150 | 2200 | 2250 | 2300 | 2400 | 2500 |
|---|---|---|---|---|---|---|---|---|---|---|---|---|---|
| **$CO_2$** | ppm | GL | 399.9 | 431.8 | 562.8 | 801.7 | 1,135.2 | 1,737.3 | 2,108.3 | 2,206.4 | 2,161.7 | 2,080.5 | 2,010.0 |
| | | NH | 401.7 | 434.3 | 567.2 | 808.5 | 1,142.3 | 1,742.0 | 2,110.7 | 2,206.4 | 2,161.7 | 2,080.5 | 2,010.0 |
| | | SH | 398.2 | 429.4 | 558.3 | 794.9 | 1,128.2 | 1,732.6 | 2,106.0 | 2,206.3 | 2,161.7 | 2,080.5 | 2,010.0 |
| **$CH_4$** | ppb | GL | 1,841.9 | 1,954.5 | 2,446.5 | 2,672.3 | 2,415.3 | 1,906.9 | 1,515.6 | 1,157.3 | 1,112.0 | 1,038.5 | 1,019.0 |
| | | NH | 1,889.7 | 2,002.6 | 2,499.2 | 2,724.9 | 2,465.2 | 1,953.8 | 1,559.4 | 1,198.1 | 1,109.0 | 1,079.3 | 1,059.8 |
| | | SH | 1,794.2 | 1,906.4 | 2,393.7 | 2,619.6 | 2,365.5 | 1,860.1 | 1,471.8 | 1,116.5 | 1,027.4 | 997.7 | 978.2 |
| **$N_2O$** | ppb | GL | 328.2 | 336.3 | 358.2 | 377.1 | 391.8 | 407.8 | 413.6 | 413.0 | 410.5 | 407.8 | 406.6 |
| | | NH | 328.5 | 336.6 | 358.5 | 377.4 | 392.1 | 408.1 | 413.9 | 413.3 | 410.8 | 408.1 | 406.9 |
| | | SH | 327.9 | 336.0 | 357.9 | 376.8 | 391.5 | 407.5 | 413.3 | 412.7 | 410.2 | 407.5 | 406.3 |

76

***Table 6 -*** Fraction of greenhouse gas induced forcing due to $CO_2$ concentrations in SSP scenarios at the point of maximal greenhouse gas induced forcing until 2300 (upper row) or in year 2100 (lower row)

| | SSP1-1.9 | SSP1-2.6 | SSP4-3.4 | SSP2-4.5 | SSP4-6.0 | SSP3-7.0 | SSP5-8.5 | SSP3-7.0-lowntcf | SSP5-3.4-OS |
|---|---|---|---|---|---|---|---|---|---|
| **Point of maximal GHG forcing over 2000 to 2300** | 68% | 74% | 70% | 83% | 81% | 86% | 92% | 90% | 75% |
| **2100** | 76% | 80% | 68% | 79% | 76% | 77% | 82% | 85% | 82% |

**Table 7 -** SSP Global Mean Surface Air Temperature (GMSAT) and Global Mean Sea Level Rise (GMSLR) projections for the end of the 21st century (2081-2100 average and 2100 estimate) and 2300. GMSAT is shown in Kelvin relative to 1750, GMSLR is shown in metres relative to the 1986-2005 average. Mean and 5th to 95th percentiles are provided for both variables.

| | GMT in K | | | GMSLR in m | | |
|---|---|---|---|---|---|---|
| | 2081-2100 | 2100 | 2300 | 2081-2100 | 2100 | 2300 |
| SSP1-1.9 | 1.2 (0.6 to 1.8) | 1.1 (0.6 to 1.8) | 0.6 (0.1 to 1.3) | 0.44 (0.30 to 0.62) | 0.47 (0.32 to 0.65) | 0.80 (0.54 to 1.19) |
| SSP1-2.6 | 1.6 (1.0 to 2.4) | 1.6 (0.9 to 2.4) | 1.3 (0.6 to 2.4) | 0.49 (0.35 to 0.69) | 0.53 (0.37 to 0.73) | 1.07 (0.69 to 1.60) |
| SSP2-4.5 | 2.6 (1.7 to 3.8) | 2.8 (1.8 to 4.1) | 3.8 (1.7 to 6.7) | 0.59 (0.41 to 0.82) | 0.66 (0.46 to 0.89) | 2.02 (1.13 to 3.12) |
| SSP4-3.4 | 2.0 (1.3 to 3.1) | 2.1 (1.3 to 3.2) | 1.8 (0.9 to 3.3) | 0.53 (0.36 to 0.75) | 0.58 (0.40 to 0.81) | 1.30 (0.82 to 1.98) |
| SSP3-7.0 | 3.8 (2.6 to 5.7) | 4.4 (3.0 to 6.5) | 9.8 (5.5 to >15**) | 0.68 (0.47 to 0.95) | 0.79 (0.56 to 1.07) | 4.51 (2.36 to 8.51) |
| SSP3-LowNTCF | 3.4 (2.3 to 5.1) | 3.9 (2.6 to 5.8) | 9.5 (5.3 to >15**) | 0.64 (0.45 to 0.89) | 0.74 (0.53 to 1.00) | 4.22 (2.22 to 7.63) |
| SSP4-6.0 | 3.3 (2.2 to 4.9) | 3.6 (2.4 to 5.3) | 6.0 (2.9 to 10.8) | 0.65 (0.45 to 0.90) | 0.74 (0.53 to 1.00) | 2.87 (1.53 to 4.72) |
| SSP5-3.4-OS | 2.1 (1.2 to 3.1) | 1.9 (1.1 to 3.0) | 1.1 (0.3 to 2.3) | 0.58 (0.40 to 0.81) | 0.62 (0.42 to 0.87) | 1.08 (0.66 to 1.68) |
| SSP5-8.5 | 5.0 (3.3 to 7.6) | 5.8 (3.8 to 8.6) | 10.8 (6.4 to >15**) | 0.79 (0.54 to 1.13) | 0.94 (0.66 to 1.29) | 5.31 (2.86 to 10.31) |

** MAGICC has an internal cutoff temperature in each land-ocean and hemispheric box at 25K. Any temperatures indications beyond 10K should be considered illustrative only given that the calibrated range of MAGICC covers only lower temperature levels.

## 11 Figures Captions

**Figure 1 -** The SSP scenarios and their five socio-economic SSP families. Shown are illustrative temperature levels relative to pre-industrial levels with historical temperatures (front band), current (2020) temperatures (small block in middle) and the branching of the respective scenarios over the 21st century along the five different socio-economic families. The small black horizontal bars on the 2100 pillars for each SSP indicate illustrative temperature levels (obtained by the MAGICC7.0 default setting used to produce the GHG concentrations) for the range of SSP scenarios that were available from the IAM community at the time of creating the benchmark SSP scenarios. The more opaque bands over the 21st century indicate the five SSP scenarios SSP1-1.9, SSP1-2.6, SSP2-4.5, SSP3-7.0 and SSP5-8.5 that are used as priority scenarios in IPCC. The more transparent bands indicate the remaining "Tier 2" SSP scenarios, namely SSP3-7.0-LowNTCF (used in AerChemMIP), SSP4-3.4, SSP4-6.0, and SSP5-3.4-OS. Also shown is a blue indicative bar on the right side, indicating the effect of mitigation action, which reduces temperature levels in 2100 and throughout the 21st century - depending on the respective reference scenario and level of mitigation.

**Figure 2 -** ~~Extensions of SSP~~The anthropogenic emission scenarios to derive SSP concentration scenarios for $CO_2$ (panels a-c), $CH_4$ (d to e), nitrous oxide (f), $NF_3$ (g) and $SF_6$ (panel i). Shown are the four SSP scenarios for which long-term CMIP6 model experiments are planned (bold lines with color-box labels), namely for SSP5-8.5 (red), SSP5-34-OS (orange), SSP1-2.6 (blue) and SSP1-1.9 (turquoise). Also shown are RCP extensions (Meinshausen et al., 2011b), and those of other SSP scenarios following the same design principles (see text). While the design principles for $CO_2$ emissions are specific, other gases from fossil and industrial sources are assumed to be phased out by 2225, and landuse-related emissions are assumed to stay constant at their 2100 values. The pre-2100 emission scenarios are derived from harmonised Integrated assessment scenarios, while the post-2100 extensions follow simple extension assumptions.

**Figure 3 -** The assumed permafrost related emissions by using MAGICC's permafrost module in its default settings for the SSP GHG concentration projections, close to the median of the probabilistic MAGICC permafrost version (Schneider von Deimling et al., 2012). In

the highest scenario, SSP5-8.5, $CO_2$ and $CH_4$ concentrations by 2300 would have been about 250 ppm and 150 ppb, respectively, lower without including the permafrost module (panel a and b). The additional $CO_2$ from mineral soil and peatland carbon decomposition reach a maximum in the highest scenario SSP5-8.5 around 2140 of about 3 GtC emissions per year (panel c), mainly due to the aerobic mineral soil decomposition (panel e). The mineral and peatland soil decomposition under aerobic conditions (panels e and g, respectively), and also the oxidised part of the methane that originates from the anaerobic decomposition (panels f and h) contribute to the net $CO_2$ emissions from permafrost thawing. The permafrost zonal bands are a simplified approach to represent the range of thawing thresholds and permafrost carbon contents and are described in Schneider von Deimling et al. (2012). See ***Table 2*** ~~***Table 2***~~ for cumulative emissions.

**Figure 4 -** Simplified parameterisation to emulate 48 Oslo Line by line model results (bright blue open numbered circles). Shown are the IPCC TAR simplified formula for $CO_2$ (three options), $CH_4$ and $N_2O$ forcing with their default parameter settings (grey-blue lines) in the background. The simplified formula results by Etminan (2016) are shown as orange lines. Adjusting pre-industrial concentration values to default 1750 values improves the fit of the Etminan simplified formula (red lines in panels a to c and red error terms in panel d). This study's simplified formula results are shown in green, matching the Oslo-line-by-line model results within rounding – and continuing a forcing approximation beyond 2000 ppm $CO_2$ in line with previously derived formulas (red dashed circle in panel a). See text.

**Figure 5 -** $CO_2$ concentrations under the SSP1-1.9 scenario. The base seasonality pattern derived from historical observations with monthly and 15° latitudinal resolution (panel a) is modulated over time using the first EOF of the residuals (panel a.1), scaled with projected NPP into the future (panel a.2). The latitudinal gradient is assumed flat in pre-industrial times, with latitudinal gradients over the observational record being derived from historical observations – and here compared with CMIP5 ESM models – see Meinshausen et al. (2017) (panel b). The projection of the latitudinal gradient uses global total $CO_2$ emissions regressed against the score (dark blue line in panel d) of the first latitudinal EOF (dark blue line in panel c). The principal component's score of the second EOF's is assumed zero in the future (turquoise line in panel c,d). Resulting surface air mole fractions fields show a return to current $CO_2$ (~2019) concentrations by the end of the 21$^{st}$ century (panel e and f). Historical NOAA surface flask station datasets (grey dots in panels f, g, h with station indicators provided in legend of panel f) are used for these future projections beyond the end of 2014 reach of the historical dataset (grey shaded background

in panels f, g, h). Various comparison datasets shown, namely the WDCGG timeseries (Tsutsumi et al., 2009), the NOAA Marine Boundary Layer (MBL) product (https://www.esrl.noaa.gov/gmd/ccgg/mbl/) and the NASA AQUA satellite data (ftp://acdisc.gsfc.nasa.gov/ftp/data/s4pa/Aqua_AIRS_Level3/AIRX3C2M.005/), the Petrenko timeseries (made available in the supplement to Buizert et al. (2012). Also shown are the MAGICC global-mean projections (bright blue line "MAGICCconc"). These overview figures are available for all 43 gases and all 9 scenarios on greenhousegases.science.unimelb.edu.au as a total of 387 so-called factsheets. See also Table 12 in Meinshausen (2017) for a description of all data labels.

**Figure 6 -** Transition between historical runs and future SSP concentrations for $CO_2$ (panel a), $CH_4$ (panel b) and $N_2O$ (panel c) surface mole fractions. The observational in situ and flask station datapoints reach into the first years of the future SSP datasets (grey dots). Derived northern-hemispheric (orange), global (black) and Southern hemispheric averages (blue) are shown with annual averages (thick lines) and monthly averages (thin lines with seasonality variability). On the right axis side, the illustrative arrows indicate the min-max range across the scenarios for Northern hemispheric, global and Southern hemispheric annual-average concentrations by 2030 across all 9 SSP scenarios. The NOAA/AGAGE global mean dataseries are shown in green. For description of labels of other comparison data, see Table 12 in Meinshausen (2017).

**Figure 7 -** Overview of all greenhouse gases within SSP scenarios and their relative importance in terms of radiative forcing. The radiative forcing contributions are stacked, starting with $CO_2$ (blue shaded area) at the bottom, followed by methane ($CH_4$), nitrous oxide ($N_2O$) and the other 40 greenhouse gases. Default radiative forcing efficiencies or parameterisations are used, with $CO_2$, $CH_4$ and $N_2O$ being based on a parameterisation of the Oslo-line-by-line model (section 2.7). Seasonal and latitudinal variation is indicated by the three bars on the right of each panel for the global average, northern hemispheric and southern hemispheric monthly mean concentrations for the year 2100. The light-blue shaded areas on the left side of each panel from 1750 to 2014 are based on historical greenhouse gas observations, the 21$^{st}$ century span from 2015 to 2100 (white area) and the extension until 2300 and beyond is based on the MAGICC7.0 model. For the IPCC

AR6, the five scenarios SSP1-1.9 (panel a), SSP1-2.6 (b), SSP2-4.5 (d), SSP3-7.0 (g) and SSP5-8.5 (i) are chosen as key scenarios for knowledge integration across chapters and Working Groups.

**Figure 8 -** Overview of SSP concentrations of $CO_2$, $CH_4$ and $N_2O$ in the context of the historical observational dataset. For the respective main ice core and firn datasets (WAIS, Law Dome, EPICA DML etc.), please see Figure 6b in Meinshausen et al. (2017). The 21st century is shown as grey vertical band.

**Figure 9 –** The 2050 $CO_2$ and $CH_4$ concentrations of SSPs (dark blue circles), RCP (orange circles) and scenarios of the IPCC Special Report on 1.5C warming database (grey dots). All scenarios' concentrations were derived by using the SSP or RCP or SR1.5 harmonised emission scenarios together with the same MAGICC7.0 default settings as used for the CMIP6 SSP concentration projections.

**Figure 10** - Atmospheric surface air mole fractions of four CFCs, namely CFC-12 (panel a), CFC-11 (panel b), CFC-113 (panel c) and CFC-114 (panel c). This study's Northern hemispheric averages (orange lines), Southern hemispheric averages (blue lines) and global averages (black lines) are shown in comparison with recent measurements of the NOAA and/or AGAGE networks (grey dots), the global averages derived by Montzka et al. (2018) and the projections by Velders and Daniel (2014b) (dashed lines with diamond markers). The latter can be seen as near-lifetime limited projections whereas observations hint to recent (since 2012) emissions increases , leading to a slower-than-projected fall in global atmospheric concentrations. For an exploration of CFC-11's decline rates, see the recent studies by Montzka et al. (2018) and Rigby et al. (2019). Note that the high "outlier" monthly mean values for CFC-11 and CFC-114 are primarily from the AGAGE Gosan station and include all data, i.e., so-called "pollution" events in which case temporary high concentration air masses pass the measurement station. The apparent disappearance of those high pollution events at the end of 2015 is due to that particular AGAGE data timeseries only having been available until then at the point of this analysis, although a recent publication (Rigby et al., 2019) shows that these enhancements continued at least through 2017.

**Figure 11 -** Overview of SSP concentrations in comparison with RCP concentrations for $CO_2$, $CH_4$ and $N_2O$. The original RCP scenarios are shown in thicker black lines and various linestyles. Applying the new MAGICC7 default setting used for the SSP scenarios to the RCP emissions results in generally higher concentrations (grey lines).

~~**Figure 12 -** Comparison of illustrative Global Mean Surface Air Temperature (GMSAT) (panel a) and global mean sea level rise (SLR) projections (panel b) under SSP and RCP scenarios. The global mean temperatures are given relative to pre-industrial (1750) levels, normalized to 0.92 C over the 1995-2014 period. Time series for the time period 2000-2100 are shown for the nine SSPs relative to 1750 with bold solid lines indicating the higher priority SSP scenarios and thin dashed lines indicating other so-called "Tier 2" scenarios. Shaded areas indicate the 5%-95% confidence intervals for each scenario. Bar plots illustrate the 2081-2100 average relative to 1750 for the nine SSPs (yellow shaded area with barplots), and the RCP scenarios, using the same MAGICC7.0 setup (left light grey shaded bar plot area) and a former MAGICC6 setup used at the time of IPCC AR5 (right light grey area). We also show the likely range of temperature and sea level rise averages as reported in IPCC AR5 for that period - based on multiple lines of evidence (dark grey shaded set of barplots on the right). Observational data for global mean surface temperatures (GMST), normalized over the same 1986-2005 period, is shown for Berkeley Earth (black solid), Cowtan & Way (Cowtan and Way, 2014) (long dashed), HadCRUT4 (Morice et al., 2012;Brohan et al., 2006) (small dashes) and NASA GISS (Lenssen et al., 2019)(dash dotted). Observational data for sea level rise is taken from NASA (Beckley et al., 2010).~~

**Figure 12~~13~~** - Warming signal induced by latitudinally and seasonally resolved GHG concentrations ("lat_mon") compared to an annually and global-mean uniform GHG concentrations ("yearmean_global") in an Earth System Model, namely CESM1.2.2 (Hurrell et al., 2013). We averaged the full historical scenario from 1850 to 2005 across all 6 ensemble members in each setup ("lat_mon" and "yearmean_global") and produced the averages for the December-January-February DJF average (panel a) and the March-April-May averages (b). The latitudinally averaged warming signals that result from using spatially and temporarily resolved GHG concentrations are

shown in the lower panels (thick blue lines), here compared against comparable one hundred differenced pairs of 930-year long control run segments (thin grey lines). In the high upper North during the MAM season, ~~approximately 97 of the 100~~the comparison with control run segment differences ~~are lower~~suggest that these ESM model results show a significant warming at the 5% level, given that only 3 to 5 of the 100 control run differences are higher.

## 12 References


Beckley, B. D., Zelensky, N. P., Holmes, S. A., Lemoine, F. G., Ray, R. D., Mitchum, G. T., Desai, S. D., and Brown, S. T.: Assessment of the Jason-2 Extension to the TOPEX/Poseidon, Jason-1 Sea-Surface Height Time Series for Global Mean Sea Level Monitoring, Marine Geodesy, 33, 447-471, 10.1080/01490419.2010.491029, 2010.

Brohan, P., Kennedy, J. J., Harris, I., Tett, S. F. B., and Jones, P. D.: Uncertainty estimates in regional and global observed temperature changes: A new data set from 1850, J. Geophys. Res.-Atmos., 111, D12106, 10.1029/2005JD006548, 2006.

Buizert, C., Martinerie, P., Petrenko, V. V., Severinghaus, J. P., Trudinger, C. M., Witrant, E., Rosen, J. L., Orsi, A. J., Rubino, M., Etheridge, D. M., Steele, L. P., Hogan, C., Laube, J. C., Sturges, W. T., Levchenko, V. A., Smith, A. M., Levin, I., Conway, T. J., Dlugokencky, E. J., Lang, P. M., Kawamura, K., Jenk, T. M., White, J. W. C., Sowers, T., Schwander, J., and Blunier, T.: Gas transport in firn: multiple-tracer characterisation and model intercomparison for NEEM, Northern Greenland, Atmos. Chem. Phys., 12, 4259-4277, 10.5194/acp-12-4259-2012, 2012.

Butchart, N., and Scaife, A. A.: Removal of chlorofluorocarbons by increased mass exchange between the stratosphere and troposphere in a changing climate, Nature, 410, 799-802, 2001.

Collins, W. J., Lamarque, J. F., Schulz, M., Boucher, O., Eyring, V., Hegglin, M. I., Maycock, A., Myhre, G., Prather, M., Shindell, D., and Smith, S. J.: AerChemMIP: quantifying the effects of chemistry and aerosols in CMIP6, Geosci. Model Dev., 10, 585-607, 10.5194/gmd-10-585-2017, 2017.

Cowtan, K., and Way, R. G.: Coverage bias in the HadCRUT4 temperature series and its impact on recent temperature trends, Quarterly Journal of the Royal Meteorological Society, 140, 1935-1944, 2014.

Cunnold, D., Steele, L., Fraser, P., Simmonds, P., Prinn, R., Weiss, R., Porter, L., O'Doherty, S., Langenfelds, R., and Krummel, P.: In situ measurements of atmospheric methane at GAGE/AGAGE sites during 1985–2000 and resulting source inferences, Journal of Geophysical Research: Atmospheres, 107, 2002.

DeConto, R. M., and Pollard, D.: Contribution of Antarctica to past and future sea-level rise, Nature, 531, 591, 2016.

Dlugokencky, E. J., P.M. Lang, A.M. Crotwell, K.A. Masarie, and M.J. Crotwell: Atmospheric Methane Dry Air Mole Fractions from the NOAA ESRL Carbon Cycle Cooperative Global Air Sampling Network, 1983-2014. NOAA (Ed.), 2015a.

Dlugokencky, E. J., P.M. Lang, K.A. Masarie, A.M. Crotwell, M.J. Crotwell: Atmospheric Carbon Dioxide Dry Air Mole Fractions from the NOAA ESRL Carbon Cycle Cooperative Global Air Sampling Network, 1968-2014. NOAA (Ed.), 2015b.

Durack, P. J., and Taylor, K.: CMIP6 Forcing datasets summary, http://goo.gl/r8up31, 46, 2019.

Edwards, T. L., Brandon, M. A., Durand, G., Edwards, N. R., Golledge, N. R., Holden, P. B., Nias, I. J., Payne, A. J., Ritz, C., and Wernecke, A.: Revisiting Antarctic ice loss due to marine ice-cliff instability, Nature, 566, 58, 2019.

Ehhalt, D., Prather, M. J., Dentener, F., Derwent, R. G., Dlugokencky, E., Holland, E., Isaksen, I. S. A., Katima, J., Kirchhoff, V., Matson, P., Midgley, P., and Wang, M.: Atmospheric Chemistry and Greenhouse Gases, in: Climate Change 2001: The Scientific Basis, edited by: Houghton, J. T., Ding, Y., Griggs, D. J., Noguer, M., van der Linden, P. J., Dai, X., Maskell, K., and Johnson, C. A., Cambridge University Press, Cambridge, UK, 892, 2001.

Engel, A., Rigby, M., Burkholder, J. B., Fernandez, R. P., Froidevaux, L., Hall, B. D., Hossaini, R., Saito, T., Vollmer, M. K., and Yao, B.: Update on Ozone-Depleting Substances (ODCss) and Other Gases of Interest to the Montreal Protocol, Chapter 1, in: Scientific Assessment of Ozone Depletion: 2018, World Meterological Organization, Geneva, Switzerland, 2018.

Etminan, M., Myhre, G., Highwood, E., and Shine, K.: Radiative forcing of carbon dioxide, methane, and nitrous oxide: A significant revision of the methane radiative forcing, Geophysical Research Letters, 43, 2016.

Eyring, V., Bony, S., Meehl, G. A., Senior, C. A., Stevens, B., Stouffer, R. J., and Taylor, K. E.: Overview of the Coupled Model Intercomparison Project Phase 6 (CMIP6) experimental design and organization, Geosci. Model Dev., 9, 1937-1958, 10.5194/gmd-9-1937-2016, 2016.

Fang, X., Park, S., Saito, T., Tunnicliffe, R., Ganesan, A. L., Rigby, M., Li, S., Yokouchi, Y., Fraser, P. J., Harth, C. M., Krummel, P. B., Mühle, J., O'Doherty, S., Salameh, P. K., Simmonds, P. G., Weiss, R. F., Young, D., Lunt, M. F., Manning, A. J., Gressent, A., and Prinn, R. G.: Rapid increase in ozone-depleting chloroform emissions from China, Nature Geoscience, 12, 89-93, 10.1038/s41561-018-0278-2, 2019.

Forkel, M., Carvalhais, N., Rödenbeck, C., Keeling, R., Heimann, M., Thonicke, K., Zaehle, S., and Reichstein, M.: Enhanced seasonal CO2 exchange caused by amplified plant productivity in northern ecosystems, Science, aac4971, 2016.

Friedlingstein, P., Cox, P., Betts, R., Bopp, L., von Bloh, W., Brovkin, V., Cadule, P., Doney, S., Eby, M., Fung, I., Bala, G., John, J., Jones, C., Joos, F., Kato, T., Kawamiya, M., Knorr, W., Lindsay, K., Matthews, H. D., Raddatz, T., Rayner, P., Reick, C., Roeckner, E., Schnitzler, K.-G., Schnur, R., Strassmann, K., Weaver, K., Yoshikawa, C., and Zeng, N.: Climate–Carbon Cycle Feedback Analysis: Results from the C4MIP Model Intercomparison, Journal of Climate, 19, 3337-3353, 10.1175/JCLI3800.1, 2006.

Friedlingstein, P., Meinshausen, M., Arora, V. K., Jones, C. D., Anav, A., Liddicoat, S. K., and Knutti, R.: Uncertainties in CMIP5 Climate Projections due to Carbon Cycle Feedbacks, Journal of Climate, 27, 511-526, 10.1175/jcli-d-12-00579.1, 2014.

Frieler, K., Meinshausen, M., Golly, A., Mengel, M., Lebek, K., Donner, S. D., and Hoegh-Guldberg, O.: Limiting global warming to 2 degrees C is unlikely to save most coral reefs, Nature Climate Change, 3, 165-170, 10.1038/nclimate1674, 2013.

Fuss, S., Lamb, W. F., Callaghan, M. W., Hilaire, J., Creutzig, F., Amann, T., Beringer, T., de Oliveira Garcia, W., Hartmann, J., and Khanna, T.: Negative emissions—Part 2: Costs, potentials and side effects, Environmental Research Letters, 13, 063002, 2018.

Gidden, M. J., Fujimori, S., van den Berg, M., Klein, D., Smith, S. J., van Vuuren, D. P., and Riahi, K.: A methodology and implementation of automated emissions harmonization for use in Integrated Assessment Models, Environmental Modelling & Software, 105, 187-200, https://doi.org/10.1016/j.envsoft.2018.04.002, 2018.

Gidden, M. J., Riahi, K., Smith, S. J., Fujimori, S., Luderer, G., Kriegler, E., van Vuuren, D. P., van den Berg, M., Feng, L., Klein, D., Calvin, K., Doelman, J. C., Frank, S., Fricko, O., Harmsen, M., Hasegawa, T., Havlik, P., Hilaire, J., Hoesly, R., Horing, J., Popp, A., Stehfest, E., and Takahashi, K.: Global emissions pathways under different socioeconomic scenarios for use in CMIP6: a dataset of harmonized emissions trajectories through the end of the century, Geosci. Model Dev., 12, 1443-1475, 10.5194/gmd-12-1443-2019, 2019.

Golledge, N. R., Keller, E. D., Gomez, N., Naughten, K. A., Bernales, J., Trusel, L. D., and Edwards, T. L.: Global environmental consequences of twenty-first-century ice-sheet melt, Nature, 566, 65, 2019.

Graven, H. D., Keeling, R. F., Piper, S. C., Patra, P. K., Stephens, B. B., Wofsy, S. C., Welp, L. R., Sweeney, C., Tans, P. P., Kelley, J. J., Daube, B. C., Kort, E. A., Santoni, G. W., and Bent, J. D.: Enhanced Seasonal Exchange of CO2 by Northern Ecosystems Since 1960, Science, 341, 1085-1089, 10.1126/science.1239207, 2013.

Gray, J. M., Frolking, S., Kort, E. A., Ray, D. K., Kucharik, C. J., Ramankutty, N., and Friedl, M. A.: Direct human influence on atmospheric CO2 seasonality from increased cropland productivity, Nature, 515, 398-401, 10.1038/nature13957, 2014.

Gütschow, J., Jeffery, M. L., Gieseke, R., Gebel, R., Stevens, D., Krapp, M., and Rocha, M.: The PRIMAP-hist national historical emissions time series, Earth Syst. Sci. Data Discuss., 2016, 1-44, 10.5194/essd-2016-12, 2016.

Hoesly, R. M., Smith, S. J., Feng, L., Klimont, Z., Janssens-Maenhout, G., Pitkanen, T., Seibert, J. J., Vu, L., Andres, R. J., Bolt, R. M., Bond, T. C., Dawidowski, L., Kholod, N., Kurokawa, J. I., Li, M., Liu, L., Lu, Z., Moura, M. C. P., O'Rourke, P. R., and Zhang, Q.: Historical (1750–2014) anthropogenic emissions of reactive gases and aerosols from the Community Emissions Data System (CEDS), Geosci. Model Dev., 11, 369-408, 10.5194/gmd-11-369-2018, 2018.

Holmes, C. D., Prather, M. J., Sovde, O. A., and Myhre, G.: Future methane, hydroxyl, and their uncertainties: key climate and emission parameters for future predictions, Atmospheric Chemistry and Physics, 13, 285-302, 2013.

Hossaini, R., Chipperfield, M., Montzka, S., Rap, A., Dhomse, S., and Feng, W.: Efficiency of short-lived halogens at influencing climate through depletion of stratospheric ozone, Nature Geoscience, 8, 186-190, 2015.

Hurrell, J. W., Holland, M. M., Gent, P. R., Ghan, S., Kay, J. E., Kushner, P. J., Lamarque, J.-F., Large, W. G., Lawrence, D., Lindsay, K., Lipscomb, W. H., Long, M. C., Mahowald, N., Marsh, D. R., Neale, R. B., Rasch, P., Vavrus, S., Vertenstein,

M., Bader, D., Collins, W. D., Hack, J. J., Kiehl, J., and Marshall, S.: The Community Earth System Model: A Framework for Collaborative Research, Bulletin of the American Meteorological Society, 94, 1339-1360, 10.1175/bams-d-12-00121.1, 2013.

Jones, C. D., Arora, V., Friedlingstein, P., Bopp, L., Brovkin, V., Dunne, J., Graven, H., Hoffman, F., Ilyina, T., and John, J. G.: C4MIP–The Coupled Climate–Carbon Cycle Model Intercomparison Project: experimental protocol for CMIP6, Geoscientific Model Development, 9, 2853-2880, 2016.

Keeling, C. D., Bacastow, R. B., Bainbridge, A. E., Ekdahl, C. A., Guenther, P. R., Waterman, L. S., and Chin, J. F.: Atmospheric carbon dioxide variations at Mauna Loa observatory, Hawaii, Tellus, 28, 538-551, 1976.

Atmospheric CO2 records from sites in the SIO air sampling network: http://cdiac.esd.ornl.gov/trends/co2/sio-keel.htm, access: May, 2004.

Lawrence, D. M., Hurtt, G. C., Arneth, A., Brovkin, V., Calvin, K. V., Jones, A. D., Jones, C. D., Lawrence, P. J., de Noblet-Ducoudré, N., and Pongratz, J.: The Land Use Model Intercomparison Project (LUMIP) contribution to CMIP6: rationale and experimental design, Geoscientific Model Development, 9, 2973-2998, 2016.

Lenssen, N. J. L., Schmidt, G. A., Hansen, J. E., Menne, M. J., Persin, A., Ruedy, R., and Zyss, D.: Improvements in the GISTEMP Uncertainty Model, Journal of Geophysical Research: Atmospheres, 124, 6307-6326, 10.1029/2018jd029522, 2019.

Matthes, K., Funke, B., Anderson, M., Barnard, L., Beer, J., Charbonneau, P., Clilverd, M., Dudok de Wit, T., Haberreiter, M., and Hendry, A.: Solar forcing for CMIP6 (v3. 2), Geoscientific Model Development, 10, 2247-2302, 2017.

Meehl, G. A., Covey, C., Delworth, T., Latif, M., McAvaney, B., Mitchell, J. F., Stouffer, R. J., and Taylor, K. E.: The WCRP CMIP3 multimodel dataset: A new era in climate change research, Bulletin of the American Meteorological Society, 88, 1383-1394, 2007.

Meinshausen, M., Meinshausen, N., Hare, W., Raper, S. C. B., Frieler, K., Knutti, R., Frame, D. J., and Allen, M. R.: Greenhouse-gas emission targets for limiting global warming to 2°C, Nature, 458, 1158, 2009.

Meinshausen, M., Raper, S. C. B., and Wigley, T. M. L.: Emulating coupled atmosphere-ocean and carbon cycle models with a simpler model, MAGICC6: Part I – Model Description and Calibration, Atmospheric Chemistry and Physics 11, 1417-1456, 2011a.

Meinshausen, M., Smith, S., Calvin, K., Daniel, J., Kainuma, M., Lamarque, J. F., Matsumoto, K., Montzka, S., Raper, S., Riahi, K., Thomson, A., Velders, G., and van Vuuren, D. P.: The RCP greenhouse gas concentrations and their extensions from 1765 to 2300, Climatic Change, 109, 213-241, 10.1007/s10584-011-0156-z, 2011b.

Meinshausen, M., Wigley, T. M. L., and Raper, S. C. B.: Emulating atmosphere-ocean and carbon cycle models with a simpler model, MAGICC6: Part 2– Applications, Atmospheric Chemistry and Physics 11, 1457-1471, 2011c.

Meinshausen, M., Vogel, E., Nauels, A., Lorbacher, K., Meinshausen, N., Etheridge, D. M., Fraser, P. J., Montzka, S. A., Rayner, P. J., Trudinger, C. M., Krummel, P. B., Beyerle, U., Canadell, J. G., Daniel, J. S., Enting, I. G., Law, R. M., Lunder, C. R., O'Doherty, S., Prinn, R. G., Reimann, S., Rubino, M., Velders, G. J. M., Vollmer, M. K., Wang, R. H. J., and Weiss, R.: Historical greenhouse gas concentrations for climate modelling (CMIP6), Geosci. Model Dev., 10, 2057-2116, 10.5194/gmd-10-2057-2017, 2017.

Mengel, M., Nauels, A., Rogelj, J., and Schleussner, C.-F.: Committed sea-level rise under the Paris Agreement and the legacy of delayed mitigation action, Nature communications, 9, 601, 2018.

Montzka, S., McFarland, M., Andersen, S., Miller, B., Fahey, D., Hall, B., Hu, L., Siso, C., and Elkins, J.: Recent trends in global emissions of hydrochlorofluorocarbons and hydrofluorocarbons: Reflecting on the 2007 adjustments to the Montreal Protocol, The Journal of Physical Chemistry A, 119, 4439-4449, 2015.

Montzka, S. A., Dutton, G. S., Yu, P., Ray, E., Portmann, R. W., Daniel, J. S., Kuijpers, L., Hall, B. D., Mondeel, D., Siso, C., Nance, J. D., Rigby, M., Manning, A. J., Hu, L., Moore, F., Miller, B. R., and Elkins, J. W.: An unexpected and persistent increase in global emissions of ozone-depleting CFC-11, Nature, 557, 413-417, 10.1038/s41586-018-0106-2, 2018.

Morgenstern, O., Braesicke, P., Hurwitz, M. M., O'Connor, F. M., Bushell, A. C., Johnson, C. E., and Pyle, J. A.: The World Avoided by the Montreal Protocol, Geophysical Research Letters, 35, 10.1029/2008gl034590, 2008.

Morice, C. P., Kennedy, J. J., Rayner, N. A., and Jones, P. D.: Quantifying uncertainties in global and regional temperature change using an ensemble of observational estimates: The HadCRUT4 data set, Journal of Geophysical Research: Atmospheres, 117, 2012.

Myhre, G., Shindell, D., Breon, F. M., Collins, W., Fuglestvedt, J., Huang, J., Koch, D., Lamarque, J. F., Lee, D., Mendoza, B., Nakajima, T., Robock, A., Stephens, G., Takemura, T., and Zhang, H.: Anthropogenic and Natural Radiative Forcing, in: Climate Change 2013: The Physical Science Basis. Contribution of Working Group I to the Fifth Assessment, Report of the Intergovernmental Panel on Climate Change, edited by: Stocker, T. F., Qin, D., Plattner, G.-K., Tignor, M., Allen, S. K., Boschung, J., Nauels, A., Xia, Y., Bex, V., and Midgley, P. M., Cambridge University Press, Cambridge, New York, 2013.

Nauels, A., Meinshausen, M., Mengel, M., Lorbacher, K., and Wigley, T. M. L.: Synthesizing long-term sea level rise projections - the MAGICC sea level model v2.0, Geoscientific Model Development, 10, 2495-2524, 10.5194/gmd-10-2495-2017, 2017.

Nisbet, E. G., Dlugokencky, E. J., Manning, M. R., Lowry, D., Fisher, R. E., France, J. L., Michel, S. E., Miller, J. B., White, J. W. C., Vaughn, B., Bousquet, P., Pyle, J. A., Warwick, N. J., Cain, M., Brownlow, R., Zazzeri, G., Lanoisellé, M., Manning, A. C., Gloor, E., Worthy, D. E. J., Brunke, E.-G., Labuschagne, C., Wolff, E. W., and Ganesan, A. L.: Rising atmospheric methane: 2007–2014 growth and isotopic shift, Global Biogeochemical Cycles, 30, 1356-1370, 10.1002/2016gb005406, 2016.

NOAA ESRL GMD: Atmospheric Carbon Dioxide Dry Air Mole Fractions from quasi-continuous measurements at American Samoa. K.W. Thoning, D. R. K., and A. Crotwell (Ed.), National Oceanic and Atmospheric Administration (NOAA), Earth System Research Laboratory (ESRL), Global Monitoring Division (GMD): Boulder, Colorado, USA, 2014a.

NOAA ESRL GMD: Atmospheric Carbon Dioxide Dry Air Mole Fractions from quasi-continuous measurements at South Pole. K.W. Thoning, D. R. K., and A. Crotwell (Ed.), National Oceanic and Atmospheric Administration (NOAA), Earth System Research Laboratory (ESRL), Global Monitoring Division (GMD): Boulder, Colorado, USA, 2014b.

NOAA ESRL GMD: Atmospheric Carbon Dioxide Dry Air Mole Fractions from quasi-continuous measurements at Mauna Loa, Hawaii. K.W. Thoning, D. R. K., and A. Crotwell (Ed.), National Oceanic and Atmospheric Administration (NOAA), Earth System Research Laboratory (ESRL), Global Monitoring Division (GMD): Boulder, Colorado, USA, 2014c.

NOAA ESRL GMD: Atmospheric Carbon Dioxide Dry Air Mole Fractions from quasi-continuous measurements at Barrow, Alaska. K.W. Thoning, D. R. K., and A. Crotwell (Ed.), National Oceanic and Atmospheric Administration (NOAA), Earth System Research Laboratory (ESRL), Global Monitoring Division (GMD): Boulder, Colorado, USA, 2014d.

O'Neill, B. C., Tebaldi, C., Vuuren, D. P. v., Eyring, V., Friedlingstein, P., Hurtt, G., Knutti, R., Kriegler, E., Lamarque, J.-F., and Lowe, J.: The scenario model intercomparison project (ScenarioMIP) for CMIP6, Geoscientific Model Development, 9, 3461-3482, 2016.

Prather, M. J., Holmes, C. D., and Hsu, J.: Reactive greenhouse gas scenarios: Systematic exploration of uncertainties and the role of atmospheric chemistry, Geophysical Research Letters, 39, 2012.

Prinn, R., Cunnold, D., Rasmussen, R., Simmonds, P., Alyea, F., Crawford, A., Fraser, P., and Rosen, R.: Atmospheric emissions and trends of nitrous oxide deduced from 10 years of ALE–GAGE data, Journal of Geophysical Research: Atmospheres, 95, 18369-18385, 1990.

Prinn, R. G., Weiss, R. F., Arduini, J., Arnold, T., DeWitt, H. L., Fraser, P. J., Ganesan, A. L., Gasore, J., Harth, C. M., Hermansen, O., Kim, J., Krummel, P. B., Li, S., Loh, Z. M., Lunder, C. R., Maione, M., Manning, A. J., Miller, B. R., Mitrevski, B., Mühle, J., O'Doherty, S., Park, S., Reimann, S., Rigby, M., Saito, T., Salameh, P. K., Schmidt, R., Simmonds, P. G., Steele, L. P., Vollmer, M. K., Wang, R. H., Yao, B., Yokouchi, Y., Young, D., and Zhou, L.: History of chemically and radiatively important atmospheric gases from the Advanced Global Atmospheric Gases Experiment (AGAGE), Earth Syst. Sci. Data, 10, 985-1018, 10.5194/essd-10-985-2018, 2018.

Ray, E. A., Moore, F. L., Elkins, J. W., Rosenlof, K. H., Laube, J. C., Röckmann, T., Marsh, D. R., and Andrews, A. E.: Quantification of the SF6 lifetime based on mesospheric loss measured in the stratospheric polar vortex, Journal of Geophysical Research: Atmospheres, 122, 4626-4638, 10.1002/2016JD026198, 2017.

Rigby, M., Montzka, S. A., Prinn, R. G., White, J. W. C., Young, D., O'Doherty, S., Lunt, M. F., Ganesan, A. L., Manning, A. J., Simmonds, P. G., Salameh, P. K., Harth, C. M., Mühle, J., Weiss, R. F., Fraser, P. J., Steele, L. P., Krummel, P. B., McCulloch, A., and Park, S.: Role of atmospheric oxidation in recent methane growth, Proceedings of the National Academy of Sciences, 114, 5373-5377, 10.1073/pnas.1616426114, 2017.

Rigby, M., Park, S., Saito, T., Western, L. M., Redington, A. L., Fang, X., Henne, S., Manning, A. J., Prinn, R. G., Dutton, G. S., Fraser, P. J., Ganesan, A. L., Hall, B. D., Harth, C. M., Kim, J., Kim, K. R., Krummel, P. B., Lee, T., Li, S., Liang, Q., Lunt, M. F., Montzka, S. A., Mühle, J., O'Doherty, S., Park, M. K., Reimann, S., Salameh, P. K., Simmonds, P., Tunnicliffe, R. L., Weiss, R. F., Yokouchi, Y., and Young, D.: Increase in CFC-11 emissions from eastern China based on atmospheric observations, Nature, 569, 546-550, 10.1038/s41586-019-1193-4, 2019.

Rogelj, J., Meinshausen, M., and Knutti, R.: Global warming under old an new scenarios using IPCC climate sensitivity range estimates, Nature Climate Change, 2, 248-253, 2012.

Rogelj, J., Schaeffer, M., Meinshausen, M., Shindell, D. T., Hare, W., Klimont, Z., Velders, G. J., Amann, M., and Schellnhuber, H. J.: Disentangling the effects of CO2 and short-lived climate forcer mitigation, Proceedings of the National Academy of Sciences, 111, 16325-16330, 2014.

Rogelj, J., Meinshausen, M., Schaeffer, M., Knutti, R., and Riahi, K.: Impact of short-lived non-CO2 mitigation on carbon budgets for stabilizing global warming, Environmental Research Letters, 10, 2015.

Royer, D. L.: CO2-forced climate thresholds during the Phanerozoic, Geochim Cosmochim Ac, 70, 5665-5675, 2006.

Saunois, M., Bousquet, P., Poulter, B., Peregon, A., Ciais, P., Canadell, J. G., Dlugokencky, E. J., Etiope, G., Bastviken, D., Houweling, S., Janssens-Maenhout, G., Tubiello, F. N., Castaldi, S., Jackson, R. B., Alexe, M., Arora, V. K., Beerling, D. J., Bergamaschi, P., Blake, D. R., Brailsford, G., Brovkin, V., Bruhwiler, L., Crevoisier, C., Crill, P., Covey, K., Curry, C., Frankenberg, C., Gedney, N., Höglund-Isaksson, L., Ishizawa, M., Ito, A., Joos, F., Kim, H. S., Kleinen, T., Krummel, P., Lamarque, J. F., Langenfelds, R., Locatelli, R., Machida, T., Maksyutov, S., McDonald, K. C., Marshall, J., Melton, J. R., Morino, I., Naik, V., O'Doherty, S., Parmentier, F. J. W., Patra, P. K., Peng, C., Peng, S., Peters, G. P., Pison, I., Prigent, C., Prinn, R., Ramonet, M., Riley, W. J., Saito, M., Santini, M., Schroeder, R., Simpson, I. J., Spahni, R., Steele, P., Takizawa, A., Thornton, B. F., Tian, H., Tohjima, Y., Viovy, N., Voulgarakis, A., van Weele, M., van der Werf, G. R., Weiss, R., Wiedinmyer, C., Wilton, D. J., Wiltshire, A., Worthy, D., Wunch, D., Xu, X., Yoshida, Y., Zhang, B., Zhang, Z., and Zhu, Q.: The global methane budget 2000–2012, Earth Syst. Sci. Data, 8, 697-751, 10.5194/essd-8-697-2016, 2016.

Schaefer, H., Fletcher, S. E. M., Veidt, C., Lassey, K. R., Brailsford, G. W., Bromley, T. M., Dlugokencky, E. J., Michel, S. E., Miller, J. B., Levin, I., Lowe, D. C., Martin, R. J., Vaughn, B. H., and White, J. W. C.: A 21st-century shift from fossil-fuel to biogenic methane emissions indicated by <sup>13</sup>CH<sub>4</sub&gt, Science, 352, 80, 10.1126/science.aad2705, 2016.

Schneider, L., and Kollmuss, A.: Perverse effects of carbon markets on HFC-23 and SF6 abatement projects in Russia, Nature Climate Change, 5, 1061, 10.1038/nclimate2772, 2015.

Schneider, L. R.: Perverse incentives under the CDM: an evaluation of HFC-23 destruction projects, Climate Policy, 11, 851-864, 10.3763/cpol.2010.0096, 2011.

Schneider von Deimling, T., Meinshausen, M., Levermann, A., Huber, V., Frieler, K., Lawrence, D. M., and Brovkin, V.: Estimating the near-surface permafrost-carbon feedback on global warming, Biogeosciences, 9, 649-665, 10.5194/bg-9-649-2012, 2012.

Schneider von Deimling, T., Grosse, G., Strauss, J., Schirrmeister, L., Morgenstern, A., Schaphoff, S., Meinshausen, M., and Boike, J.: Observation-based modelling of permafrost carbon fluxes with accounting for deep carbon deposits and thermokarst activity, Biogeosciences, 12, 3469-3488, 2015.

Smith, C. J., Kramer, R. J., Myhre, G., Forster, P. M., Soden, B. J., Andrews, T., Boucher, O., Faluvegi, G., Fläschner, D., Hodnebrog, Ø., Kasoar, M., Kharin, V., Kirkevåg, A., Lamarque, J.-F., Mülmenstädt, J., Olivié, D., Richardson, T., Samset,

B. H., Shindell, D., Stier, P., Takemura, T., Voulgarakis, A., and Watson-Parris, D.: Understanding Rapid Adjustments to Diverse Forcing Agents, Geophysical Research Letters, 45, 12,023-012,031, 10.1029/2018gl079826, 2018.

Smith, P., Davis, S. J., Creutzig, F., Fuss, S., Minx, J., Gabrielle, B., Kato, E., Jackson, R. B., Cowie, A., and Kriegler, E.: Biophysical and economic limits to negative CO 2 emissions, Nature climate change, 6, 42-50, 2016.

Stevens, B., Fiedler, S., Kinne, S., Peters, K., Rast, S., Müsse, J., Smith, S. J., and Mauritsen, T.: MACv2-SP: A parameterization of anthropogenic aerosol optical properties and an associated Twomey effect for use in CMIP6, Geoscientific Model Development, 10, 433-452, 2017.

Taylor, K. E., Stouffer, R. J., and Meehl, G. A.: An overview of CMIP5 and the experiment design, Bulletin of the American Meteorological Society, 93, 485-498, 2012.

Toohey, M., Stevens, B., Schmidt, H., and Timmreck, C.: Easy Volcanic Aerosol (EVA v1.0): an idealized forcing generator for climate simulations, Geosci. Model Dev., 9, 4049-4070, 10.5194/gmd-9-4049-2016, 2016.

Tsutsumi, Y., Mori, K., Hirahara, T., Ikegami, M., and Conway, T. J.: Technical report of global analysis method for major greenhouse gases by the World Data Center for greenhouse gases, WMO/TD, 2009.

Velders, G., and Daniel, J.: Uncertainty analysis of projections of ozone-depleting substances: mixing ratios, EESC, ODPs, and GWPs, Atmospheric Chemistry and Physics, 14, 2757-2776, 2014a.

Velders, G. J. M., Andersen, S. O., Daniel, J. S., Fahey, D. W., and McFarland, M.: The importance of the Montreal Protocol in protecting climate, P Natl Acad Sci USA, 104, 4814-4819, 2007.

Velders, G. J. M., and Daniel, J. S.: Uncertainty analysis of projections of ozone-depleting substances: mixing ratios, EESC, ODPs, and GWPs, Atmos. Chem. Phys., 14, 2757-2776, 10.5194/acp-14-2757-2014, 2014b.

Velders, G. J. M., Fahey, D. W., Daniel, J. S., Andersen, S. O., and McFarland, M.: Future atmospheric abundances and climate forcings from scenarios of global and regional hydrofluorocarbon (HFC) emissions, Atmospheric Environment, 123, 200-209, https://doi.org/10.1016/j.atmosenv.2015.10.071, 2015.

Vollmer, M. K., Young, D., Trudinger, C. M., Mühle, J., Henne, S., Rigby, M., Park, S., Li, S., Guillevic, M., Mitrevski, B., Harth, C. M., Miller, B. R., Reimann, S., Yao, B., Steele, L. P., Wyss, S. A., Lunder, C. R., Arduini, J., McCulloch, A., Wu, S., Rhee, T. S., Wang, R. H. J., Salameh, P. K., Hermansen, O., Hill, M., Langenfelds, R. L., Ivy, D., O'Doherty, S., Krummel, P. B., Maione, M., Etheridge, D. M., Zhou, L., Fraser, P. J., Prinn, R. G., Weiss, R. F., and Simmonds, P. G.: Atmospheric histories and emissions of chlorofluorocarbons CFC-13 (CClF3), ΣCFC-114 (C2Cl2F4), and CFC-115 (C2ClF5), Atmos. Chem. Phys., 18, 979-1002, 10.5194/acp-18-979-2018, 2018.

Welp, L. R., Patra, P. K., Rödenbeck, C., Nemani, R., Bi, J., Piper, S. C., and Keeling, R. F.: Increasing summer net CO2 uptake in high northern ecosystems inferred from atmospheric inversions and remote sensing, Atmos. Chem. Phys.(Discuss), submitted, 2016.

WMO: Scientific Assessment of Ozone Depletion: 2006, World Meteorological Organization, Geneva, Switzerland, 572, 2006.

WMO: Scientific Assessment of Ozone Depletion: 2014, World Meteorological Organization, Geneva, Switzerland, 416, 2014.

Worden, J. R., Bloom, A. A., Pandey, S., Jiang, Z., Worden, H. M., Walker, T. W., Houweling, S., and Röckmann, T.: Reduced biomass burning emissions reconcile conflicting estimates of the post-2006 atmospheric methane budget, Nature Communications, 8, 2227, 10.1038/s41467-017-02246-0, 2017.

475

476

477

478

479

480

481

482

483

484 **13 Figures**